AN ABSTRACT OF THE THESIS OF

Wenqian (Winnie) Zhang for the degree of Master of Science in Bioresource Engineering and Civil Engineering presented on July 17, 1995. Title: Use of Pore-scale Network to Model Three-phase Flow in a Bedded Unsaturated Zone.

Redacted for Privacy

Abstract approved: _____

John S. Selker

Redacted for Privacy

_____

Jonathan D. Istok

Contamination of ground water by non-aqueous phase liquids (NAPLs) has received increasing attention. The most common approach to numerical modeling of NAPL movement through the unsaturated zone is the use of the finite difference or finite element methods to solve a set of partial differential equations derived from Darcy's law and the continuity equations (Abriola and Pinder, 1985; Kaluarachchi and Parker, 1989). These methods work well in many settings, but have given little insights as to why certain non-ideal flow phenomena will occur. The network modeling method, which considers flow at the pore-scale, was used in this study to better understand macroscopic flow phenomena in porous media.

Pore-scale network models approximate porous medium as a connected network of pores and channels. Two and three-dimensional pore-scale network models were constructed in this study. A uniform statistical distribution was assumed to represent the random arrangement of pore and tube sizes. Both hysteristic scanning curves and

intermediate fluid distribution are studied. The simulation results suggested that network models may be used to predict the characteristic curves of three-phase systems. The results also suggested that three-dimensional models are necessary to study the three-phase problems. Two-dimensional models do not provide realistic results as evidenced by their inability to provide scale-invariant representation of flow processes. The network sizes used in this study ranged from 10 x 5 (50) to 156 x 78 (12168) pores for two-dimensional and from 10 x 5 x 5 (250) to 100 x 50 x 5 (25000) pores for three-dimensional domains. The domain size of 100 x 50 x 5 pores was large enough to provide descriptions independent of the domain scale.

The one important limitation of network models is the considerable computational requirements. The use of very high speed computers is essential. Except for this limitation, the network model provides an invaluable technique to study fluid transport mechanisms in the vadose zone.

Use of Pore-scale Network to Model Three-phase Flow in a Bedded Unsaturated Zone

by

Wenqian (Winnie) Zhang

A THESIS

submitted to

Oregon State University

in partial fulfillment of
the requirements for the
degree of

Master of Science

Completed July 17, 1995
Commencement June 1996

Master of Science thesis of Wenqian (Winnie) Zhang presented on July 17, 1995.

APPROVED:

Redacted for Privacy

Co-major Professor, representing Bioresource Engineering

Redacted for Privacy

Co-major Professor, representing Civil Engineering

Redacted for Privacy

Head of Department of Bioresource Engineering

Redacted for Privacy

Head of Department of Civil Engineering

Redacted for Privacy

Dean of Graduate School

I understand that my thesis will become part of the permanent collection of Oregon State University libraries. My signature below authorized release of my thesis to any reader upon request.

Redacted for Privacy

Wenqian (Winnie) Zhang, Author

Acknowledgment

At first, I would like to thank my advisors, Dr. John Selker, and Dr. Jonathan Istok. Without their invaluable, enthusiastic help, and their expertise, the completeness of this project will be impossible. Especially, I would like to thank Dr. John Selker of his financial support for offering me the research assistantship through my graduate study at Oregon State University. It is indeed a great honor to have the opportunity to work under their guides in my graduate program.

Many thanks to my committee members Dr. Andrew Hashimoto, Dr. Peter Nelson, and Dr. Kenneth Johnson for their invaluable advice, and taking time out of their busy schedule to review my work.

Special thanks to everybody, who helped me in one way or another to make this project possible. I especially thank Bob Schneckenburger for his very educational help in keeping all the computers running; Dr. Chaur-Fong Chen for his great way of teaching me how to use UNIX workstation, Janet Lee for her invaluable help in keeping SUN station running.

I would like to take a chance to thank my colleagues, Steve, Florian, Weidong, Shaun, Rick, Martin, etc. They helped me in many discussions about my questions in this project and friendly encouragement through my good and bad times at Oregon State University.

Also, my great respect and thanks go to the entire staff, faculty and many graduate students in Department of Bioresource Engineering and Department of Civil

Engineering, who always made me feel warm like at home and helped me in many different ways.

Especially, I would like to express my greatest appreciation, respect, and warm thanks to my parents for their unquestioning support and encouragement. The same applies to all of my friends.

Without the people I mentioned above, my time at Oregon State University will not be so memorable.

Table of Contents

Table of Contents (continued)

Table of Contents (continued)

List of Figures

List of Figures (continued)

List of Figures (continued)

List of Figures (continued)

List of Figures (continued)

List of Figures (continued)

List of Figures (continued)

Use of Pore-scale Network to Model Three-phase Flow in a Bedded Unsaturated Zone

Chapter 1. Introduction

Contamination of ground water by organic wastes is a serious problem in many countries. Many of these waste materials are organic liquids such as liquid petroleum products. Those which are not readily water soluble are called non-aqueous phase liquids (NAPLs). The need to clean up NAPL contamination leads to the need to predict NAPL movement. To model the movement in the unsaturated zone, we must consider a system of three different fluid phases ---- air, NAPL and water. Many researchers are engaged in work on this problem using both experimental and numerical methods.

The most common approach to numerical modeling the movement of NAPLs through the unsaturated zone is the use of the finite difference or finite element methods to solve a set of partial differential equations derived from Darcy's law and the continuity equations (one for each phase) (Abriola and Pinder, 1985; Kaluarachchi and Parker, 1989). Even though these methods have been successful in some cases, this approach gives little insight as to why certain non-continuous flow phenomena occur; e.g., the movement of NAPLs along the isolated sets of large pores.

In this thesis, a network modeling approach is employed, constructed by considering the flow at the pore scale, to better understand macroscopic flow phenomena in porous media. The model describes the medium by a connected network of pores and channels.

The main objectives of this work are: (1) to develop a methodology to apply a network model to a three-phase flow system, (2) to use the network model to simulate the capillary pressure-saturation scanning curves in homogeneous and bedded sand media, and (3) to apply the network model to several infiltration processes to determine the significance of antecedent conditions on fluid distribution.

This thesis applies the network model to both two-dimensional and three-dimensional domains. Chapter 2 gives a brief review of previous research. Chapter 3 describes the methodology used to apply a network model to the three-phase system. Chapter 4 and Chapter 5 present the results from the two-dimensional and three-dimensional domains, respectively. Chapter 6 provides discussion and conclusions.

Chapter 2. Literature Review

The problem of modeling multi-phase flow in porous media has received increasing attention, especially modeling using pore-scale networks to describe the porous media.

The spherical pack model is the earliest pattern used to describe porous media (Hazen, 1892; Slichter, 1899). One example of this pattern has uniform sized spherical particles packed orderly in three-dimensional space (Figure 1). Hazen suggested that the effective size of sand grains can be used to represent the great range of sand sizes. Here the effective size is defined as the size such that 10 percent of the porous media mass is smaller and 90 percent is larger. His experimental results showed that those sizes which are smaller than the effective size have as much influence upon the infiltration as those coarse 90 percent. This finding indicated that the smaller 10 percent of grain sizes determined the frictional resistance, the capillary suction, during the infiltration processes. He developed an empirical formula to estimate the capillary pressure head, h, at which a saturated media would de-saturate:

$$h = \frac{1.5}{d^2}, \tag{1}$$

where d is the effective grain size. Here all units are in millimeters. However, this is not consistent with capillary pressure heads and predicted by the Laplace Equation. Hazen's formula may only fit a special case of sand grain size. Obviously, the volumes of pore space between particles are complicated to calculate. Slichter (1899) gave a detailed theoretical derivation of the volume of pore space and mean velocity of the fluid traveling

through a porous medium based on assumption that pore space is made up of tubes with triangular cross section. Since Slichter assumed that all of the particles are of one size, these arrangements are not suitable for describing hysteresis in the capillary pressure-saturation relationship. Because of its complexity and poor fit to the observed data, the development of this model is limited.

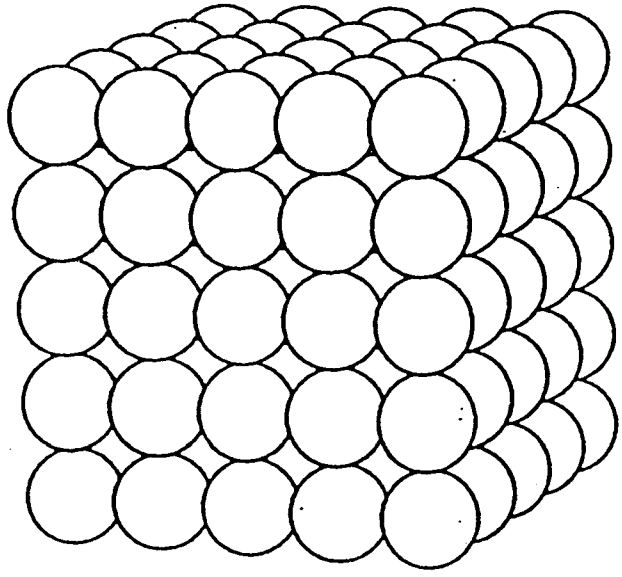

Figure 1. The spherical pack model.

The first effective model for porous media saturated with multiple fluids was the "bundle-of-tubes" model discussed by Green and Ampt (1911) and Blake (1922). In this model, the pore space is represented as a bundle of independent parallel tubes, each of which may have a different radius (Figure 2). As mentioned by Ferrand et al. (1990), this model relates microscopic lengths to macroscopic quantities, such as permeability and porosity (Cushman, 1990). Compared to the spherical pack model, this model is much simpler, but only suitable for one-dimensional case.

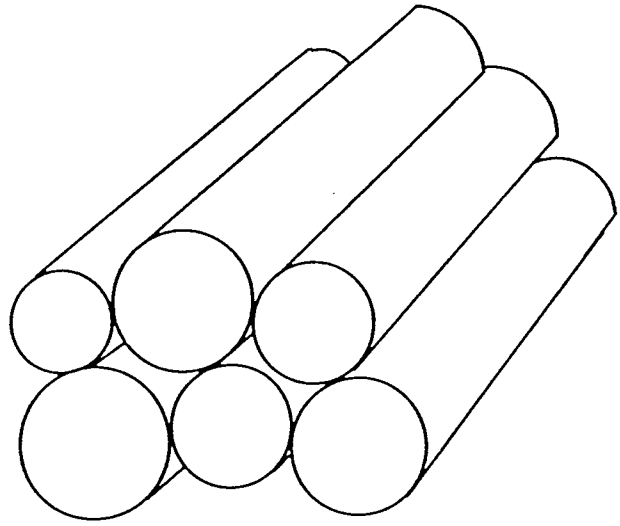

Figure 2. The "bundle-of-tubes" model.

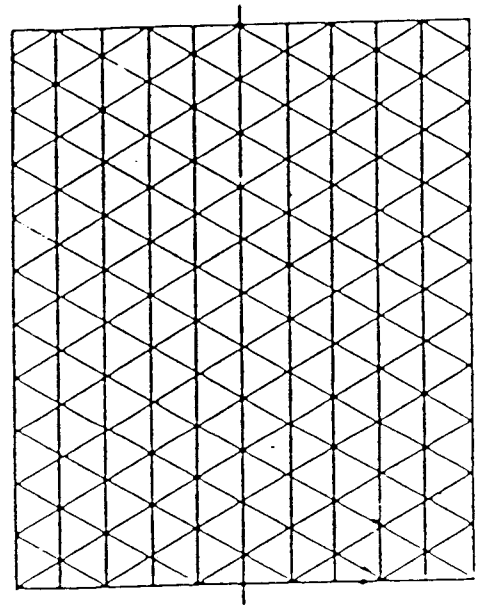

Figure 3. Fatt's (1956a) network model

The first network model was developed by Fatt (1956a). He combined the spherical pack model and "bundle-of-tubes" model to build the network model. He used

the cylinder tube and the triple hexagonal network (Figure 3). In his pivotal paper, Fatt applied the network of tube model in studying the influence of tube size distribution on capillary pressure-saturation curves and the dynamic properties of network (e.g., flow resistance in network). He found that the capillary pressure-saturation curve is more sensitive to changes in tube radius distribution than to changes in connectivity of tubes in the network. This result can be used to simplify the geometry of a network. The other major finding of Fatt was that the relative permeability curves obtained from this model were similar to those obtained from experiments, demonstrating network models as a powerful tool to understand flow through porous media.

2.1 Two-dimensional Models

Since 1956, many researchers have engaged in the development and application of network models. Koplik (1982) introduced a two-dimensional square-grid "pore and throat" network to study the creeping flow using the "effective medium theory". This theory was developed to obtain the effective bulk network conductivity from the radius or conductivity distribution of the individual elements. Using the same model, Chandler et al. (1982) studied capillary displacement to investigate the residual saturation of a displaced phase, which was found to depend strongly upon the domain size (width, or the shorter side of domain) but weakly on the pore size distribution. This means that pore size distribution may change the path of infiltration, but may not change the residual saturation. They also developed an empirical formula to show the relationship of domain width W and residual saturation S for two-dimensional models:

$$S(W) = 1 - 0.95W^{-0.17} \quad (2)$$

Here, width W is represented by the number of pores. When domain width increases, the residual saturation will increase. It is notable that when $W \rightarrow \infty$, $S \rightarrow 1$. It seems that there was no threshold domain width for which the residual saturation became constant.

Koplik and Lasseter (1985) used an irregular network to study oil-water two-phase flow in homogeneous porous media. They were the first author to discuss modeling using partially filled pores. Dias and Payatakes (1986) introduced a sinusoidal tube and square frame two-dimensional network model to study two-phase flow micro displacement and the movement of oil ganglia (entrapped oil). They discussed the effects of the viscosity and capillary number on the displacement of the non-wetting fluid and the motion of oil ganglia. The capillary number mentioned here is used to express the ratio of viscous stresses in water to the capillary pressure. Even with the complicated tube space, the displacement patterns from this model were similar to Koplik's model.

Touboul et al. (1987) compared the results from the stochastic and the pore-scale network models for the two-dimensional drainage case to those from micro model experiments and found similar displacement patterns. This demonstrated that the pore-scale network model was just as powerful as the stochastic physical network model but simpler. Here, the stochastic network models were based on percolation theory, or on diffusion limited aggregation algorithm, which is related to the Monte Carlo technique, to describe displacement in porous media. Compared to pore-scale network models, these

models lack the physical basis, but they are still capable of predictions of the geometry and transport properties of a given network.

Since the development of more powerful computation tools, network models have been used more widely (Kueper and McWhorter, 1992; Ewing and Gupta, 1993a & 1993b; Ferrand et al., 1994). Kueper and McWhorter (1992) introduced the concept of a local-scale network, which assigns each pore and tube in the network a porosity, permeability, and capillary pressure-saturation relationship. This concept was combined with the effective medium theory (based on a random local-scale permeability distribution) and network percolation theory (represent the porous media as an ordered lattice). This theory can be used to simulate the flow in heterogeneous porous media. Ewing and Gupta (1993) introduced a domain network model in which the volume of soil to be modeled is discretized into domains, and all pore throats in a domain are assumed to have identical equivalent radii. This theory can be used to model a porous medium with a wide range of pore size distribution.

Detailed literature reviews on network modeling have been carried out by Lenormand (1990) and Dullien (1990). Lenormand's review concentrated on fingering flow in two-dimensional porous media comparing network models with statistical models and the experimental methods. Dullien carried out an extensive review of pore-scale models applied to transport problems governed by the Laplace equation. Sorbie (1990) provided an in depth review of network models used to simulate flow and the conductivity problem that is governed by Poiseuille's law.

2.2 Three-dimensional Models

Network models have been extended to three dimensions to obtain more physically realistic results. Lapidus et al. (1985) developed a three-dimensional network with pores and tubes to interpret the porosimetry data obtained from mercury injection. Kantzas and Chatzis (1988) developed a three-dimensional network model to simulate relative permeability curves of two-phase flow in porous media. They found that the pore size distribution was not the only factor in predicting effective permeability. Other factors which were found to be influential included porosity and the pore geometry (shape, pore distance, etc.) in the pore network. However, the simplified geometry of cylindrical pores do give a good approximation of the permeability values. To simulate consolidated rocks, Constantinides and Payatakes (1989) developed a three-dimensional network model with a randomized lattice, in an attempt to make the model more closely match to the pore size and distance of real rocks. Currently, researchers continue to apply three-dimensional network models to study two-phase flow (Blunt and King, 1991; Blunt et al., 1992).

2.3 Three-phase Models

Scientists began to apply network modeling techniques to the study of three-phase flow more than ten years ago. Heiba et al. (1984) used a statistical network to study the relative permeability of multi-phase flow. Oren et al. (1992) set up a two-dimensional etched glass micro-model to study the influence of spreading coefficients on the displacement of three-phase flow. Soll et al. (1993) used a similar etched glass micro-model to study both the processes of infiltration and the capillary pressure-saturation

relationships in three-phase systems. This micro-model was pressure-controlled, unlike Oren's, to efficiently provide the quantitative description of capillary pressure-saturation relationships. Both Soll and Oren's micro-models only allowed one advancing fluid at a given time, a constraint which does not exist in the real world. Soll et al. found that the fluid interfaces of the three-phase system are locally two-phase at the pore scale, a fact which can be used to simplify computational modeling. Soll and Celia (1993) also developed a pore-scale network model to simulate their experiments. The results show that their computational model could reproduce many of the important aspects of the laboratory-scale capillary pressure-saturation experiments.

Although a number of network models have been developed for a variety of purposes, network models have not been used to study multi-phase flow in bedded porous media. This study seeks to develop the methodology to apply the pore-scale network model to a three-phase flow system in two and three-dimensional domains.

Chapter 3. Theory and Methodology

3.1 Theory

Network models for porous media may be based on two-dimensional or three-dimensional interconnected networks of pores and throats. Different rules of computation must be followed depending on the system being studied. In this thesis, we will only discuss the transport problem.

In the present research we define a transport problem to be an attempt to predict the movement of fluids in porous media. We specifically focus here on bulk fluid imbibition and drainage, and do not attempt to address issues of solute transport, adsorption, or inter-phase mass transfer. In typical naturally occurring porous media, the size of pores and throats are very small (i.e., from about 0.1 to 300 μm). At this scale, capillary forces are dominant compared to gravitational and viscous forces. Therefore, we neglect the influence of these two forces to simplify the model.

Capillary pressure across a fluid with a curved interface, P_c, can be calculated by Young-Laplace equation:

$$P_c = \sigma \left(\frac{1}{r_1} + \frac{1}{r_2}\right) \tag{3}$$

where r_1 and r_2 are the principal radii of curvature, and σ is the surface tension. Assuming that $r_1 = r_2 = r$, as is true for the cylindrical tubes employed here, equation (3) can be rewritten as:

$$P_c = \sigma(\frac{2}{r}) \tag{4}$$

In cylindrically symmetrical system, the contact angle can be defined as:

$$\cos\theta = \frac{R}{r} \tag{5}$$

where R is the local radius of curvature and θ is the contact angle. Laplace equation for a two-phase system may be rewritten as:

$$P_c = \frac{2\,\sigma_{ab}\cos\theta_{ab}}{R} \tag{6}$$

where θ_{ab} is the contact angle between phase **a** and phase **b** (solid-fluid or fluid-fluid) interface, R is the radius of the pore or throat (depending on which process will be concerned, i.e., wetting or draining), σ_{ab} is the surface tension of the interface, **a** is the advancing fluid index, and **b** is the resident fluid index. Fluids with contact angles $\theta < 90°$ are called wetting fluids, and fluids with contact angles $\theta > 90°$ are referred to as non-wetting fluids.

At a fluid-fluid interface, the pressure difference between wetting and non-wetting fluid ΔP_{nw} can be defined as:

$$\Delta P_{nw} = P_n - P_w \tag{7}$$

where P_n is the non-wetting fluid pressure and P_w is the wetting fluid pressure. When ΔP_{nw} equals the interface capillary pressure P_c, the system is in a state of equilibrium and the interface will not move. When $\Delta P_{nw} < P_c$, the larger P_c, the larger difference of ΔP_{nw} and P_c, so that the wetting fluid will displace the non-wetting fluid from the smallest radius aperture along the fluid interface. When $\Delta P_{nw} > P_c$, the smaller P_c will give the

larger difference of ΔP_{nw} and P_c, and the non-wetting fluid will displace the wetting fluid from the largest radius aperture along the fluid interface. The process of wetting fluid displacing non-wetting fluid is called wetting, and the process of non-wetting fluid displacing wetting fluid is called draining.

Based on the above theory, when pore sizes are much larger than tube sizes, wetting is a pore size-controlled process and draining is a tube size-controlled process. It is of note that the sequence of displacements for a particular network pore geometry will be identical for any pair of fluids under the same displacement process (e.g., wetting fluid displace non-wetting fluid). Thus the pattern of imbibition of water into an air filled network will be identical to that of oil into an air filled network, or water into a oil filled network.

3.2 Methodology

Models are developed to simplify the complicated real world so that we may gain greater understanding of natural phenomena. The assumptions which are made in developing a model dictate both the simplicity of the model and the desired accuracy of model's predictions. The main assumptions and observations employed in this study to develop a network model to simulate multi-phase flow in porous media are discussed below.

3.2.1 Assumptions

The assumptions used in this model are summarized below. We stress that the present model is conceived to give insight to capillary displacement processes, where displacement is slow enough to make capillary forces dominant.

1. There are only two kinds of fluids existing at any given interface. This assumption is strongly supported by Soll's experimental work (Soll et al., 1993).

2a. All non-equilibrium fluid displacement occurs instaneously.

2b. All the displacement is in steady-state. Time is not considered.

3. Only one fluid may occupy an individual pore or throat at any given time. Partially filled pores are not in an equilibrium state. Under the condition of steady-state, partially filled pores will not occur. This assumption was also confirmed by Soll's experiments.

4. All of the pore sizes are larger than all of the tube sizes. Compared to the volume of a pore, the fluid volume existing in a tube can be neglected.

5. We neglect the effects of gravitation and viscosity.

6. Contact angles at the interface of two different fluids equal zero.

3.2.2 Parameters

A network domain can be expressed by its dimension, connectivity, and aperture size distribution, which are therefore the defining parameters of a network model.

The dimension of a network is a measure of the number of orthogonal axes of allowed flow. One, two and three-dimensional networks are easy to visualize. But it is worth noting that from formal and mathematical perspectives, N-dimensional networks

may be constructed easily too. If we define the size of a domain as the number of connected pores along any one axis, say R, it is clear that the number of pores or nodes goes up with R^n. Thus, the memory requirements and computational effort go up exponentially with the number of dimensions. Such considerations quickly become constraints regardless of the size and speed of the computational facilities. The results of this thesis are composed of two parts. The first part considers a two-dimensional domain, while the second part contrasts these results with those from a three-dimensional domain.

The term connectivity is defined as the number of adjacent pores or tubes which connect to a given pore or tube respectively. For a given network, the connectivity of pores and tubes may be different. The connectivity of a network reflects the geometry of the model domain. The network domain used in this model is similar to Koplik's model (1982) which is a square-grid, pore and throat network with an ordered lattice. The shapes of a pore and a throat are a sphere and a cylinder respectively. In a two-dimensional domain, the connectivity of pores and tubes are 4 and 6, respectively (Figure 4 and 5). In a three-dimensional domain, the connectivity of pores and tubes are 6 and 10, respectively.

Since the dimensions of the numerical matrices which describe the pores and tubes are different, we chose random pore and tube size distributions independently, only constrained by the assumptions in Section 3.2.1. Pore sizes were chosen from an assumed uniform distribution ranging from 0.09 to 0.13mm for fine sand and from 0.25 to 0.5mm for coarse sand. Tube size was chosen uniformly distributed from 0.009 to 0.013mm for fine sand and from 0.025 to 0.05mm for coarse sand.

The final set of important parameters required are the interfacial tensions at the fluid-fluid interfaces which depend on the type of fluids in the domain. The oils we used were soltrol-220 and mineral oil. The interfacial tensions between the two fluids are shown in the following table:

Interfacial tensions used in the simulations.

	Interfacial	tension	(N/m)
Fluid	Water*1	Soltrol-220*2	mineral oil*3
Air	0.0727	0.0245	0.0309
Water		0.0399	0.0534

*1 Value from Jury, et al. (1991, p.37).
*2 Phillips 66 Petroleum Co., Bartlesville, OK (McBride, et al., 1992).
*3 Medi-kay Laboratories, Bucklin, MO (Heavy Mineral Oil Laxative). (McBride, et al., 1992)

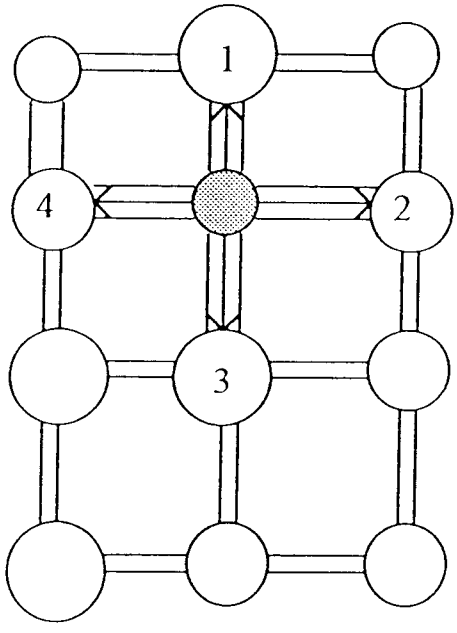

Figure 4. Illustration of connectivity of pores in a 2-D square lattice network

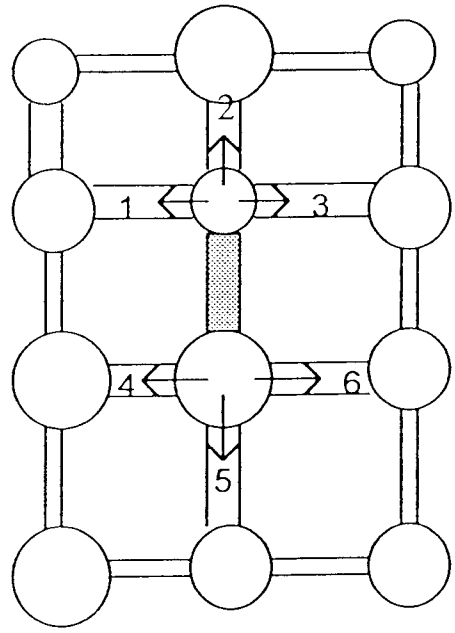

Figure 5. Illustration of connectivity of tubes in a 2-D square lattice network

3.2.3 Boundary Conditions

As stated in Section 3.2.1, all movement within the network is governed exclusively by fluid pressures and aperture size. In the model employed here, the fluid reservoir dictates the fluid pressure.

There are two types of boundaries in this model. A boundary attached to a reservoir is a specified pressure boundary. Any boundary not attached to a reservoir is a no-flow boundary. The water and oil reservoirs are at the top of the domain, and the air reservoir is at the bottom of the domain (Figure 6 and 7).

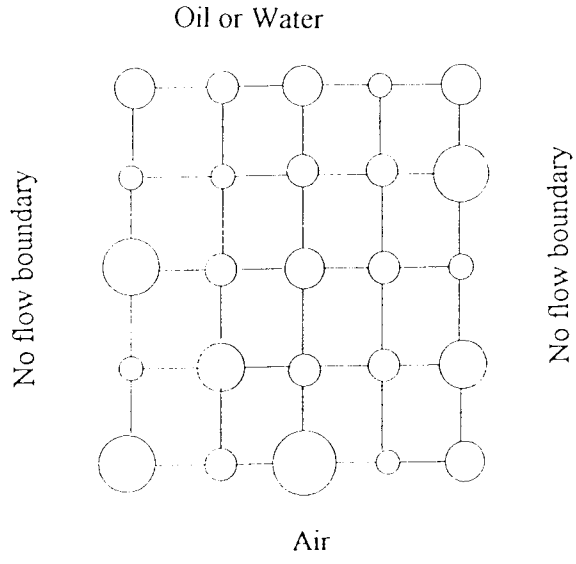

Figure 6. A 5 x 5 two-dimensional model domain.

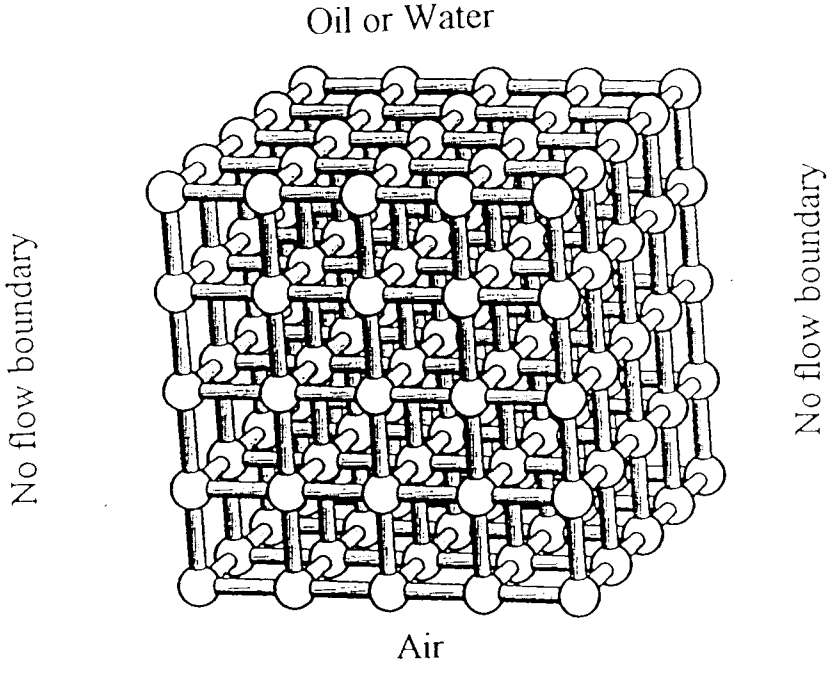

Figure 7. A 5 x 5 x 5 three-dimensional model domain.

(Note: Radii of tubes and spheres may be random, although shown as single sized.)

3.2.4 Procedures

In the following section we discuss the central methods required to implement the network model. We first define terminology, then discuss issues of trapped pores, wetting front identification and infiltration simulation.

The displacement matrix DAOW (distribution of air, oil, and water) is used to store the distribution of all species of fluid in the model domain. It is a two or three dimensional matrix depending on the dimension of model domain. The size of DAOW is the same as pore matrix. The "pore matrix" is used to store the randomized pore sizes, and the "tube matrix" is used to store the randomized tube sizes. The number of rows and columns in pore matrix and tube matrix are different. The advancing fluid is defined as the fluid whose reservoir provides a pressure to make this fluid move. The resident fluid is defined as the fluid whose reservoir does not provide a pressure.

In DAOW, we use index numbers to represent the fluids and boundary. The indexes 1, 2, 3, and 0 represent the least wetting fluid, the intermediate wetting fluid, the most wetting fluid, and the boundary respectively.

3.2.4.1 Identifying the Trapped and Non-trapped Pores

Non-trapped pores are defined as the pores filled by a fluid which can follow a continuous route to its reservoir, while trapped pores are defined as the pores filled by a fluid which can not follow a continuous route to its reservoir.

There are two methods to identify the trapped pores. One is called the space sweeping method. The other one is called the tracing method. We discuss each below.

Space Sweeping Method

This method identifies connected pores based on the search of the domain following the sequence of column by column and row by row in each case identifying neighboring connected pores. The process is repeated until no changes in computed pore connection are obtained between sequential sweeps. The procedures to apply this method are stated below.

1. Write all fluid **i** (**i=1,2,3**) filled pores from displacement matrix DAOW to matrix A. In matrix A, we only have two index numbers ---- **i** and **0**.

2. Assign the pores on the nearest row to **i** reservoir which are filled by **i** a particular number other than **i** or **0** (e.g., **5**).

3. From left to right, check if the four pores connecting to a **5** filled pore on this row are **i** filled. If so, assign them **5**.

4. Repeat step 3 from the second nearest row to farthest row to **i** reservoir.

5. Use the checking method of step 3 and 4 to search from right to left and from nearest row to farthest row to **i** reservoir.

6. Use the same method to search from right to left and from farthest row to nearest row to **i** reservoir.

7. Use the same method to search from left to right and from farthest row to nearest row to **i** reservoir.

8. Repeat step 3 to step 7 for N times (N equals the number of rows).

9. Write all **5** filled pores in matrix A to matrix B. Matrix B is used to store all the pores filled by **i** and not trapped. All the pores left in matrix A assigned the value **i** are trapped pores.

Tracing Method

This method is based on the search of the domain following the sequence from trees to branches. From the view of algorithms (Goodman and Hedetniemi, 1977), both the depth-first search (DFS) and breadth-first search (BFS) are called tracing methods. In this thesis, we use the depth-first search, which involves the search of one tree structure by another. The procedures to apply this method are presented below.

1. Write all fluid **i** (**i=1,2,3**) filled pores from displacement matrix DAOW to matrix A.

2. Starting from one end of the nearest row to **i** reservoir (e.g., left), check if it is **i** filled. If so, write this pore to matrix C. Assign this pore in matrix A a particular number (e.g., **5**). If not, go to the second left pore. Here matrix C is an one dimensional matrix which used to store all the pores need to be checked.

3. For every pore in the matrix C, check if any of the pores in matrix A connecting to this pore is **i** filled. If so, write them to matrix C. Assign them a particular number in matrix A. Assign the already checked pores in matrix C a particular number so that they will not be checked again. Repeat this step until all the pores in matrix C have been checked.

4. Repeat step 2 and step 3 from second left to the last left pore on the nearest row to **i** reservoir.

5. Write all **5** filled pores in matrix A to matrix B, which used to store all the pores filled by **i** and not trapped.

Both the space sweeping and tracing methods were implemented in the course of this study. From the perspective of computational efficiency, no difference between the two methods was seen. The tracing method was more amenable to code implementation, and thus was employed in this study.

3.2.4.2 Identifying the Wetting Front

The wetting front is defined as the border between not trapped advancing fluid to the not trapped resident fluid. Fluid displacement can only occur along this front. Following the method in last step, we can identify the non-trapped pores for each kind of fluid, making this boundary easy to identify.

From theory, the process of wetting fluid infiltration is controlled by the pore size. Thus we assign the wetting front to be on the border belonging to the resident fluid to simplify the programming. When a non-wetting fluid is the advancing fluid, the infiltration process is controlled by the tube size. In this case the wetting front on the border is assigned to belong to the advancing fluid.

We know water is the most wetting fluid in the domain. When water infiltrates a pore, it will fill all the tubes connected to this pore at the same time. No trapped tubes

occur in this process. On the other side, air is the least wetting fluid in the domain. When air infiltrates a pore, it will not fill all the tubes connected to this pore, so trapped tubes occur in the air infiltration process. These factors must be considered in identifying the wetting front.

3.2.4.3 Infiltration

As pressure increases at either the water or oil reservoir, the advancing fluid will infiltrate the model domain following the theory described above. The procedures employed to implement these rules are presented below.

1. By the equation (6) and (7), calculate ΔP_{nw} - P_c for every pore or tube on or adjacent to the wetting front.

From the assumptions, we know when **a** $\neq$ **b**, $\cos\theta = 1$. Let $C_{ab} = 2\sigma_{ab}$, where **a** is the advancing fluid index number (**1** to **3**) and **b** is the resident fluid index number (**1** to **3**). The units of C_{ab} are the same as σ_{ab} (force/length). We have at most three kinds of fluid, so C_{ab} may be expressed as a matrix with size of 3x3. When **a** = **b**, $\theta_{ab} = 90°$ hence $C_{ab} = 0$. The matrix C_{ab} used in the programming is shown below:

$$\mathbf{C} = \begin{pmatrix} 0 & C_{12} & C_{13} \\ C_{21} & 0 & C_{23} \\ C_{31} & C_{32} & 0 \end{pmatrix}$$

We take $C_{ab} = C_{ba}$, but note that hysteresis in contact angle can be modeled by having $C_{ab} \neq C_{ba}$.

2. Find the pore or tube with smallest or largest value of ΔP_{nw} - P_c depending on

which fluid is advancing following the pressure control condition (hence obtain the element which will be displaced first). Here, P_c is the absolute value. Since the sign is taken into account in equation (6).

3. Displace this matrix element and write this value of ΔP_{nw} - P_c to the pressure file.

4. Calculate ΔP_{nw} - P_c respectively for each of four matrix elements around this displaced element, then compare the values of ΔP_{nw} - P_c and determine if these four elements have values of ΔP_{nw} - P_c which will indicate movement. If not, go back to step 3.2.4.1. If so, check if these elements which are candidates for infiltration are trapped. If trapped; they will not be filled, go back to step 3.2.4.1. If the pores are not trapped, displace fluid into these elements. For each displaced element, repeat this step until no further displacement occurs at this pressure. Calculate the saturation at this pressure.

5. Go back to step 3.2.4.1, repeat above procedures until the desired limit of pressure is achieved.

The size distribution matrix used in this model is the combined pore size and tube size matrix. Under the condition that the most wetting fluid is advancing, this matrix can be simplified to be only the pore size matrix since both pressure and saturation can be calculated from pore-size.

Chapter 4. Two-dimensional Model Results

In this chapter, a two-dimensional pore-scale network model was tested. The objectives were: (1) Compare the results from single layer sand media to those from double layer bedded sand media. For single layer sand media, fine sand occupies the whole domain. For bedded sand media, fine sand occupies the top layer and coarse sand occupies the bottom layer. (2) Compare the results for small domains (10 x 5 pores) to those for larger domains (up to 100 x 50 pores). (3) Compare the results for different oils (soltro-220 vs. mineral oil). (4) Compare the results from different infiltration processes (water-air-oil-air vs. oil-air-water-air).

4.1 Capillary Pressure-saturation Relationships

4.1.1. Single Layer Sand Media with Water-air-water-air-water-air Infiltration Processes

Model domains were set up with dimensions of 10 x 5 or 100 x 50 pores filled with fine sand. Water was first infiltrated into the initially dry domain from the water reservoir at the upper surface until only trapped air filled pores remained free of water. Next, air was infiltrated to the domain from the bottom air reservoir. These processes were repeated two more times. The simulation results are shown in Figures 8 and 9.

As shown in Figure 8, at the pressure of -16.05 cmH_2O, water started to infiltrate the domain until reached the maximum saturation of 0.64, then air was infiltrated, with entry at the pressure of -114.36 cmH_2O continuing until the residual

saturation of 0.09 was reached at a pressure of -162.61 cmH_2O. The second infiltration started at the pressure of -16.05 cmH_2O and reach the maximum saturation of 0.61 at -11.75 cmH_2O, then drained starting at the pressure of -114.36 cmH_2O and reached the residual saturation of 0.15 at a pressure of -162.61 cmH_2O. The third infiltration was observed to repeat the same path with the second infiltration. As can be readily seen, the second infiltration achieves a lower maximum saturation than the first infiltration. This can be understood by noting that during each infiltration, water can only infiltrate non-trapped air filled pores. Those pores which become trapped in the second infiltration process increase the total volume of trapped air, thus decreasing the maximum saturation. It is noted that there is a significant pressure jump between wetting and draining process. This is due to the assumption that mean pore sizes are ten times larger than mean tube sizes. There is also a crossing between the hysterestic loops of the first infiltration and the second infiltration.

Figure 9 shows features similar to those obtained from the small domain, except much lower maximum saturation (0.33). The residual saturation increased in comparison to the small domain. As observed in the Figure 8, the third infiltration again followed the same path as the second infiltration. This phenomena may be caused by the dimension effect, as this was not observed in the results from the three-dimensional models.

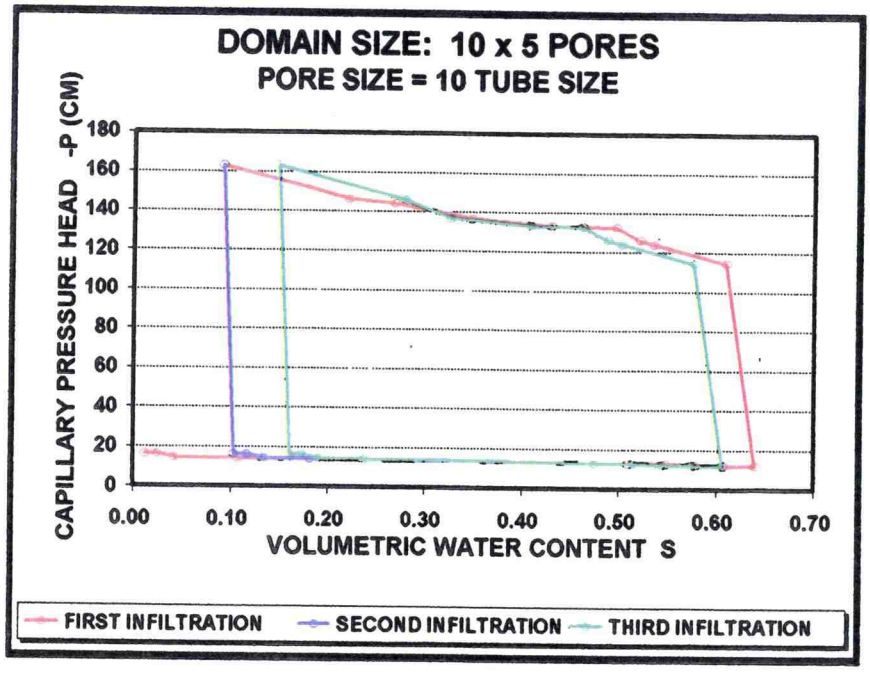

Figure 8. W-A-W-A-W-A capillary pressure-saturation scanning curves for single layer sand media with the size of 10 x 5 pores.

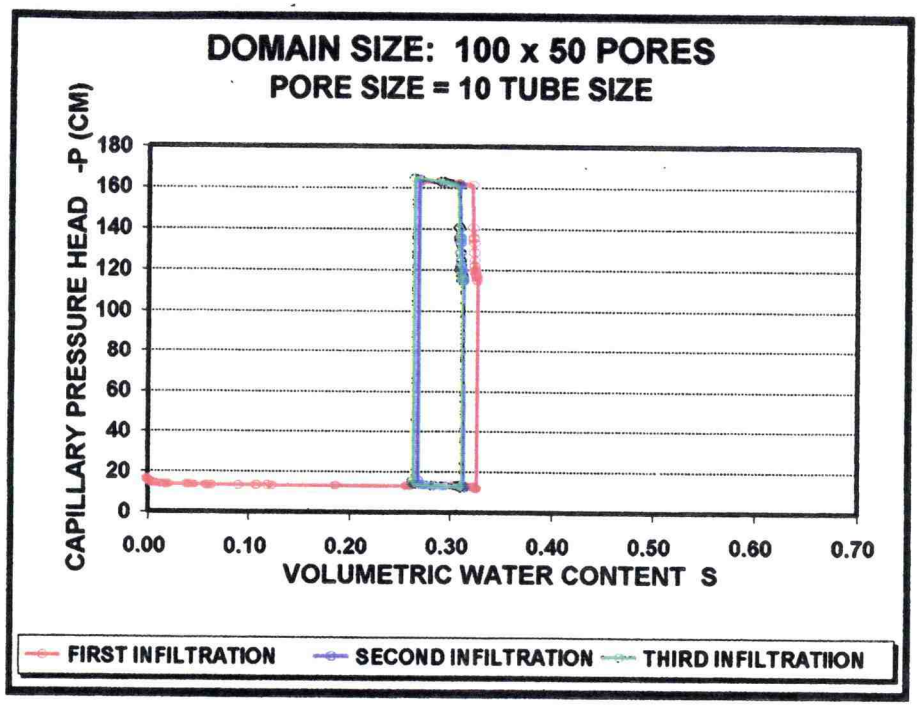

Figure 9. W-A-W-A-W-A capillary pressure-saturation scanning curves for single layer sand media with the size of 100 x 50 pores.

4.1.2. Double Layer Sand Media with Water-air-water-air-water-air Infiltration Processes

Model domains were set up with dimensions of 10 x 5 and 100 x 50 pores with top layer occupied by fine sand and bottom layer occupied by coarse sand. The infiltration processes are the same as those stated in section 4.1.1. The simulation results are shown in Figures 10 and 11.

As shown in Figure 10, at the pressure of -16.05 cmH_2O, water was infiltrated into the domain. When water was infiltrated to the intermediate boundary from fine sand to coarse sand, a pressure jump occurred from -12.73 cmH_2O to -4.64 cmH_2O. The infiltration was stopped when water reached the maximum saturation of 0.55. Next, air was infiltrated to the domain at the pressure of -32.15 cmH_2O. There was a pressure jump from -43.42 cmH_2O to -131.26 cmH_2O occurred at the intermediate boundary from coarse sand to fine sand. The air infiltration continued until reached the residual saturation of 0.25. The second infiltration started at the pressure of -16.05 cmH_2O. After water reached the intermediate boundary, the infiltration path was observed to repeat the same path as the first infiltration. The third infiltration was observed to follow the same path with the second infiltration. This may be caused by the size and dimension effect.

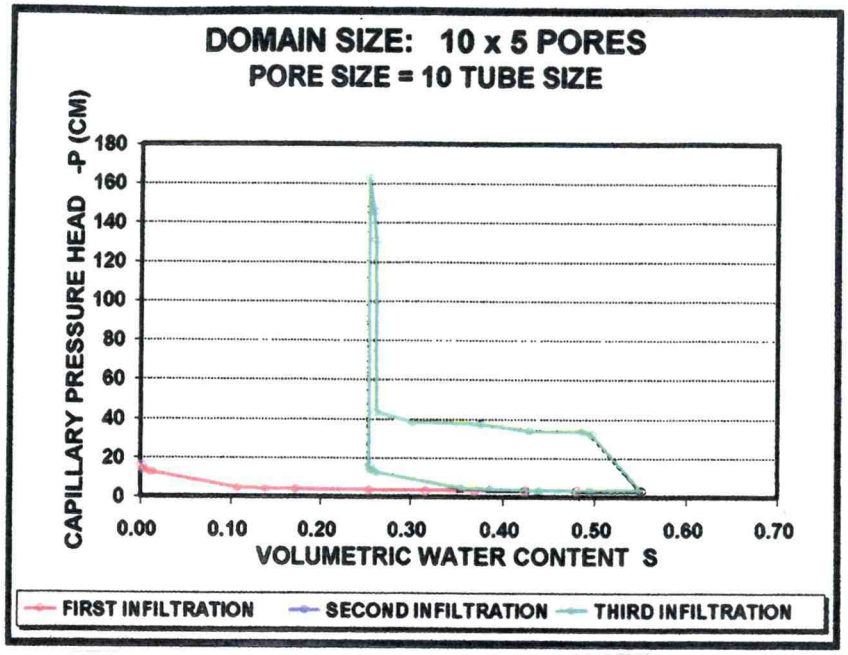

Figure 10. W-A-W-A-W-A capillary pressure-saturation scanning curves for double layer sand media with the size of 10 x 5 pores.

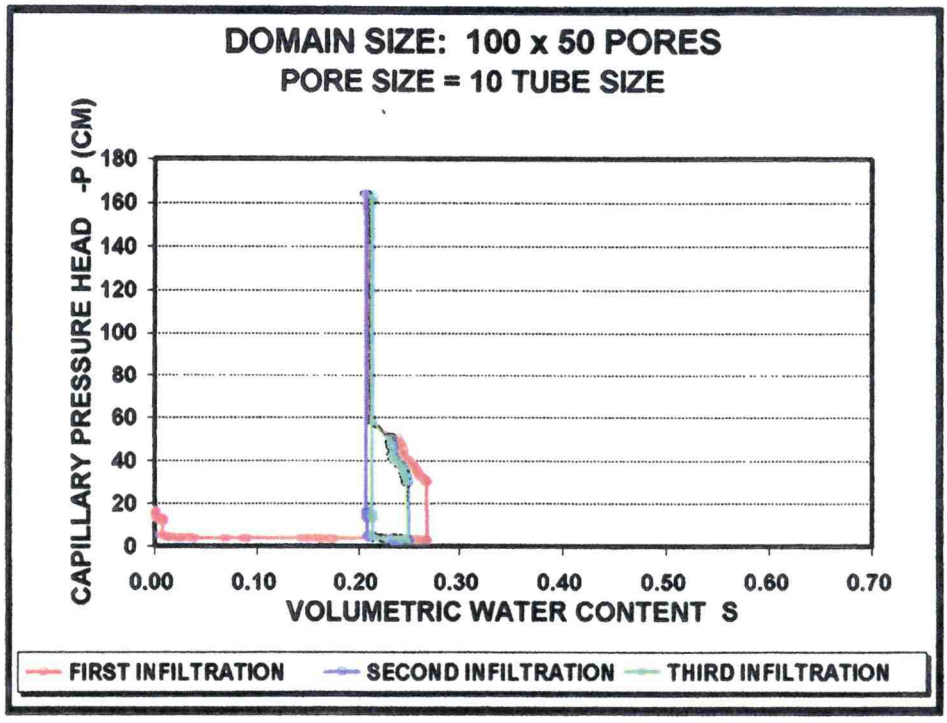

Figure 11. W-A-W-A-W-A capillary pressure-saturation scanning curves for double layer sand media with the size of 100 x 50 pores.

Figure 11 shows the similar behavior as in Figure 10 except that maximum saturations were smaller. The path of the third infiltration was again observed to follow the second infiltration, however, the path of the second infiltration did not follow the first infiltration. This again demonstrated that this path repeating may be caused by the size and dimension effect or the boundary effect.

4.1.3. Double Layer Sand Media with Water-air-oil-air Infiltration Processes

Model domains are the same as those stated in section 4.1.2. Water was first infiltrated into the initially dry domain from the top water reservoir and drained by infiltration of air from the bottom air reservoir. Next, oil was infiltrated from the top oil reservoir and then drained by air infiltration from the bottom.

Figure 12 shows that during the soltrol-220 infiltration, the minimum air content increased compared to the water infiltration in Figure 10 (from 0.45 to 0.52). This is because more air is trapped during oil infiltration. The values of the pressure head were also lower than those in the Figure 10 during the second infiltration. This is due to the larger interfacial tension of water-air than that of oil-air. Figure 13 shows the similar relationship except higher minimum air content.

As would be expected from inspection of the governing equations for the network model, the mineral oil results are identical to those of soltrol-220 shown in Figures 12 and 13, but with scaled pressure values during oil infiltration and draining due to the differences in interfacial tension. An example of mineral oil infiltration is shown in Figure 14. These findings do not correspond to the experimental results obtained by

Simmons, et al. (1986), where soltrol-220 and mineral oil did act differently during the infiltration. We believe that the discrepancy resulted from the assumption that film flow could be neglected. The spreading oil is known to have greater film flow than the non-spreading oil. With our assumption, the spreading oil acts like the non-spreading oil, which will be seen clearly in the graphs of fluid distribution in a later section. This feature is one of the major limitation of this model, however inclusion of film flow is conceptually at odds with basic notion of network modeling methods as the fluid pressure along the film is not well defined, nor is the limit of film extent.

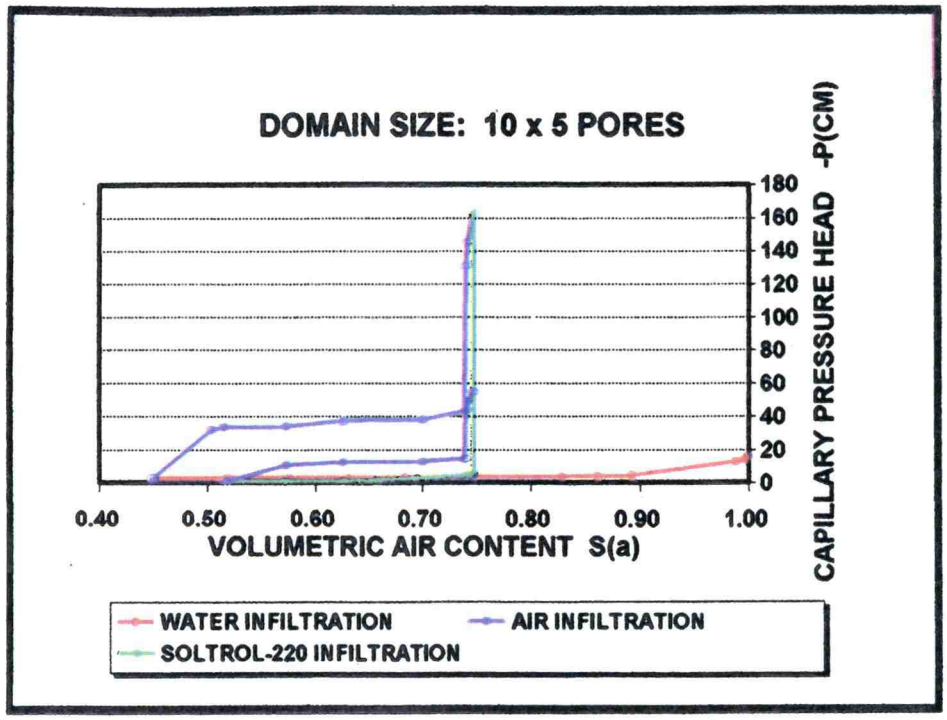

Figure 12. W-A-O-A capillary pressure-saturation scanning curves for double layer sand media with the size of 10 x 5 pores (soltrol-220).

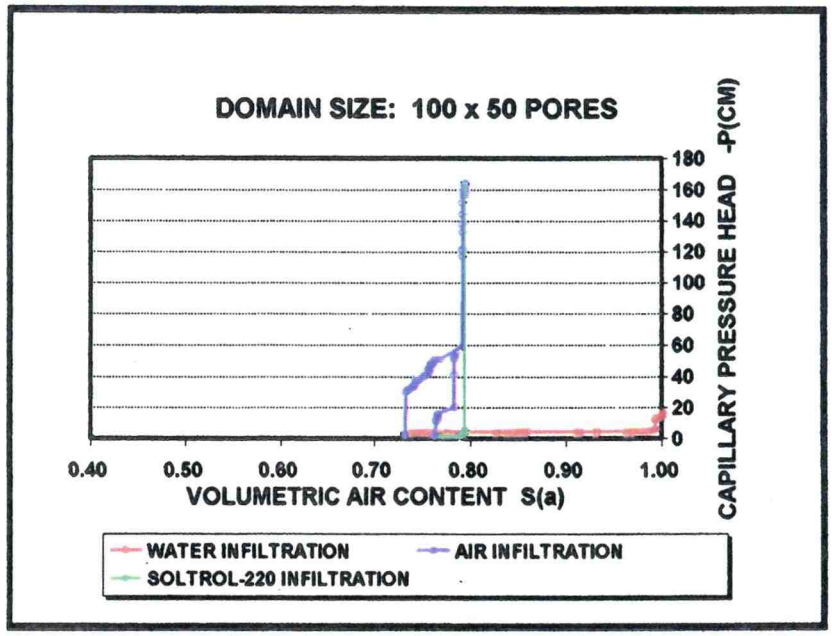

Figure 13. W-A-O-A capillary pressure-saturation scanning curves for double layer sand media with the size of 100 x 50 pores (soltrol-220).

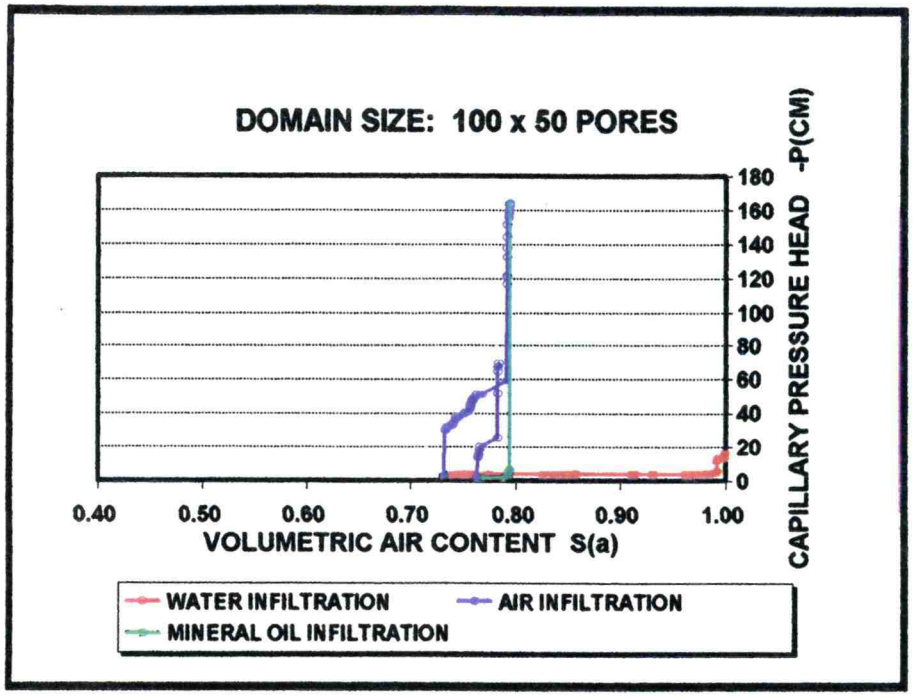

Figure 14. W-A-O-A capillary pressure-saturation scanning curves for double layer sand media with the size of 100 x 50 pores (mineral oil).

4.1.4. Double Layer Sand Media with Oil-air-water-air Infiltration Processes

Model domain settings for this series of experiments were the same as those employed in last section. The infiltration sequence was oil-air-water-air for both kind of oil --- soltrol-220 and mineral oil. The simulation results for soltrol-220 are shown in Figures 15 and 16.

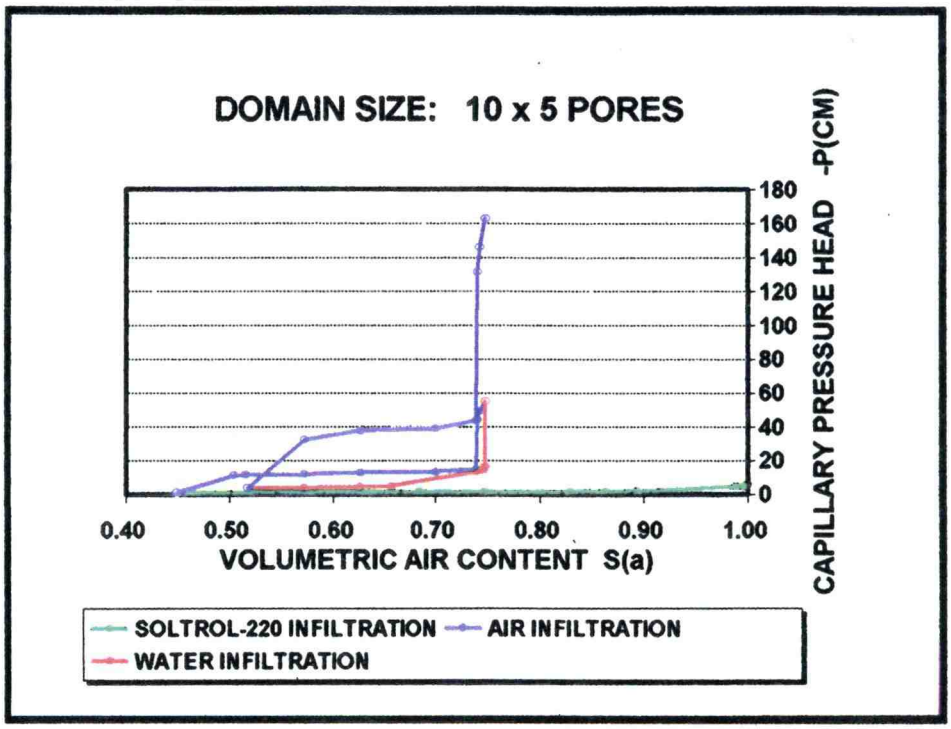

Figure 15. O-A-W-A capillary pressure-saturation scanning curves for double layer sand media with the size of 10 x 5 pores (soltrol-220).

It can be observed that Figure 15 and 16 have the same saturation for each intermediate steps as those in Figure 12 and 13 respectively, but have different pressure values. This difference is due to different surface tension when different fluids occur at interface. As before, the results for mineral oil were identical to those of soltrol-220

except for scaling the oil pressure by the ratio of the surface tension of mineral oil to soltrol-220.

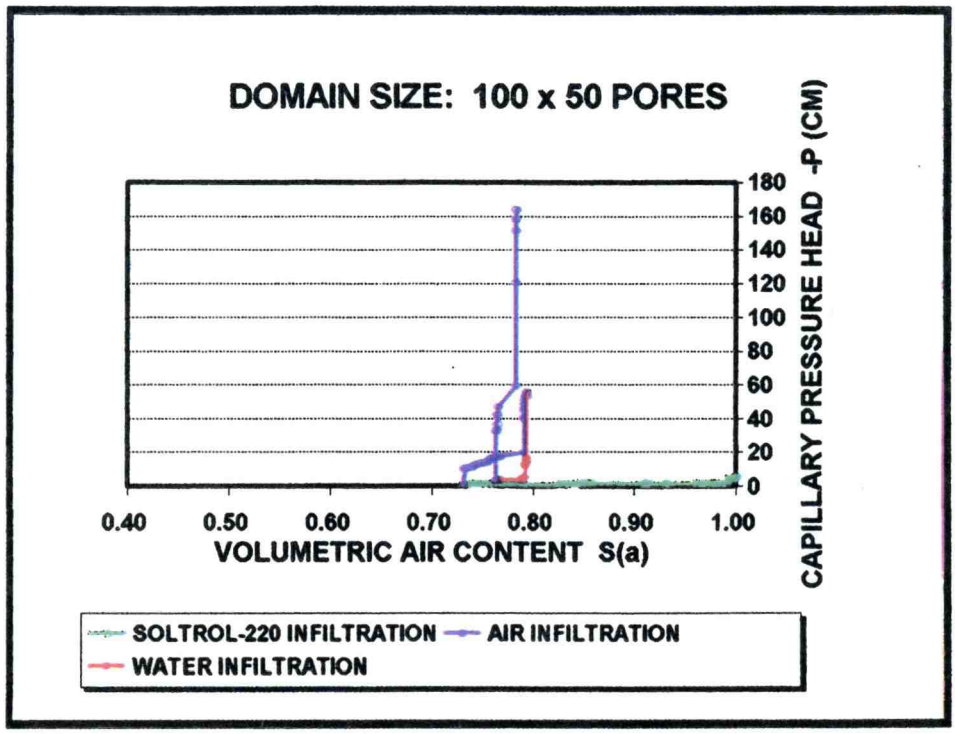

Figure 16. O-A-W-A capillary pressure-saturation scanning curves for double layer sand media with the size of 100 x 50 pores (soltrol-220).

4.2 Fluid Distribution

4.2.1. Single Layer Sand Media with Water-air Infiltration Processes

Model domain settings and infiltration processes are the same as those described in section 4.1.1. The simulation results are presented in Figures 17, 18, 19, and 20.

Figures 17 and 18 show the intermediate distribution of fluid during wetting and draining respectively for the domain size of 10 x 5 pores and Figures 19 and 20 for the

domain size of 100 x 50 pores. During water infiltration, water was infiltrated into the domain step by step until reached the air reservoir. During air infiltration, air was infiltrated step by step. Since air infiltration is a tube-controlled process, fluid trapped in tubes was the primary trapping-mechanism which occurred, although not specifically shown on these graphs. Also, we did not consider the moving trapped areas. If any trapped air area was developed in water infiltration, it would stay trapped during air infiltration. This can be seen more clearly in the water-air-oil-air experiments discussed in a later section. It was notable that in each experiment there are areas of trapped air developing with linear extent which is of the same scale as the domain. There are similar areas of trapped water when drained (Figure 20).

4.2.2. Double Layer Sand Media with Water-air Infiltration Processes

Model domain settings and infiltration processes are the same as described in section 4.1.2. The simulation results are presented in Figures 21, 22, 23, and 24.

Figure 21 and 23 show that wetting fluid will fill fine sand first followed by infiltration into coarse sand. As described in section 3.1, wetting fluid will displace the non-wetting fluid from the smallest radius aperture along the fluid interface. Fine sand has smaller pore sizes, thus those pattern showed in Figure 21 and 23 demonstrate the principle we stated before. Again, there are areas of trapped air occurring with the length of the same scale as the domain. This phenomena, which is not seen in physical porous media, is a limitation of two-dimensional network models which is not seen in the results from three-dimensional model runs.

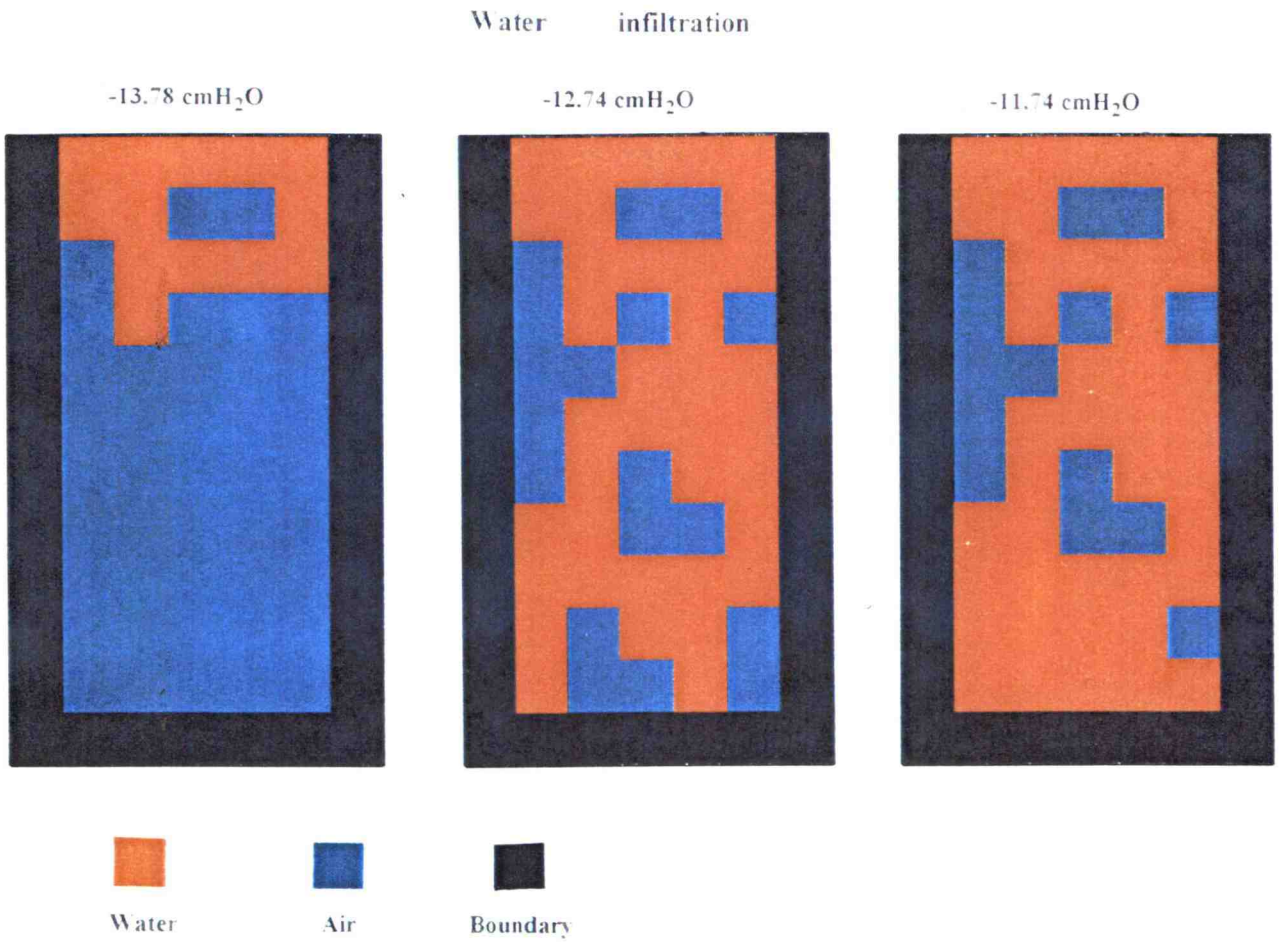

Figure 17 Fluid displacement of water infiltration for single layer sand media with domain size of 10 x 5 pores

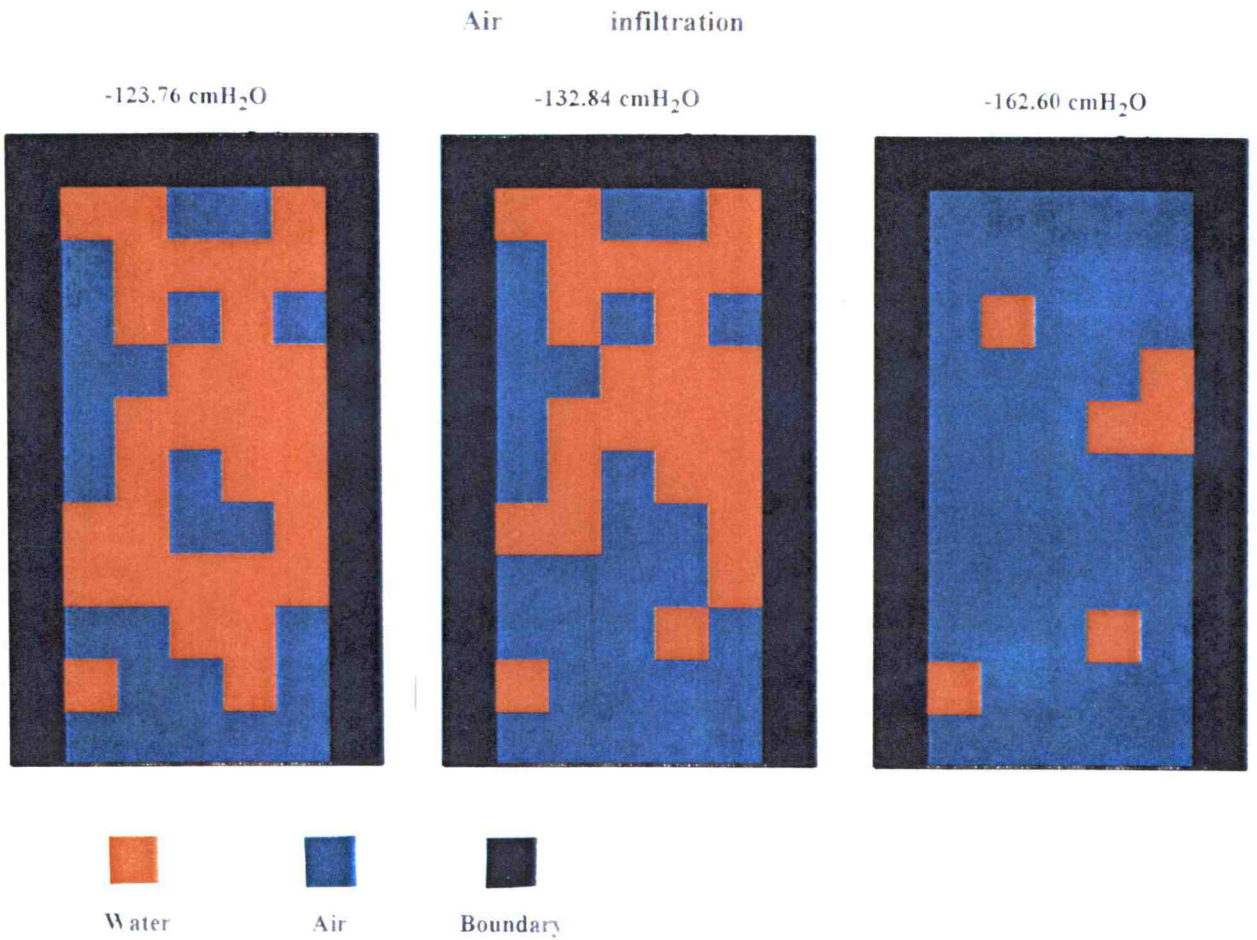

Figure 18 Fluid displacement of air infiltration for single layer sand media with domain size of 10 x 5 pores

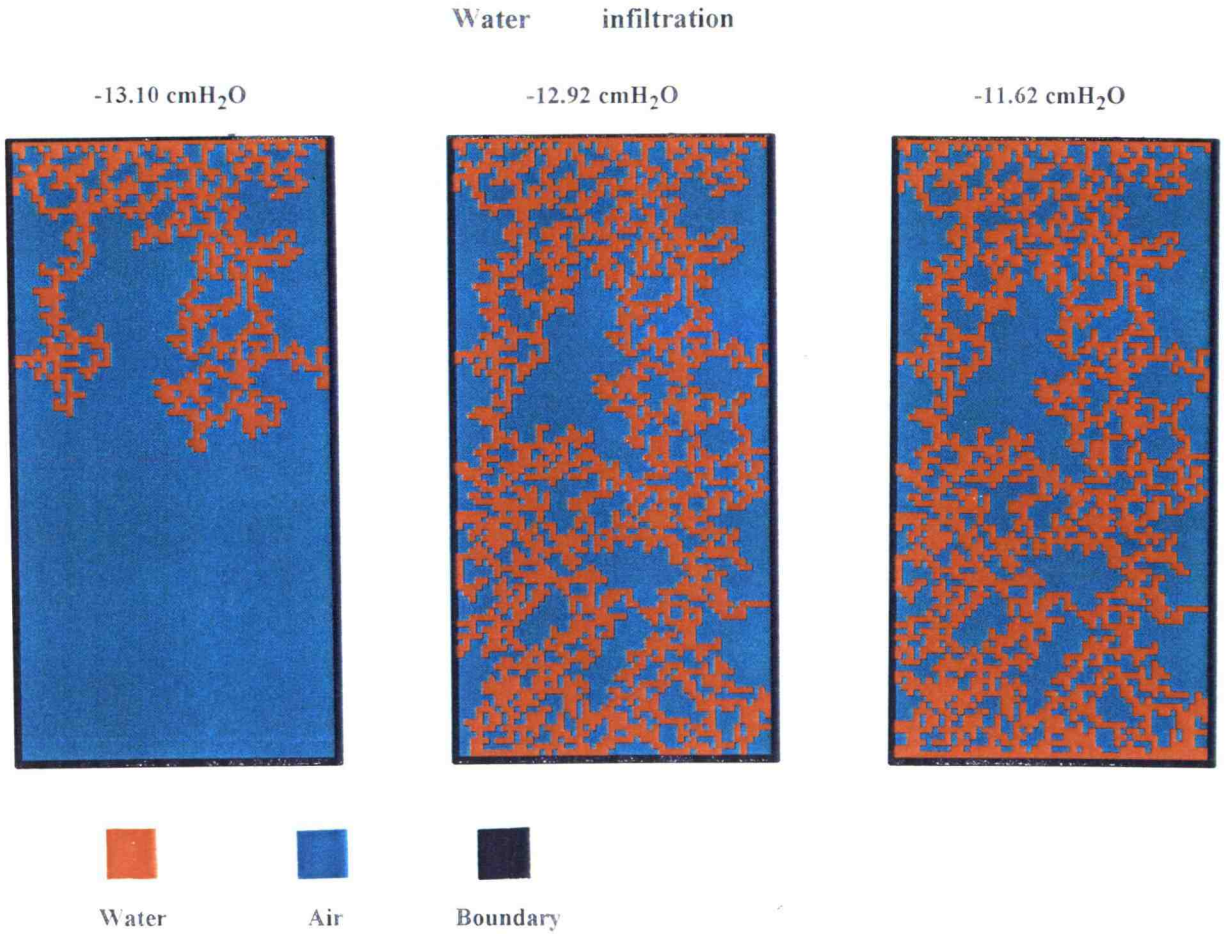

Figure 19. Fluid displacement of water infiltration for single layer sand media with domain size of 100 x 50 pores

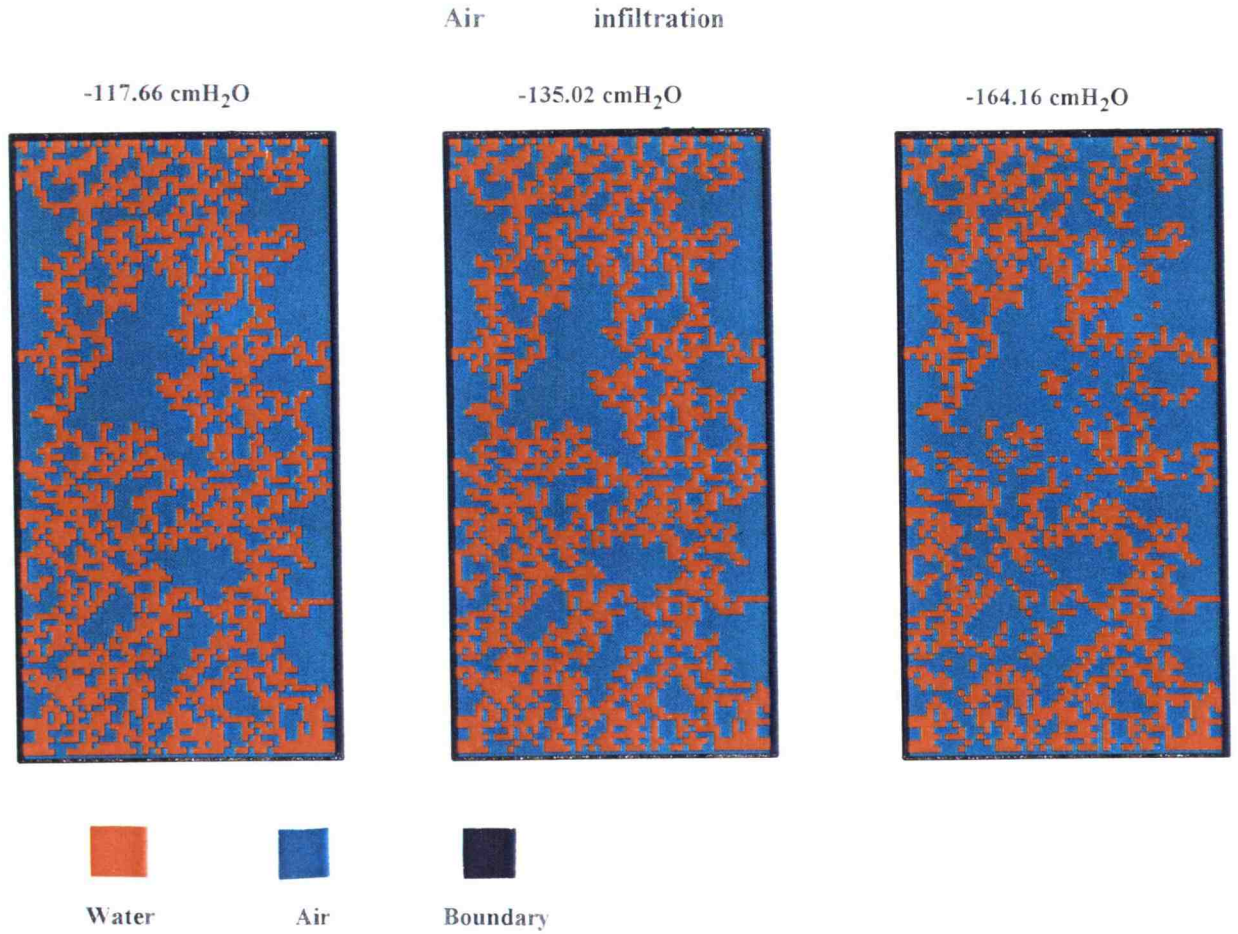

Figure 20. Fluid displacement of air infiltration for single layer sand media with domain size of 100 x 50 pores.

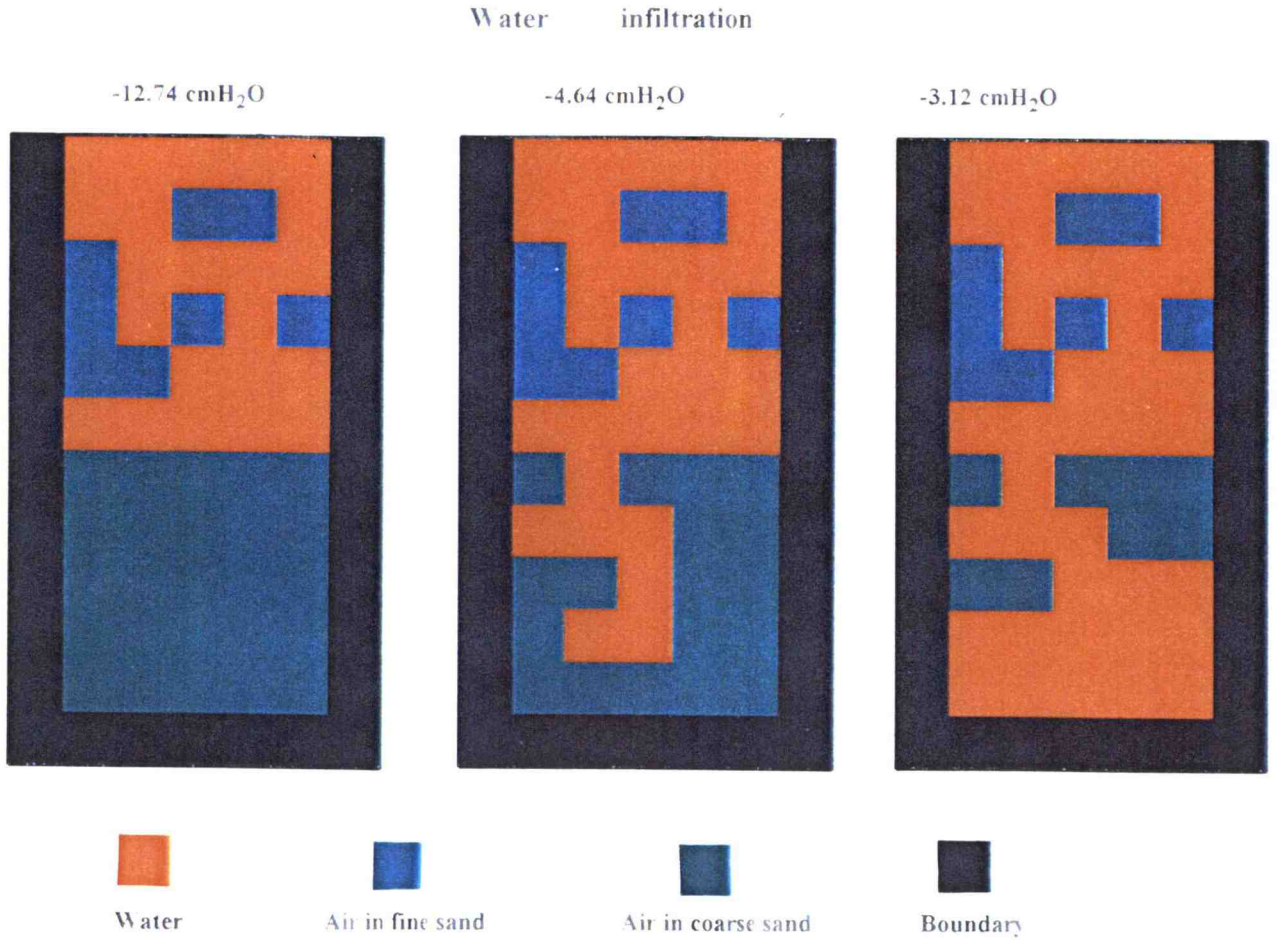

Figure 21 Fluid displacement of water infiltration for double layer sand media with domain size of 10 x 5 pores

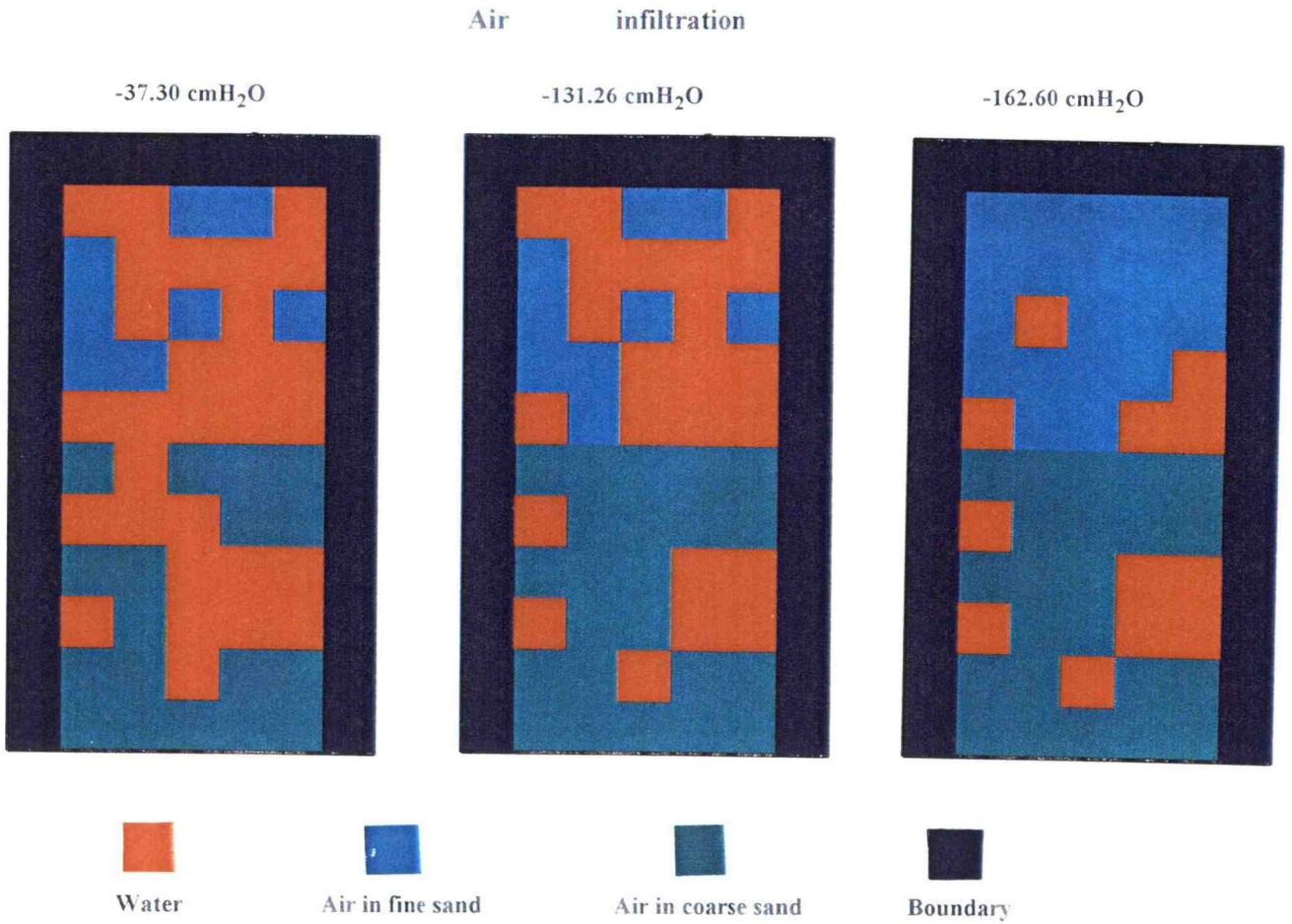

Figure 22 Fluid displacement of air infiltration for double layer sand media with domain size of 10 x 5 pores

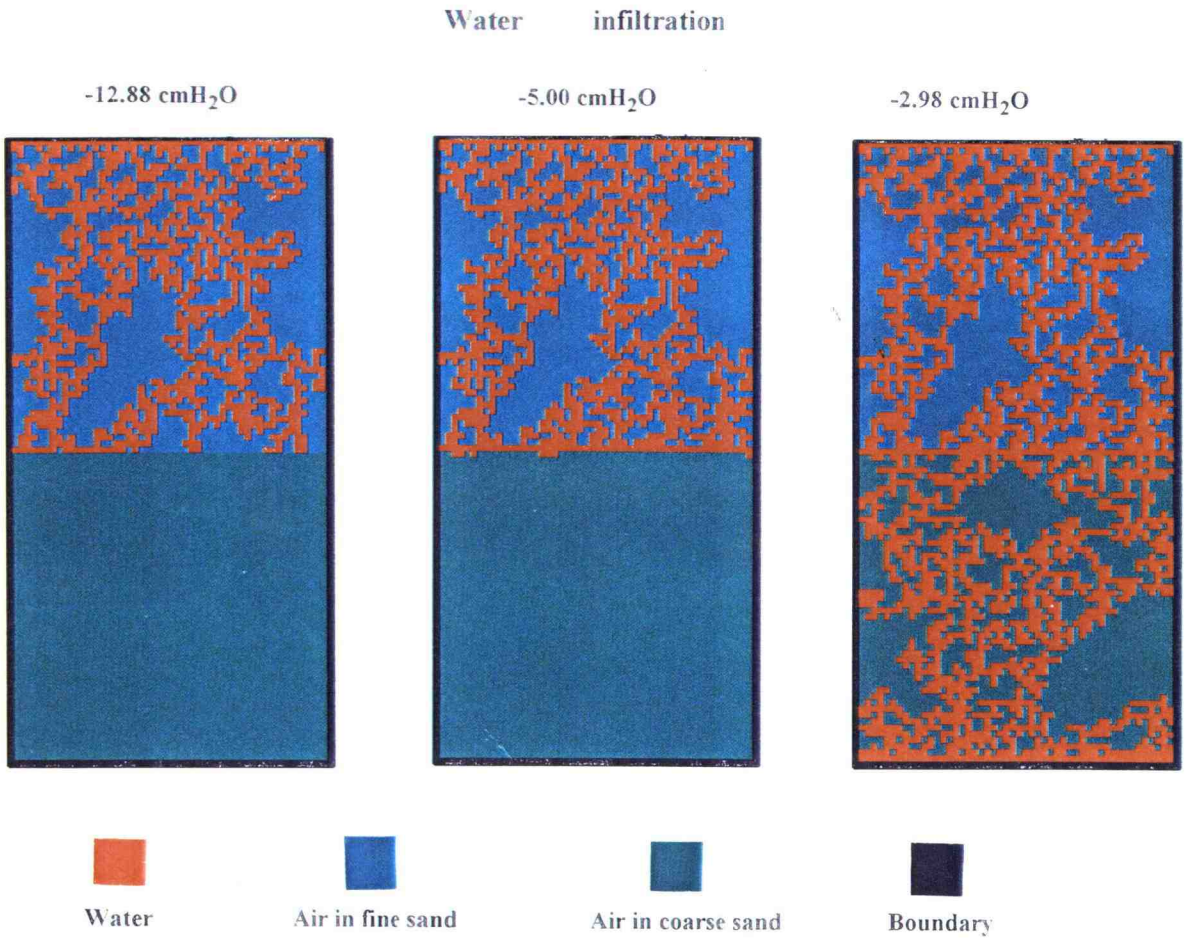

Figure 23. Fluid displacement of water infiltration for double layer sand media with domain size of 100 x 50 pores

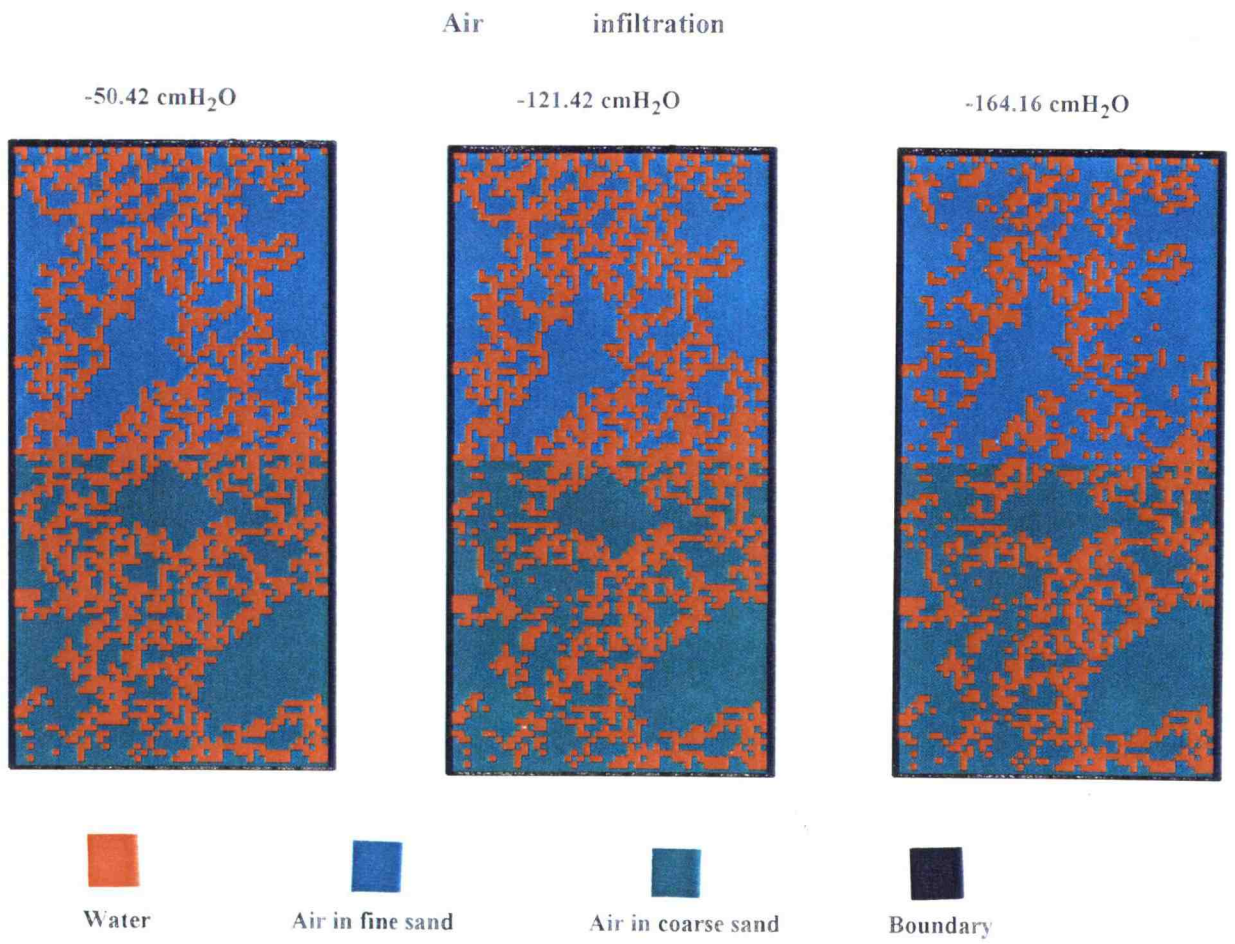

Figure 24 Fluid displacement of air infiltration for double layer sand media with domain size of 100 x 50 pores

4.2.3. Double Layer Sand Media with Water-air-oil-air Infiltration Processes

Model domain settings and infiltration processes are the same as described in section 4.1.3. The fluid distribution pattern of oil infiltration and draining are presented in Figures 25 26, 27, and 28.

Figures 25 and 27 show that, when oil infiltration takes place into media with residual water, infiltration is constricted to isolated fingers, similar to that seen experimentally with non-spreading NAPLs by Simmons et al. (1986). This indicates the fundamentally notable nature of non-wetting fluids displacing wetting fluids. Even though soltrol-220 is a spreading oil, however, film flow was not considered in this model, which is the major difference between spreading and non-spreading oil. Figure 28 shows that when oil is drained, trapped oil remains in the domain. No oil was trapped in the 10 x 5 pores network, this appears to be due to the small size of the domain. As shown in Figure 28, it is noted that the remaining oil fingers seemed connecting to the reservoir, however, they were not on the wetting front. Because no non-trapping air (advancing fluid) was touched to these non-trapping oil (resident fluid). As mentioned in an earlier section, all trapped air developed in previous processes will remain trapped in the next process. There are large amount of trapped air remaining in the domain, although sometimes it can not be seen clearly in the graphs.

4.2.4. Double Layer Sand Media with Oil-air-water-air Infiltration Processes

Model domain settings and infiltration processes are the same as described in section 4.1.4. The fluid distribution pattern of oil infiltration and draining are identical to

the patterns presented in Figures 21 to 28 with oil and water switching roles. This demonstrates that the sequence of displacements for a particular network pore geometry will be identical for any pair of fluids under the same displacement process.

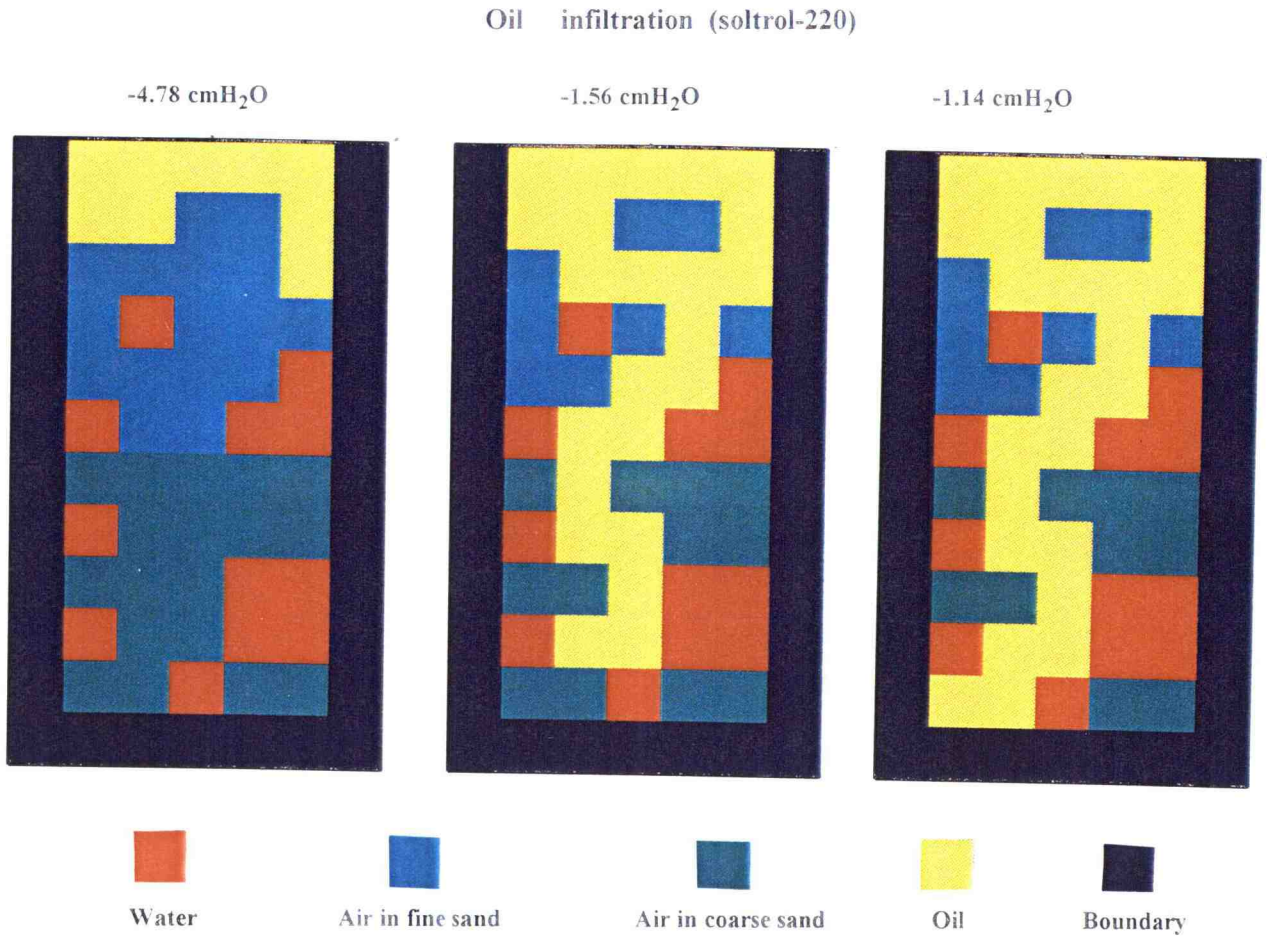

Figure 25. Fluid displacement of oil infiltration for double layer sand media with domain size of 10 x 5 pores.

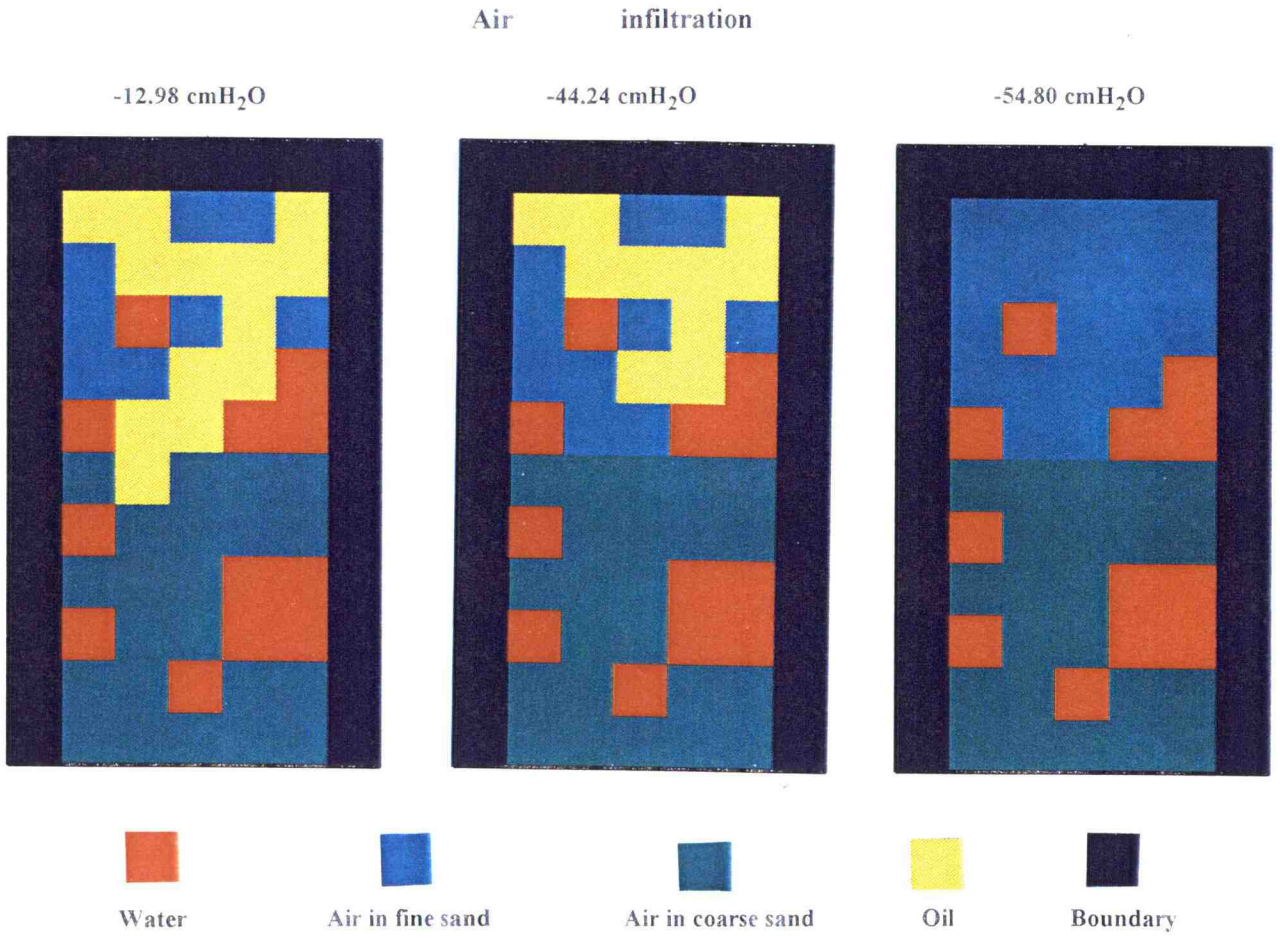

Figure 26. Fluid displacement of air infiltration for double layer sand media with domain size of 10 x 5 pores

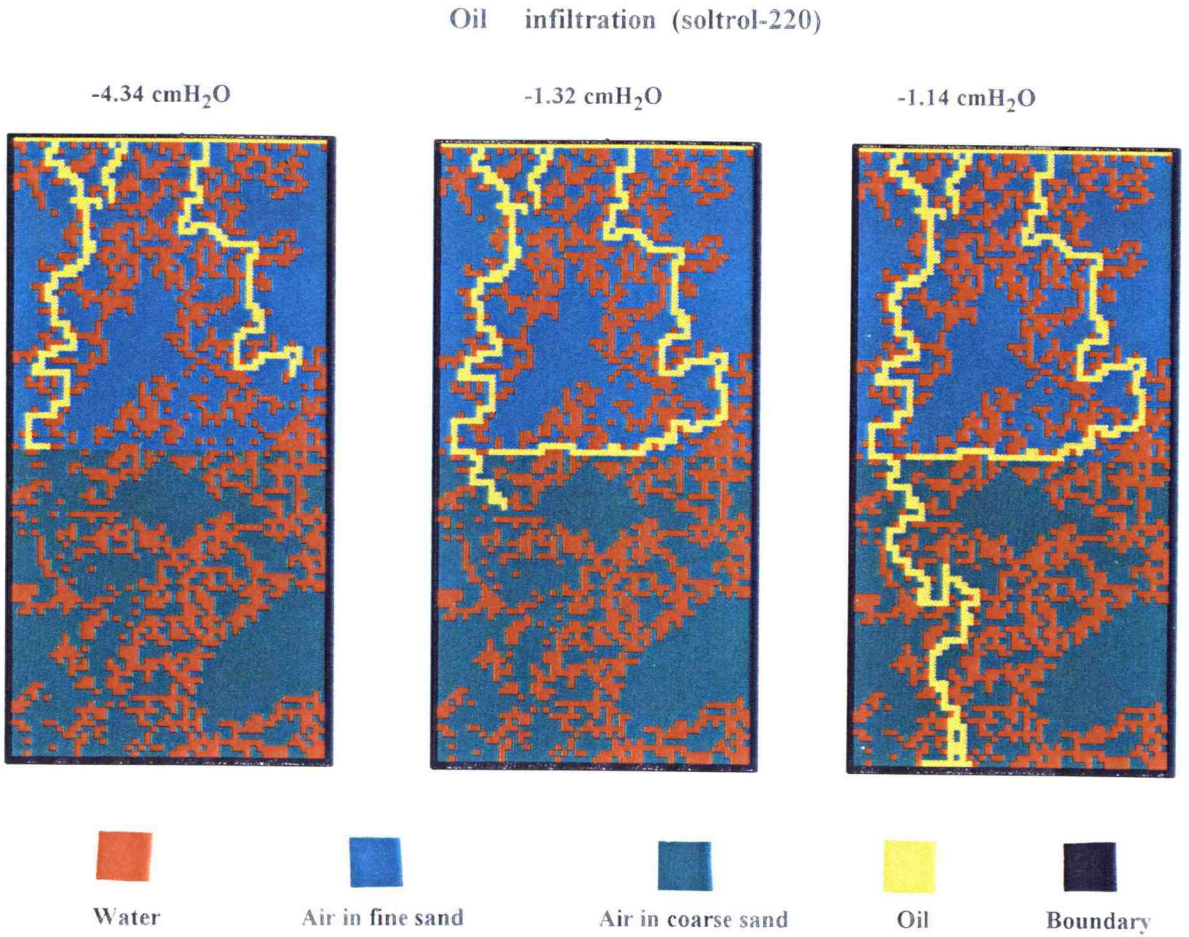

Figure 27 Fluid displacement of oil infiltration for double layer sand media with domain size of 100 x 50 pores

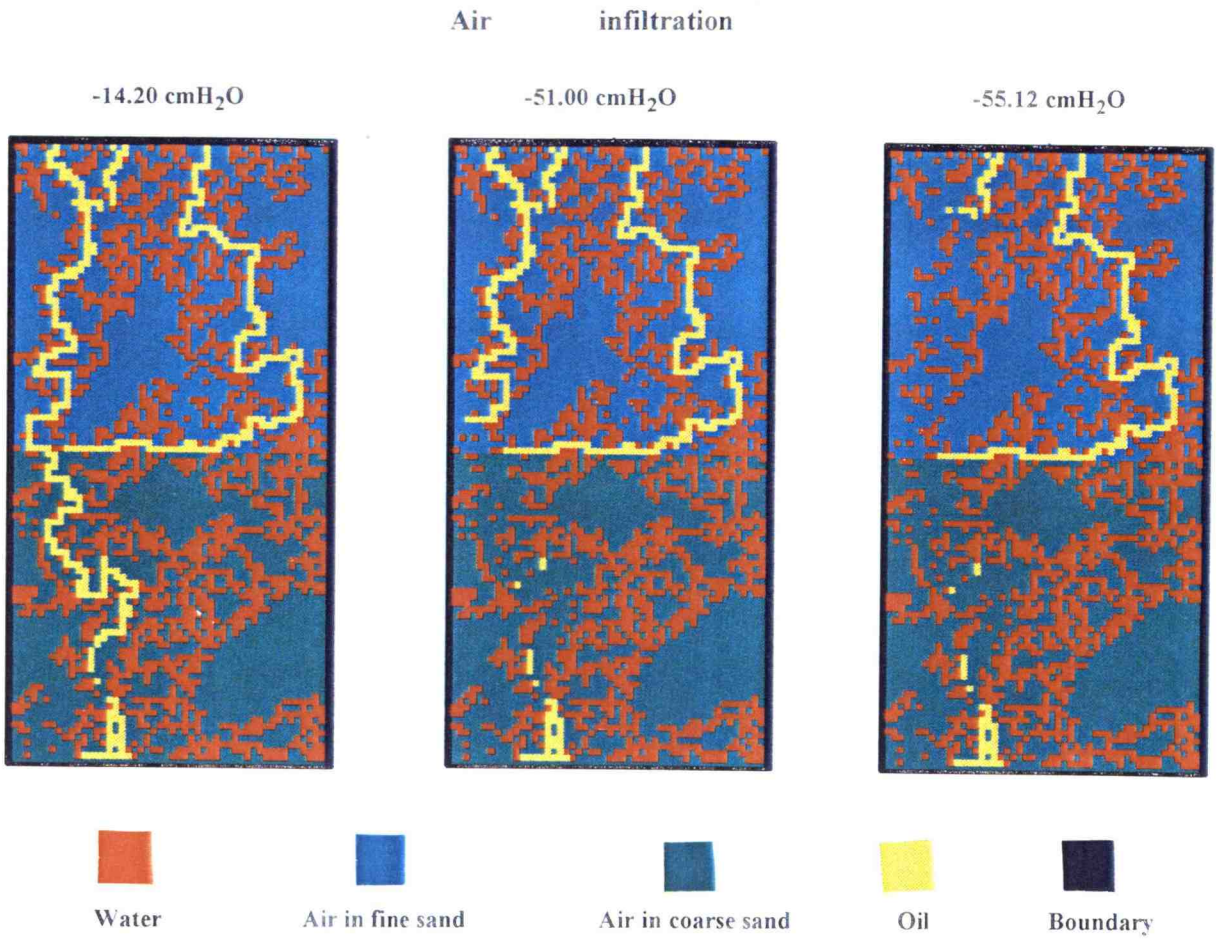

Figure 28 Fluid displacement of air infiltration for double layer sand media with domain size of 100 x 50 pores

Chapter 5. Three-dimensional Model Results

During the simulation with two-dimensional network models, we found areas of trapping pores developing with the domain size. It appears to be the results of the ability to trap pores by simply encribing a group of pores with a line. This behavior does not correspond to experimental results. In this chapter, we will explore the flow behavior in a three-dimensional system.

Our goals for the three-dimensional model run are outlined as: (1) Compare the results from single layer sand media to those from double layer bedded sand media. For single layer sand media, fine sand occupies the whole domain. For bedded sand media, fine sand occupies the top layer and coarse sand occupies the bottom layer. (2) Compare the results from different domain sizes (10 x 5 x 5 pores, 20 x 10 x 5 pores, 40 x 20 x 5 pores, 100 x 50 x 5 pores) to see if the three-dimensional models can overcome the limitations observed in two-dimensional system, and identify a useful representative elementary volume (R.E.V.) for the system. (3) Compare the results from different infiltration processes (water-air-oil-air versus water-air-water-air-water-air).

5.1 Capillary Pressure-saturation Relationships

5.1.1. Single Layer Sand Media with Water-air-water-air-water-air Infiltration Processes

Three model domain sizes, 10 x 5 x 5, 20 x 10 x 5, and 40 x 20 x 5 pores, were employed using the fine sand characteristics. Water first infiltrated the initial dry domain

from the top reservoir until the only air filled pores remaining were trapped. Following this, air was infiltrated through the bottom reservoir. These processes were repeated for a total of three complete cycles. The simulation results are shown in Figures 29 to 31.

Figures 29 and 31 showed some shift between first and second infiltration processes. However, all three graphs showed that the second infiltration has lower maximum saturation than the first infiltration, and the third infiltration has lower maximum saturation than the second infiltration. This finding is similar to that observed in the two-dimensional models except the cycle repeating.

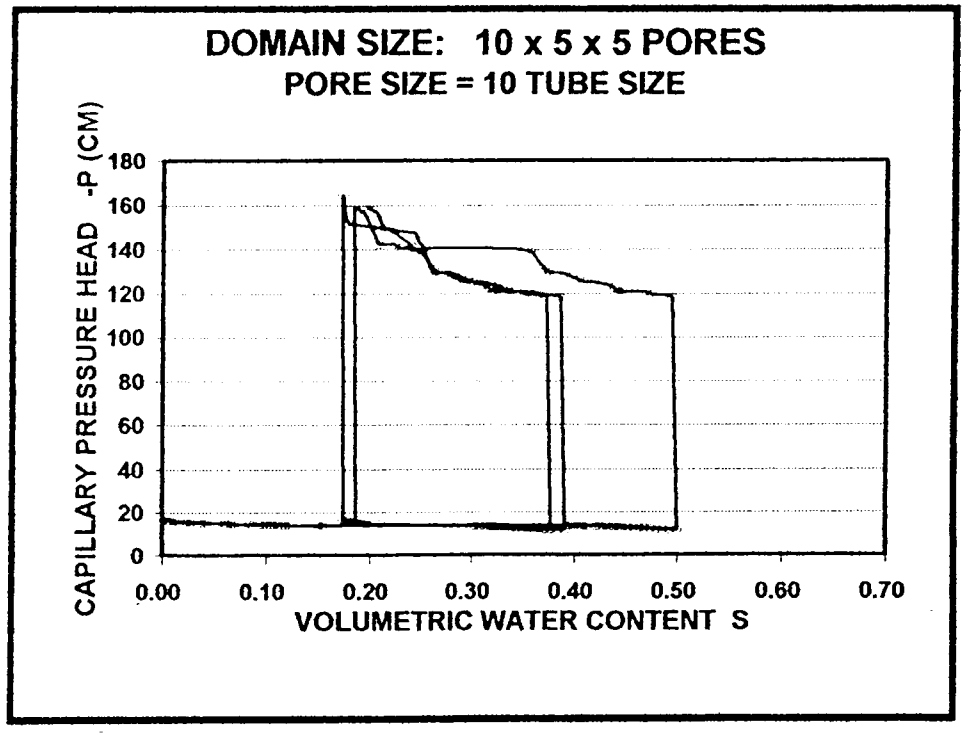

Figure 29. W-A-W-A-W-A capillary pressure-saturation scanning curves for single layer sand media with the size of 10 x 5 x 5 pores.

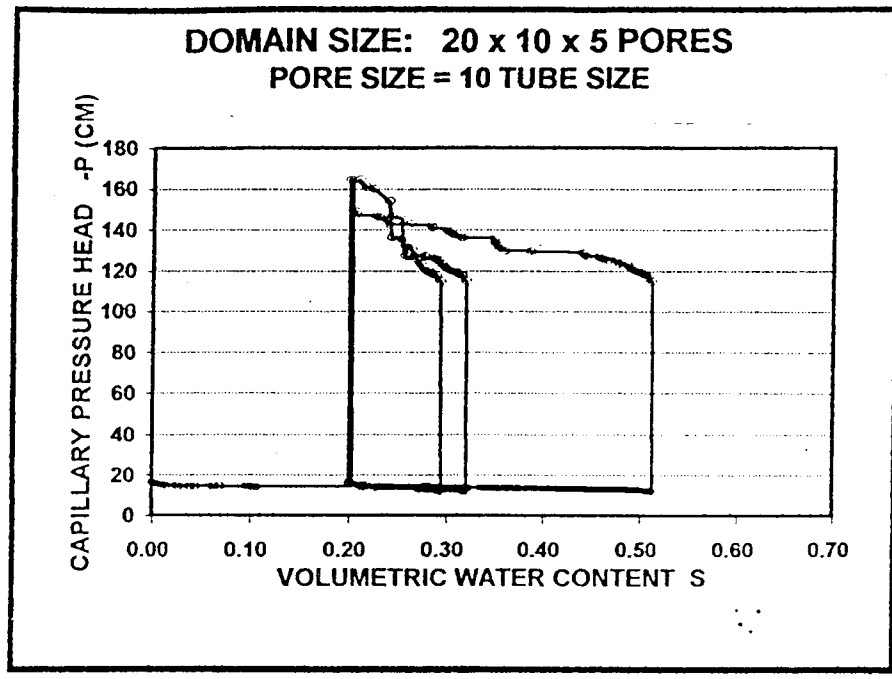

Figure 30. W-A-W-A-W-A capillary pressure-saturation scanning curves for single layer sand media with the size of 20 x 10 x 5 pores.

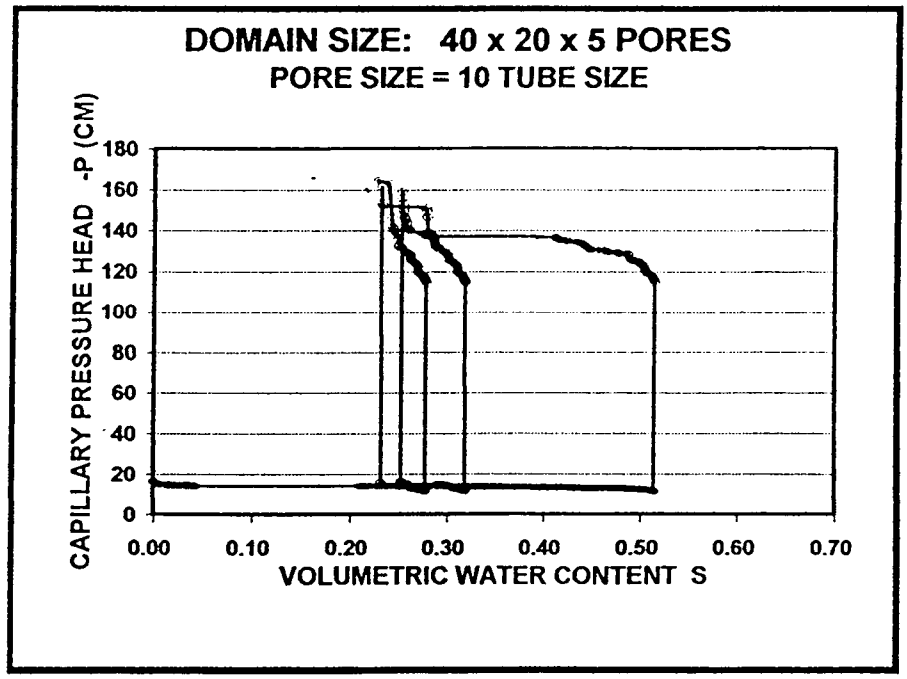

Figure 31. W-A-W-A-W-A capillary pressure-saturation scanning curves for single layer sand media with the size of 40 x 20 x 5 pores.

5.1.2. Double Layer Sand Media with Water-air-water-air-water-air Infiltration Processes

Model domains were set up with 10 x 5 x 5, 20 x 10 x 5, 40 x 20 x 5, and 100 x 50 x 5 pores with top half layer occupied by fine sand and bottom half layer occupied by coarse sand. The infiltration processes are the same as those stated in section 5.1.1. The simulation results are shown in Figures 32 to 35.

The results from small domain sizes (Figures 32 to 34) showed some crossing lines in the system characteristic curves, however, the result from the larger domain (Figure 35) showed no shift between infiltration processes. Figures 32 to 35 also showed that the larger the domain size, the lower the initial maximum saturation.

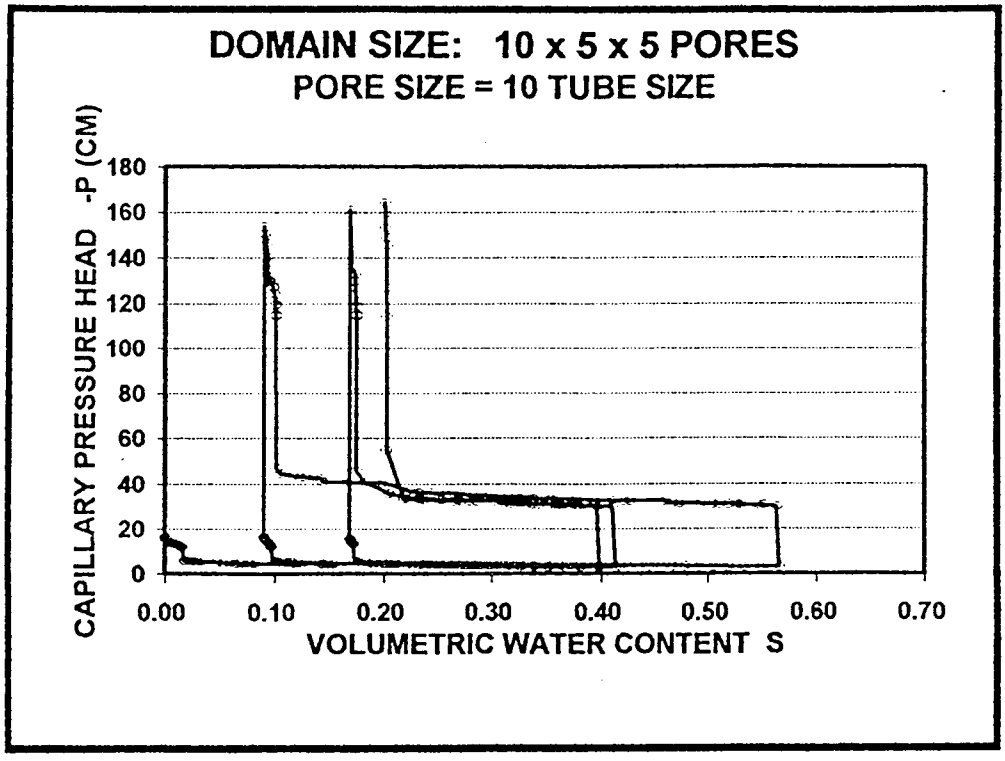

Figure 32. W-A-W-A-W-A capillary pressure-saturation scanning curves for double layer sand media with the size of 10 x 5 x 5 pores.

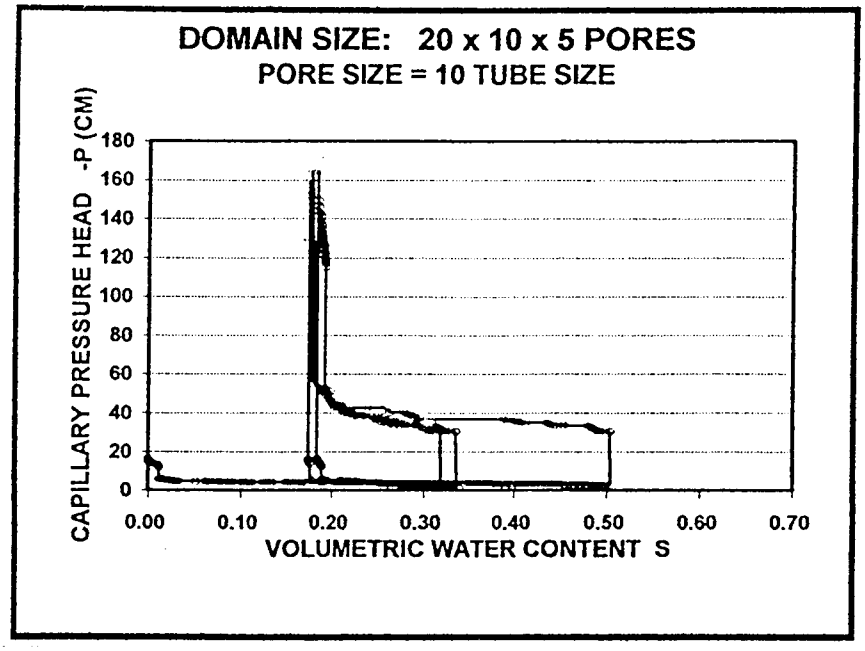

Figure 33. W-A-W-A-W-A capillary pressure-saturation scanning curves for double layer sand media with the size of 20 x 10 x 5 pores.

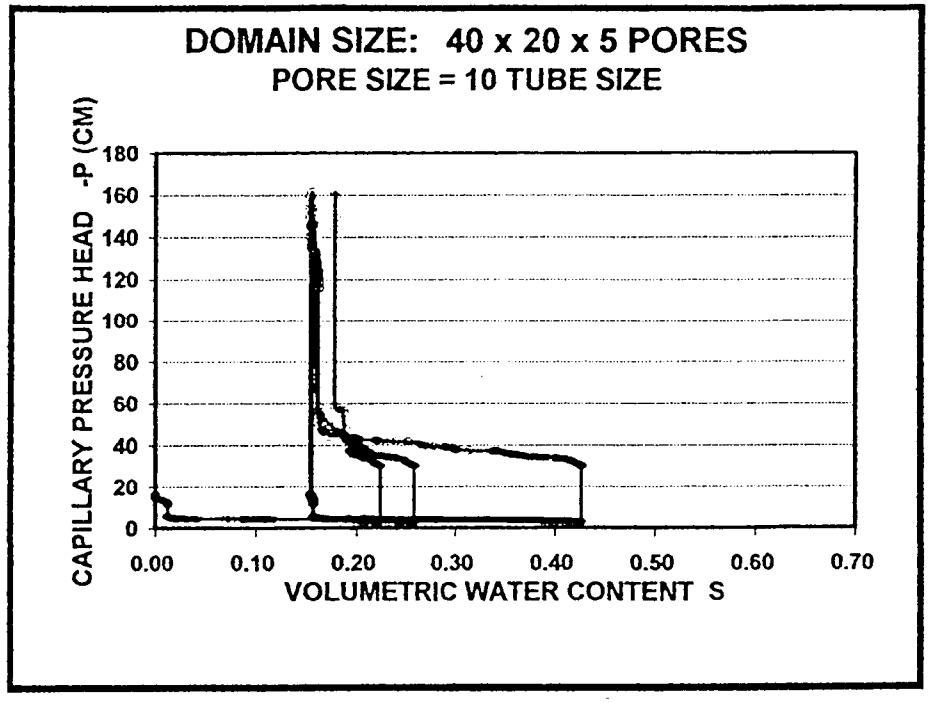

Figure 34. W-A-W-A-W-A capillary pressure-saturation scanning curves for double layer sand media with the size of 40 x 20 x 5 pores.

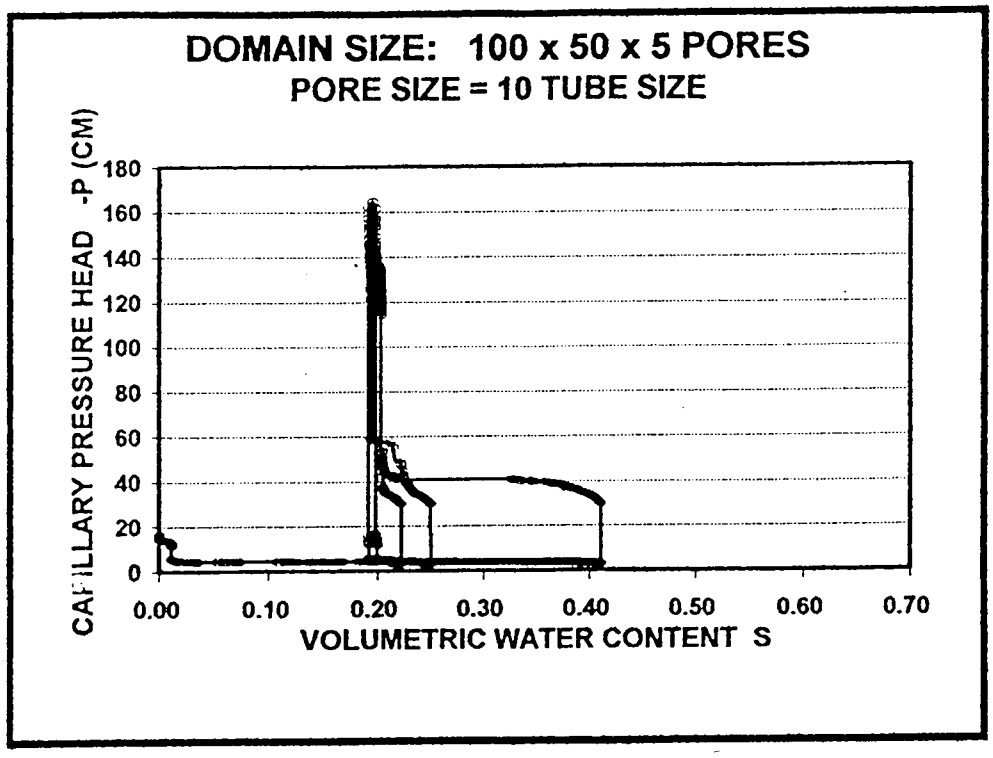

Figure 35. W-A-W-A-W-A capillary pressure-saturation scanning curves for double layer sand media with the size of 100 x 50 x 5 pores.

5.1.3. Double Layer Sand Media with Water-air-oil-air Infiltration Processes

For these simulations the model domains are the same as those stated in section 5.1.2. Water first infiltrated the air filled domain from the top reservoir and was then drained by infiltration of air from the bottom reservoir. Then oil infiltrated the water-wetted domain from the top oil reservoir and drained by air infiltration. We only use soltrol-220 in this run. The simulation results are shown in Figures 36 to 39.

Figures 36 to 39 show that there is lower maximum saturation following the first water infiltration process for larger domains. So does the oil saturation in oil infiltration process.

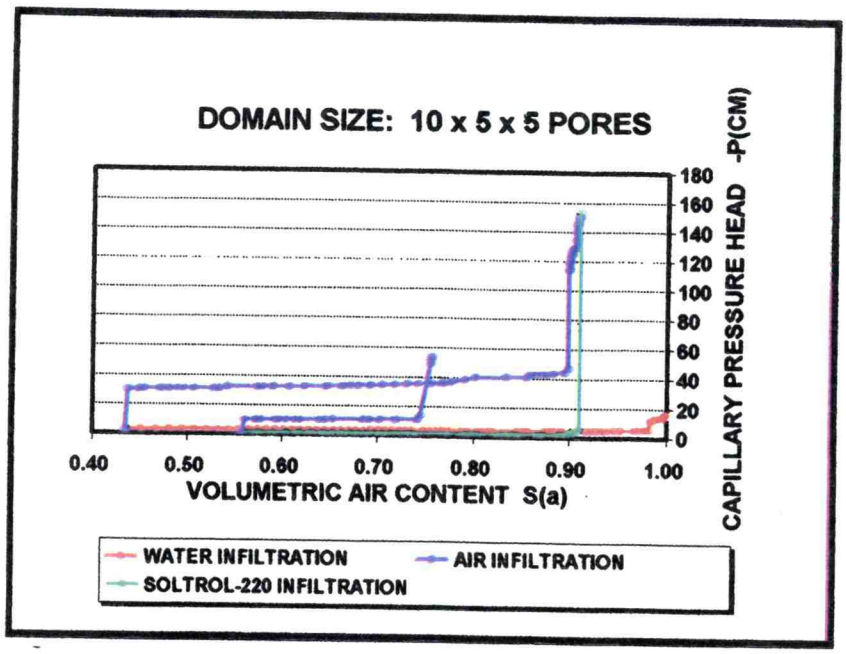

Figure 36. W-A-O-A capillary pressure-saturation scanning curves for double layer sand media with the size of 10 x 5 x 5 pores.

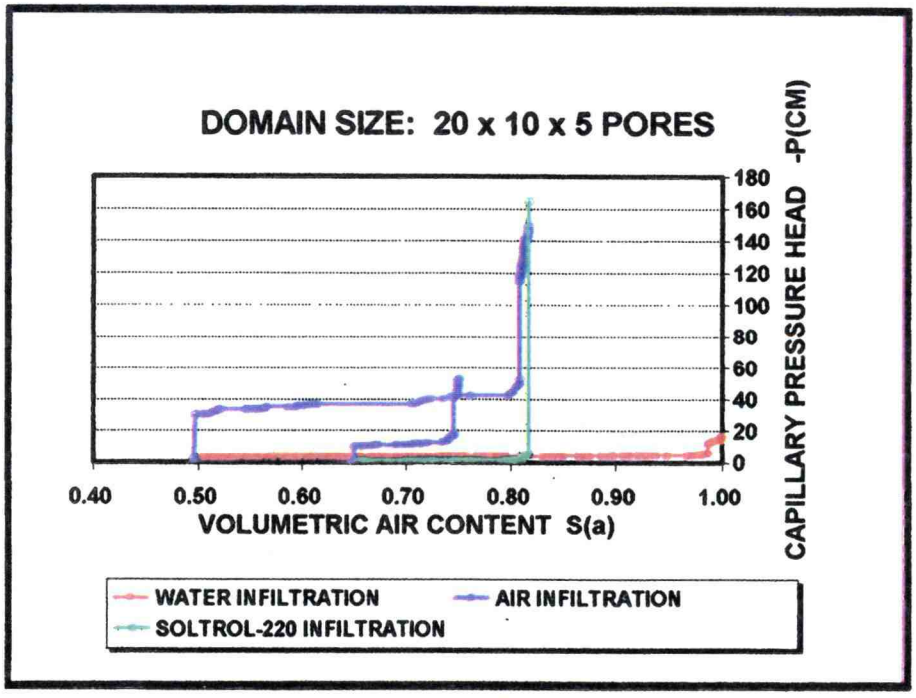

Figure 37. W-A-O-A capillary pressure-saturation scanning curves for double layer sand media with the size of 20 x 10 x 5 pores.

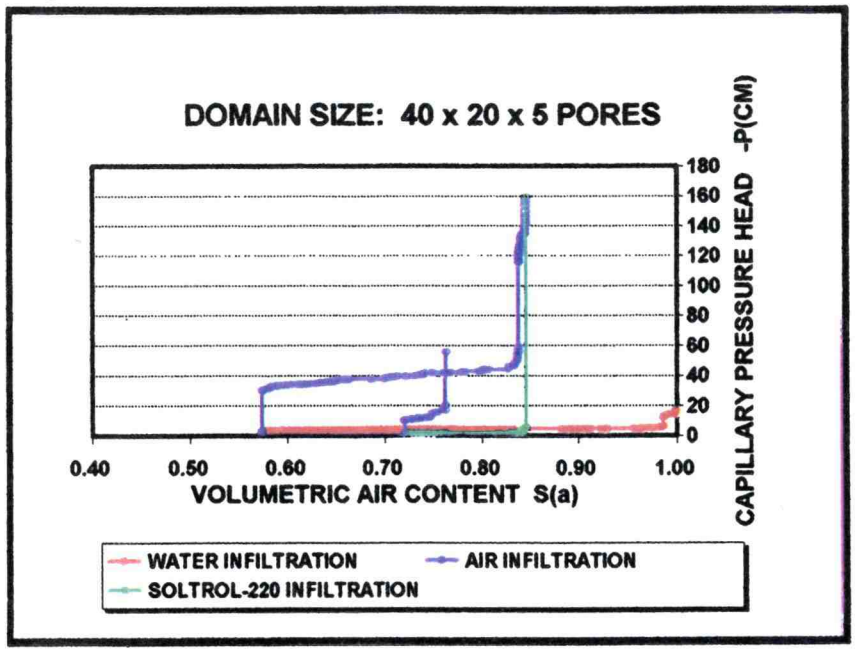

Figure 38. W-A-O-A capillary pressure-saturation scanning curves for double layer sand media with the size of 40 x 20 x 5 pores.

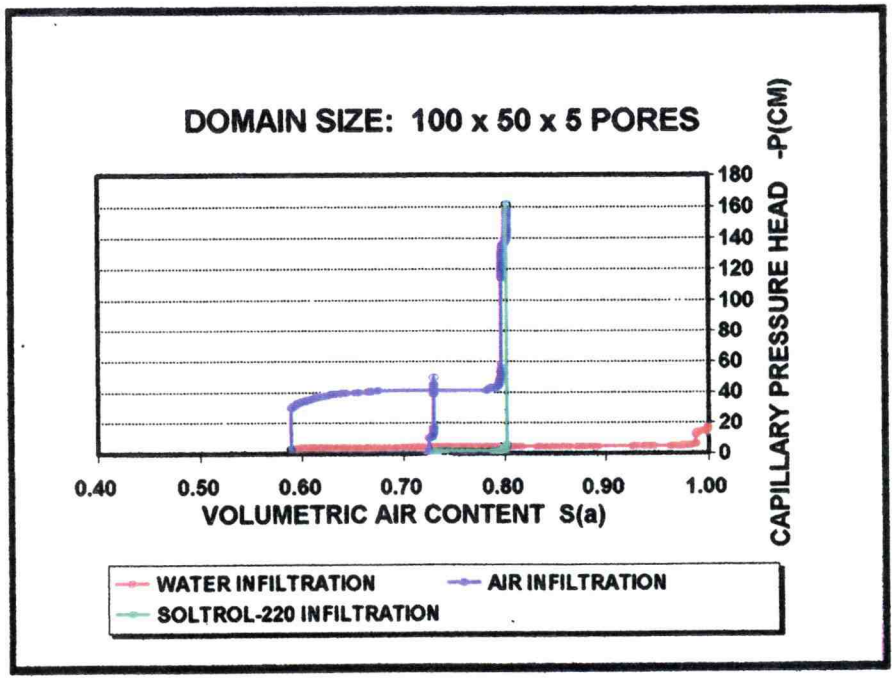

Figure 39. W-A-O-A capillary pressure-saturation scanning curves for double layer sand media with the size of 100 x 50 x 5 pores.

5.2 Fluid Distribution

5.2.1. Single Layer Sand Media with Water-air Infiltration Processes

The model domain setting employed to study air-water saturation relationships are the same as described in section 5.1.1. Water first infiltrated the initially dry domain, then drained by air infiltration. The simulation results of water saturation distribution (by summation the water volume along Z axis and divided by total pore volume along Z axis) are presented in Figures 40, 41, and 42 for domain sizes of 10 x 5 x 5, 20 x 10 x 5, and 40 x 20 x 5 pores respectively. The graphs showed that the saturation were randomly distributed and strongly dependent on local pore sizes.

The fluid distribution of intermediate pressure steps for domain sizes of 10 x 5 x 5 and 40 x 20 x 5 pores are shown by slices in Figures 43 to 50. These results are significantly different from those found in the two-dimensional domains, water are more averagely distributed in the domain after wetting process, no big area of trapped air developed (Figures 47 and 48). This is one of the major differences between two-dimensional and three-dimensional results.

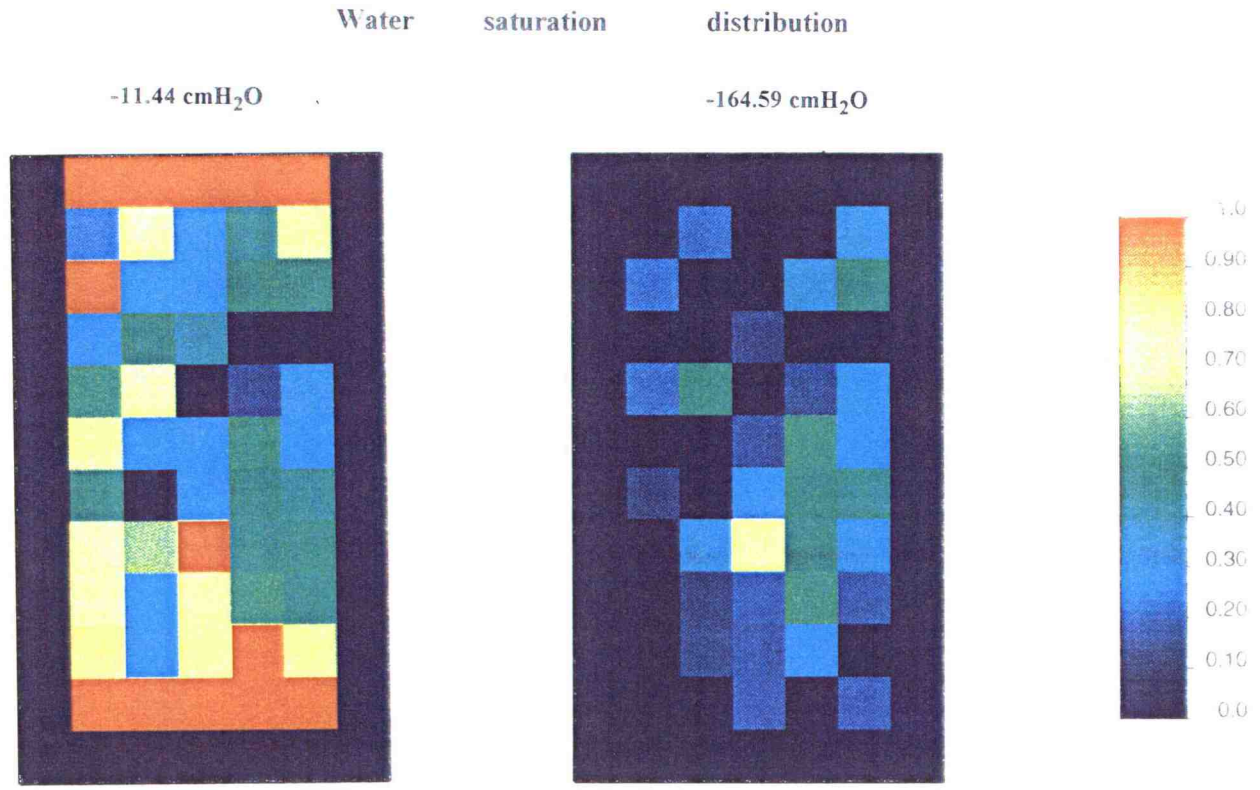

Figure 40. Water saturation distribution after water and air infiltration for single layer sand media with domain size of 10 x 5 x 5 pores

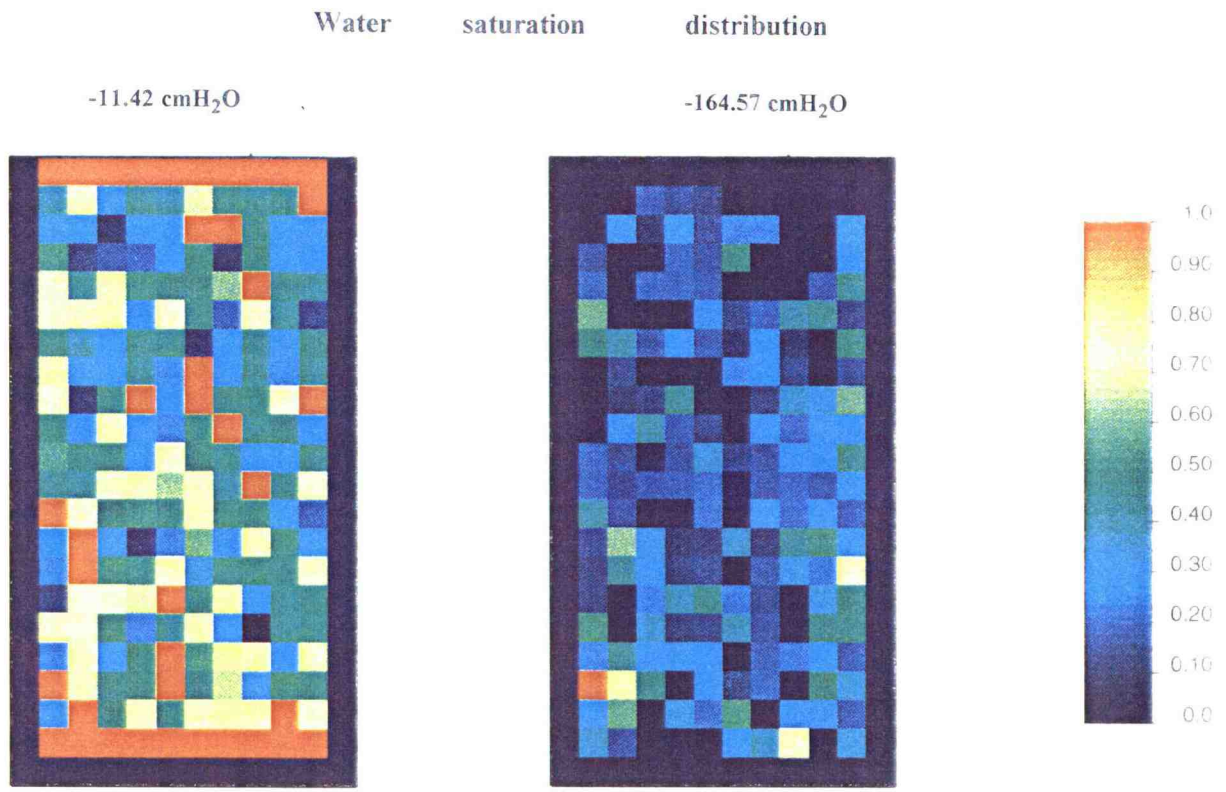

Figure 41. Water saturation distribution after water and air infiltration for single layer sand media with domain size of 20 x 10 x 5 pores

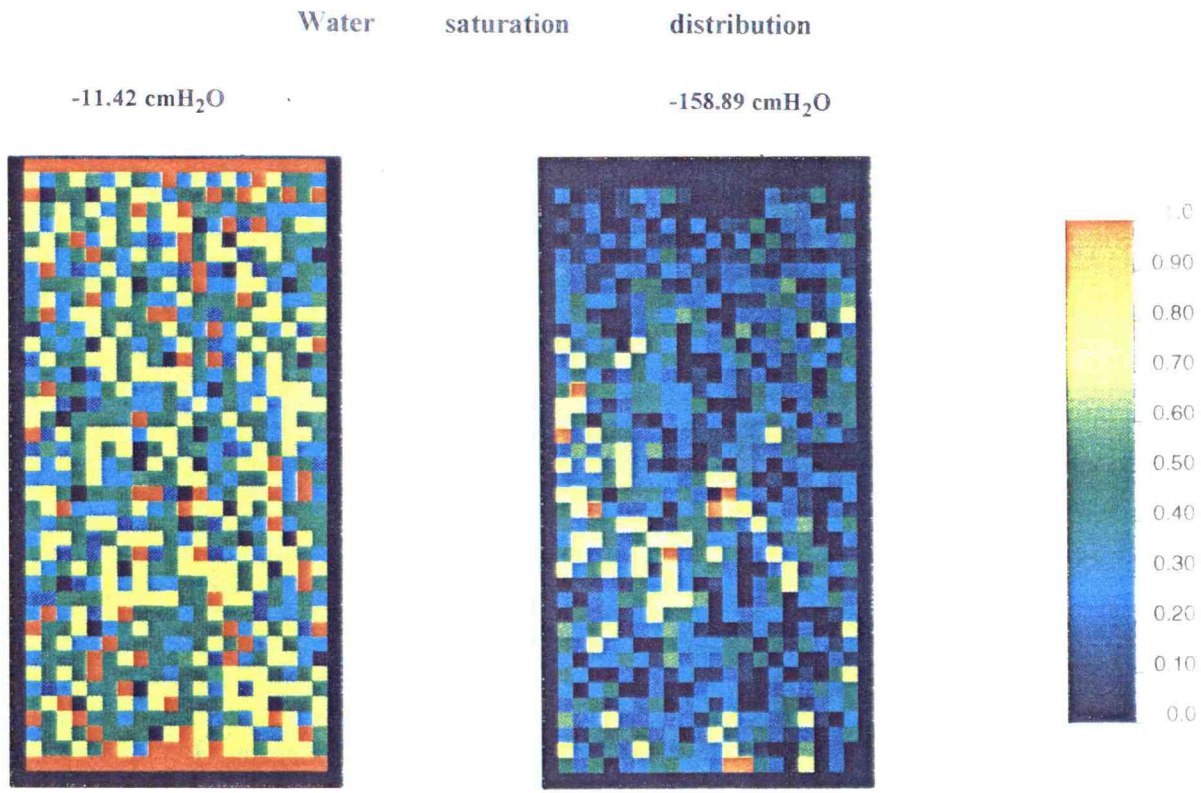

Figure 42. Water saturation distribution after water and air infiltration for single layer sand media with domain size of 40 x 20 x 5 pores.

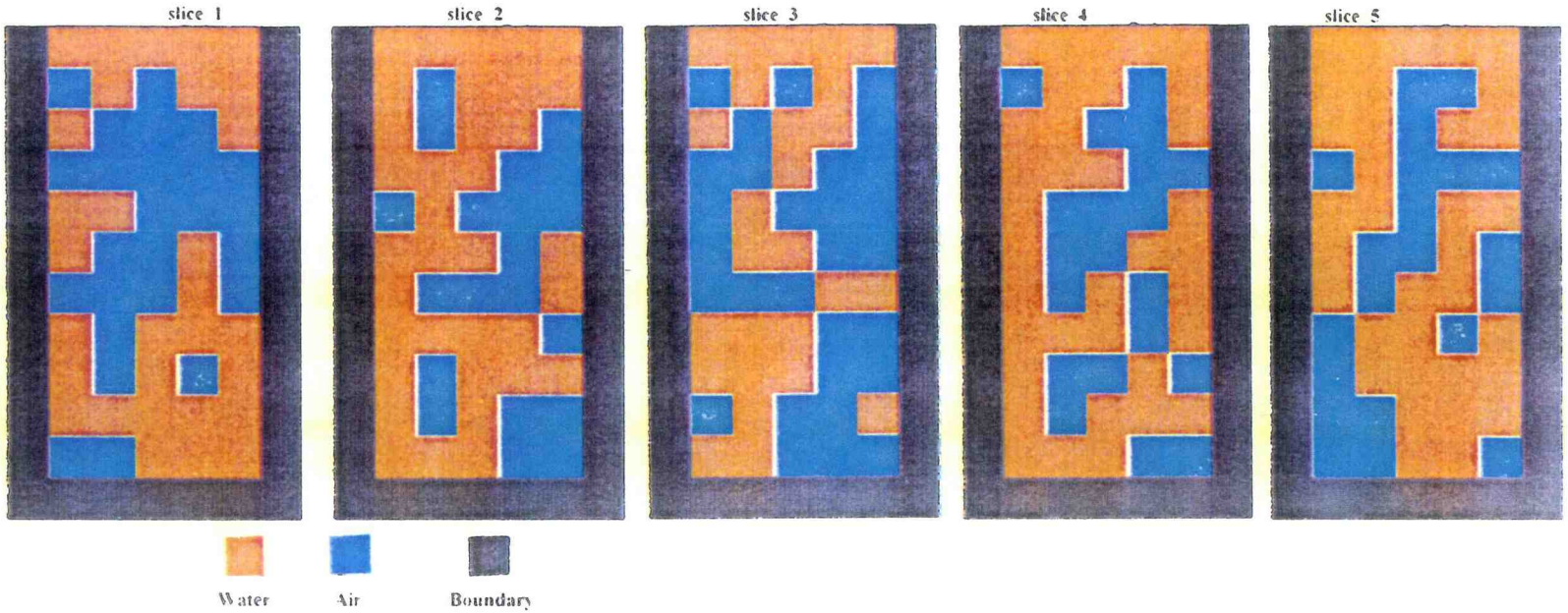

Figure 43 Fluid displacement after infiltration for single [illegible] model with [illegible] pores

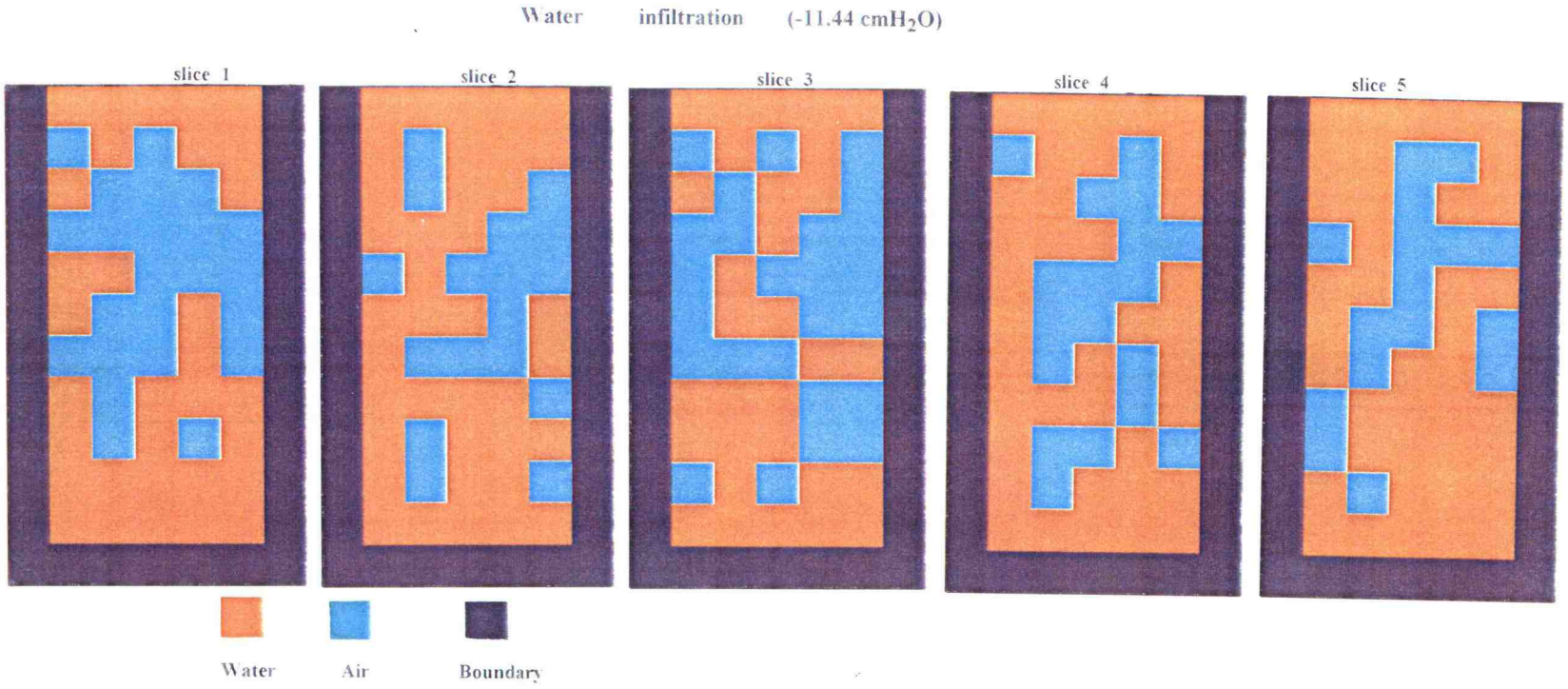

Figure 44 Fluid displacement of water infiltration for single layer sand media with domain size of 10 x 5 x 5 pores

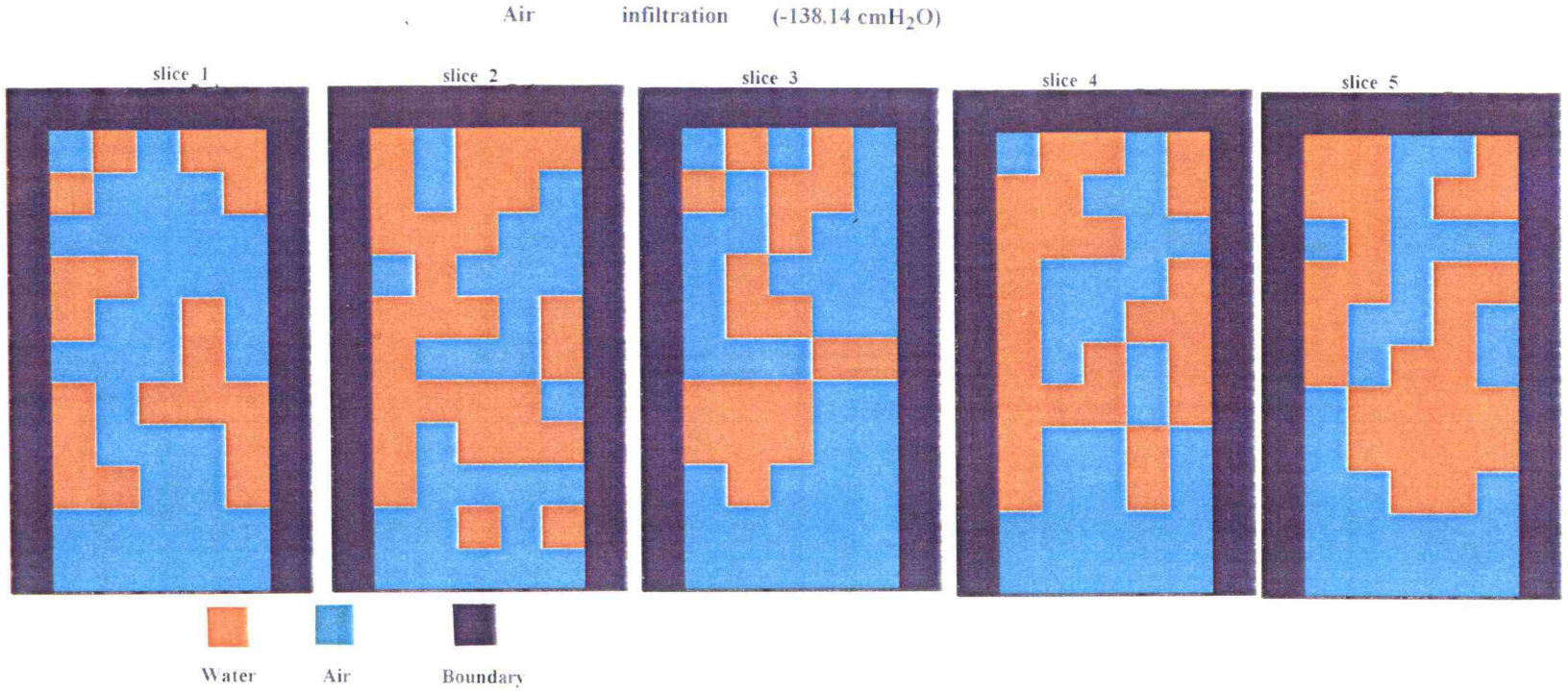

Figure 45. Fluid displacement of air infiltration for single layer sand media with domain size of 10 x 5 x 5 pores

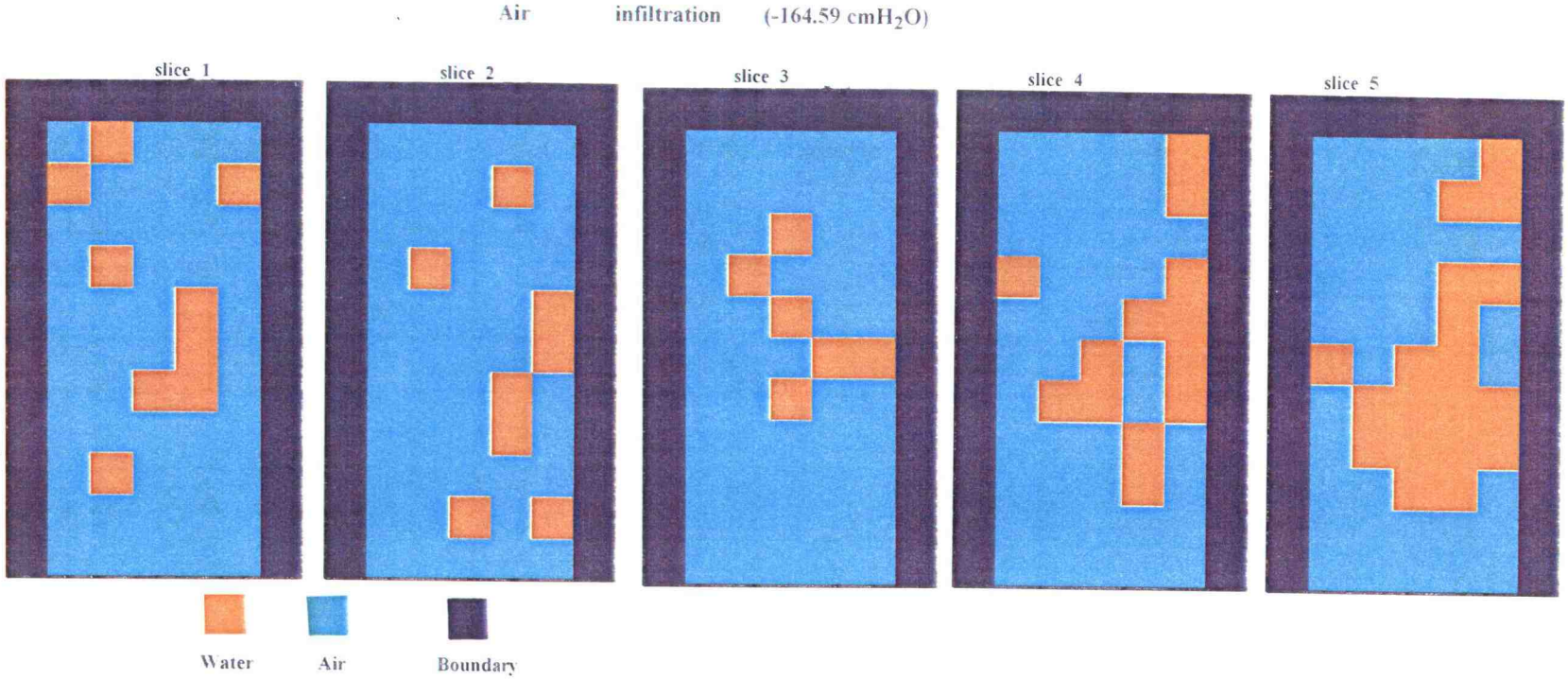

Figure 46. Fluid displacement of air infiltration for single layer sand media with domain size of 10 x 5 x 5 pores

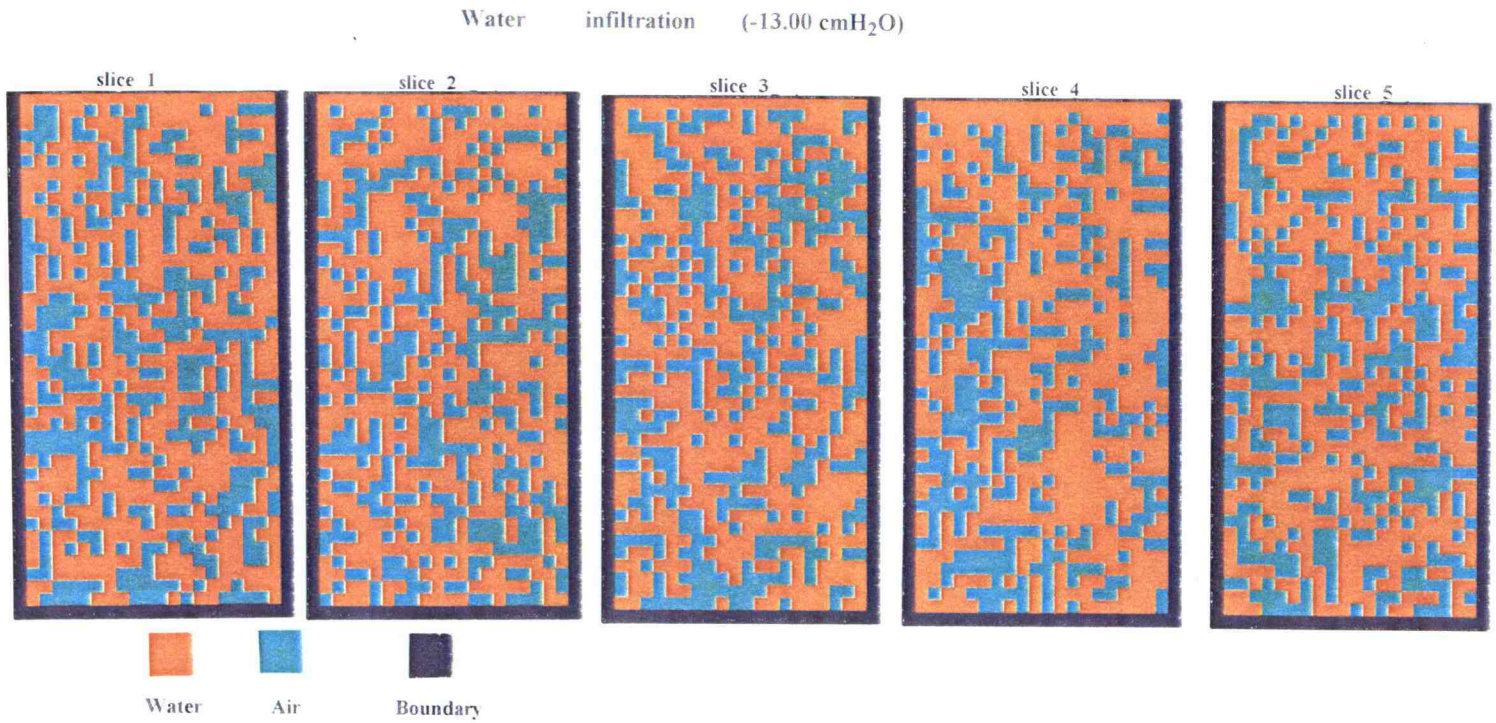

Figure 47. Fluid displacement of water infiltration for single layer sand media with domain size of 40 x 20 x 5 pores

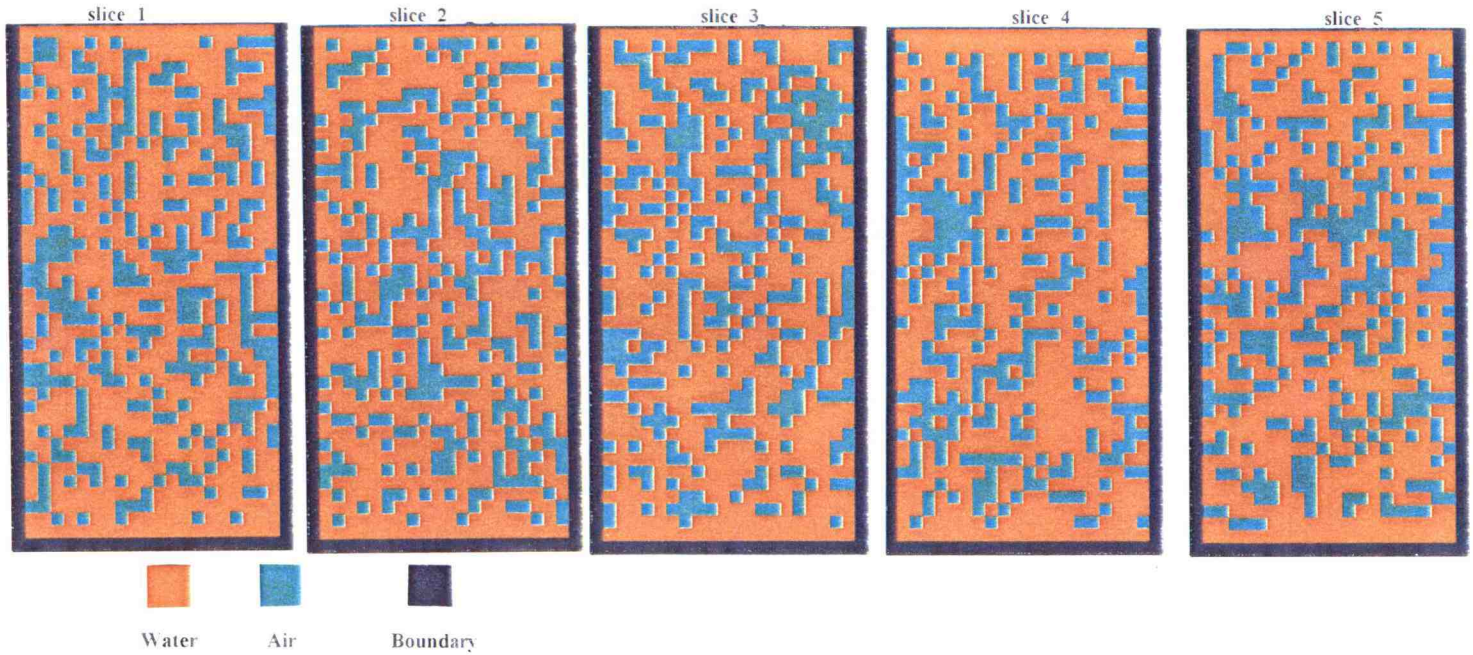

Figure 48 Fluid displacement of water infiltration for single layer sand media with domain size of 40 x 20 x 5 pores

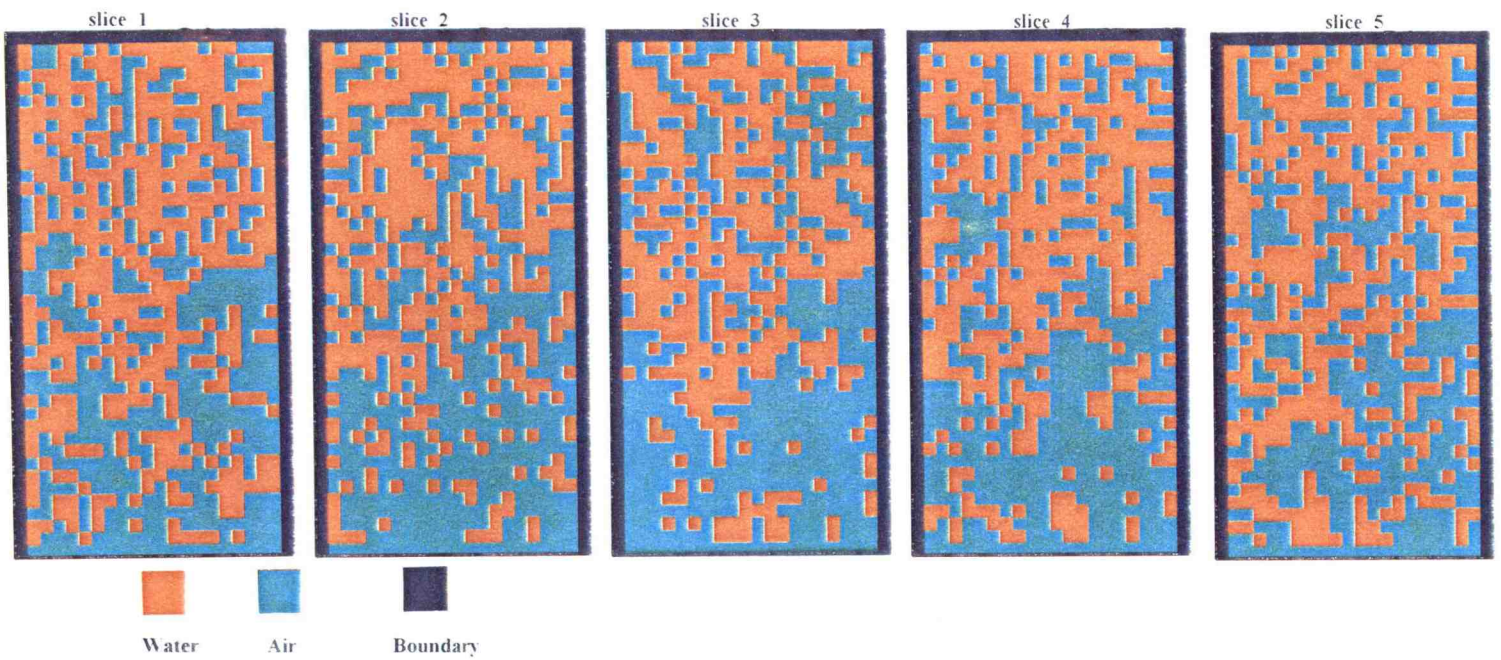

Figure 49. Fluid displacement of air infiltration for single layer sand media with domain size of 40 x 20 x 5 pores

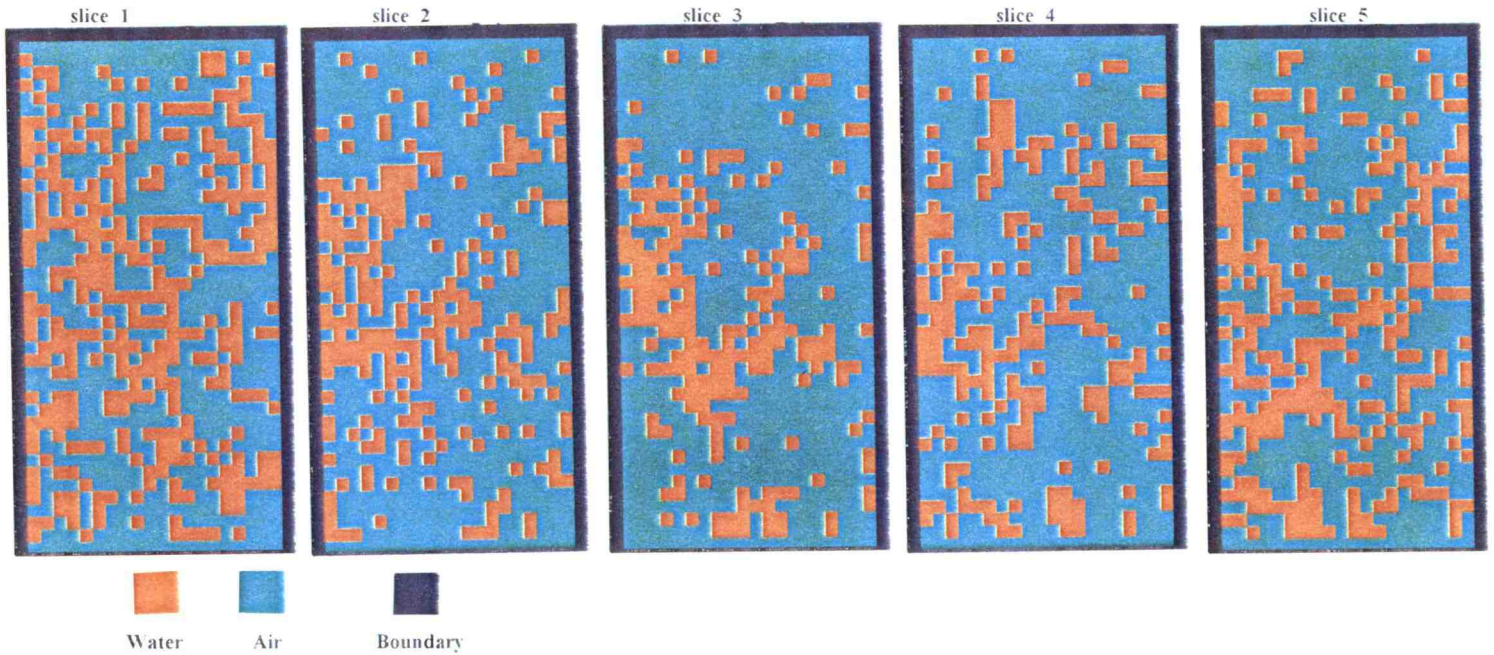

Figure 50. Fluid displacement of air infiltration for single layer sand media with domain size of 40 x 20 x 5 pores

5.2.2. Double Layer Sand Media with Water-air Infiltration Processes

The domain geometry employed for double-layer air-water simulation in a 3-dimensional network model are the same as described in section 5.1.2. Water infiltrated the initially dry domain, then drained by air infiltration. The simulation results of water saturation distribution are shown in Figures 51, 52, 53, and 54 for domain sizes of 10 x 5 x 5, 20 x 10 x 5, 40 x 20 x 5, and 100 x 50 x 5 pores respectively. The saturation were randomly distributed. It is totally saturated at the border of find sand to coarse sand after wetting process. This again demonstrates that wetting fluid (water) will be retained in the fine sand at greater pressures than in the coarse sand.

The fluid distributions of intermediate infiltration steps for domain sizes of 10 x 5 x 5, 40 x 20 x 5, and 100 x 50 x 5 pores are shown by slices in Figures 55 to 64. Water are averagely distributed in the whole domain. The graphs also show that wetting fluid will be more likely to stay in fine sand than in coarse sand during wetting process. This result is the same as that from two-dimensional model.

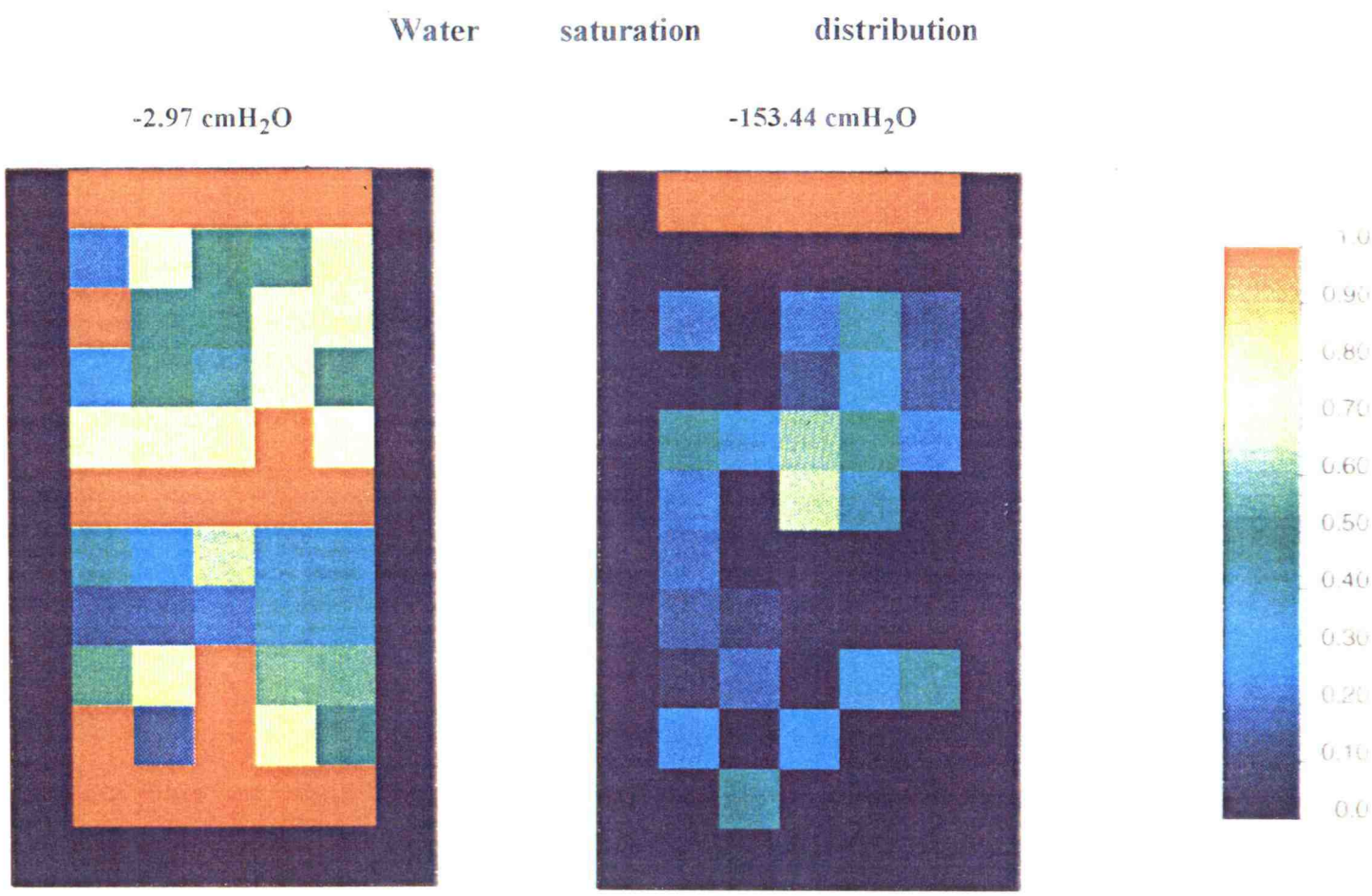

Figure 51. Water saturation distribution after water and air infiltration for double layer sand media with domain size of 10 x 5 x 5 pores.

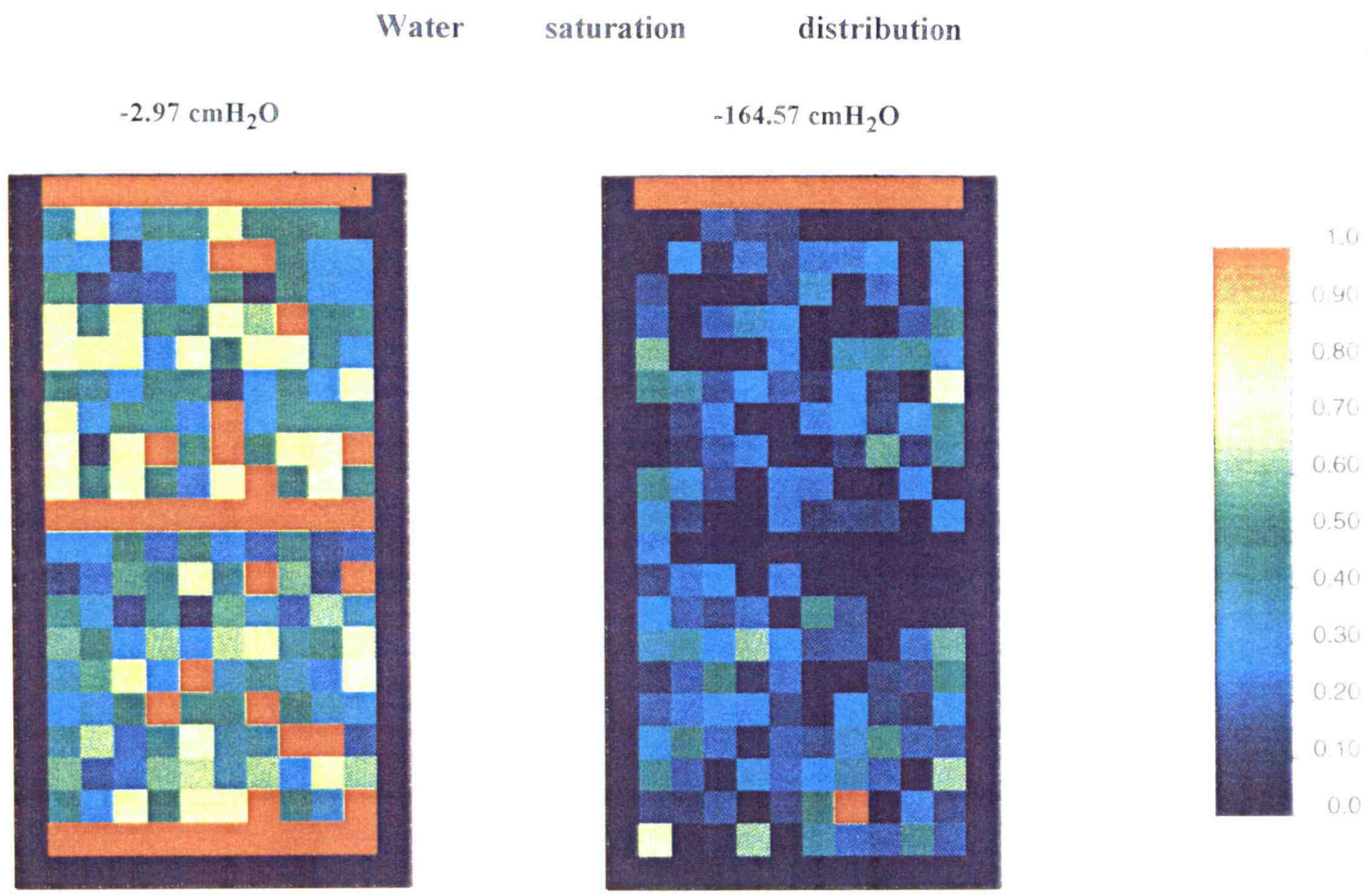

Figure 52. Water saturation distribution after water and air infiltration for double layer sand media with domain size of 20 x 10 x 5 pores.

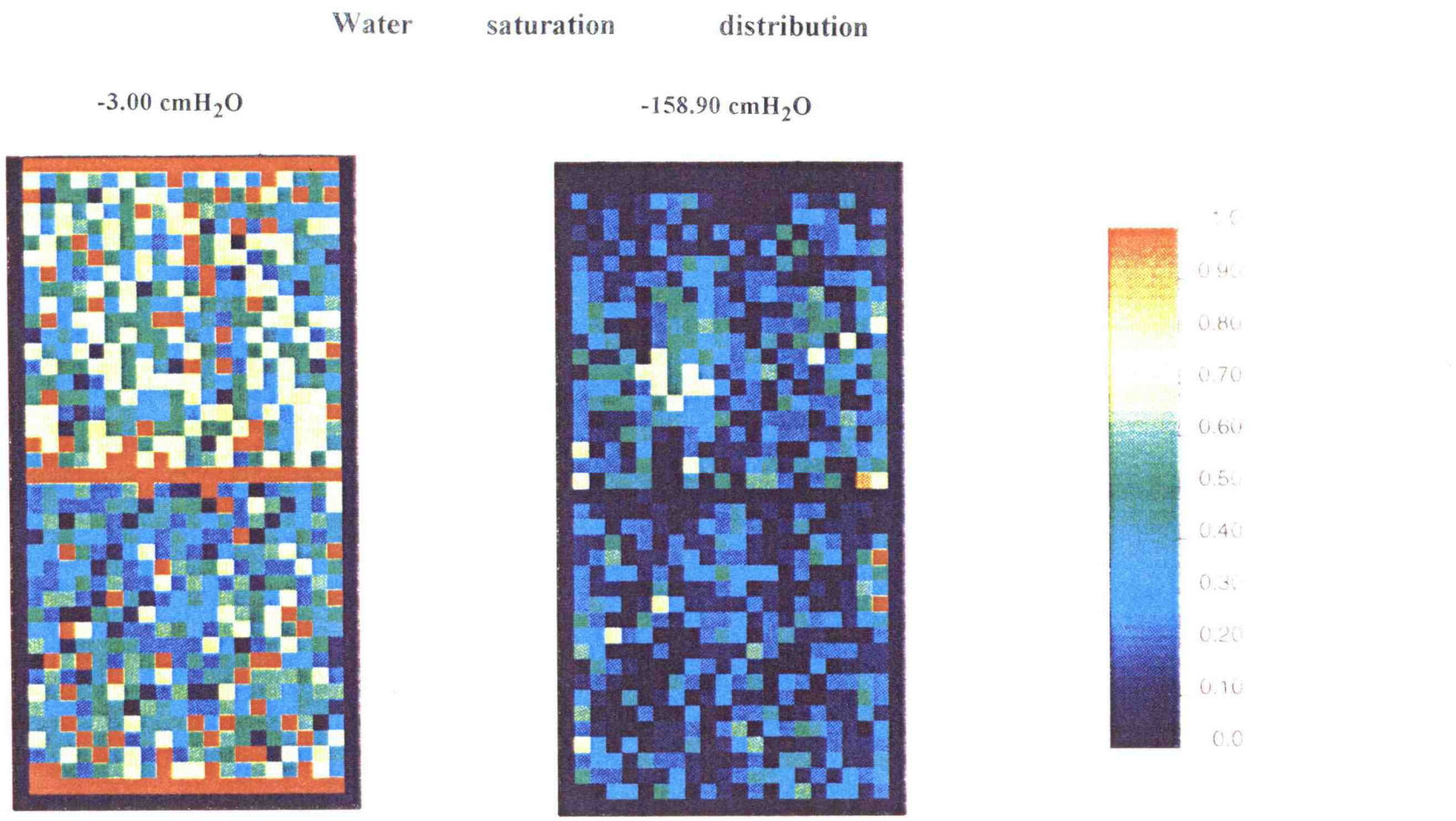

Figure 53. Water saturation distribution after water and air infiltration for double layer sand media with domain size of 40 x 20 x 5 pores.

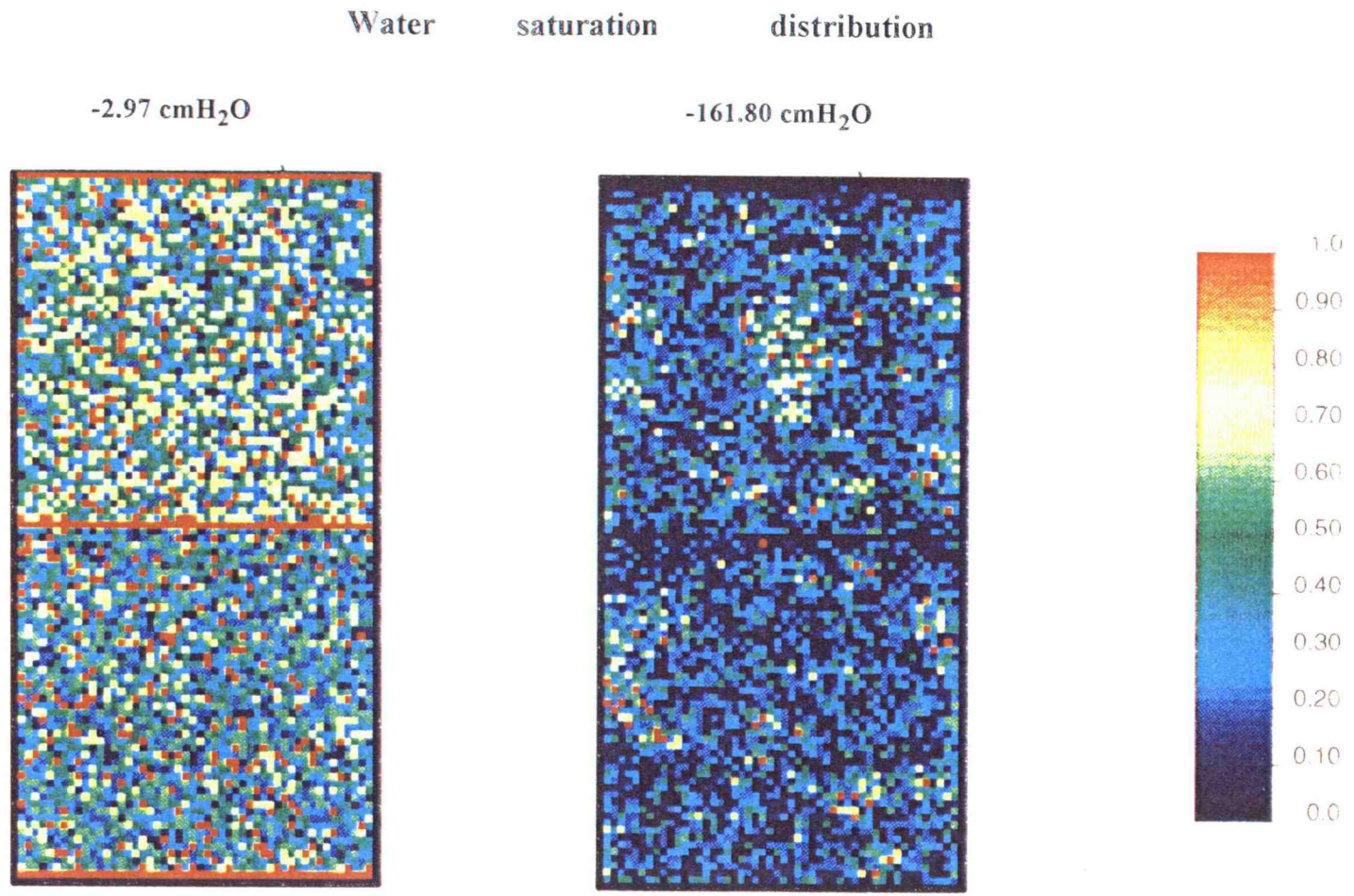

Figure 54. Water saturation distribution after water and air infiltration for double layer sand media with domain size of 100 x 50 x 5 pores.

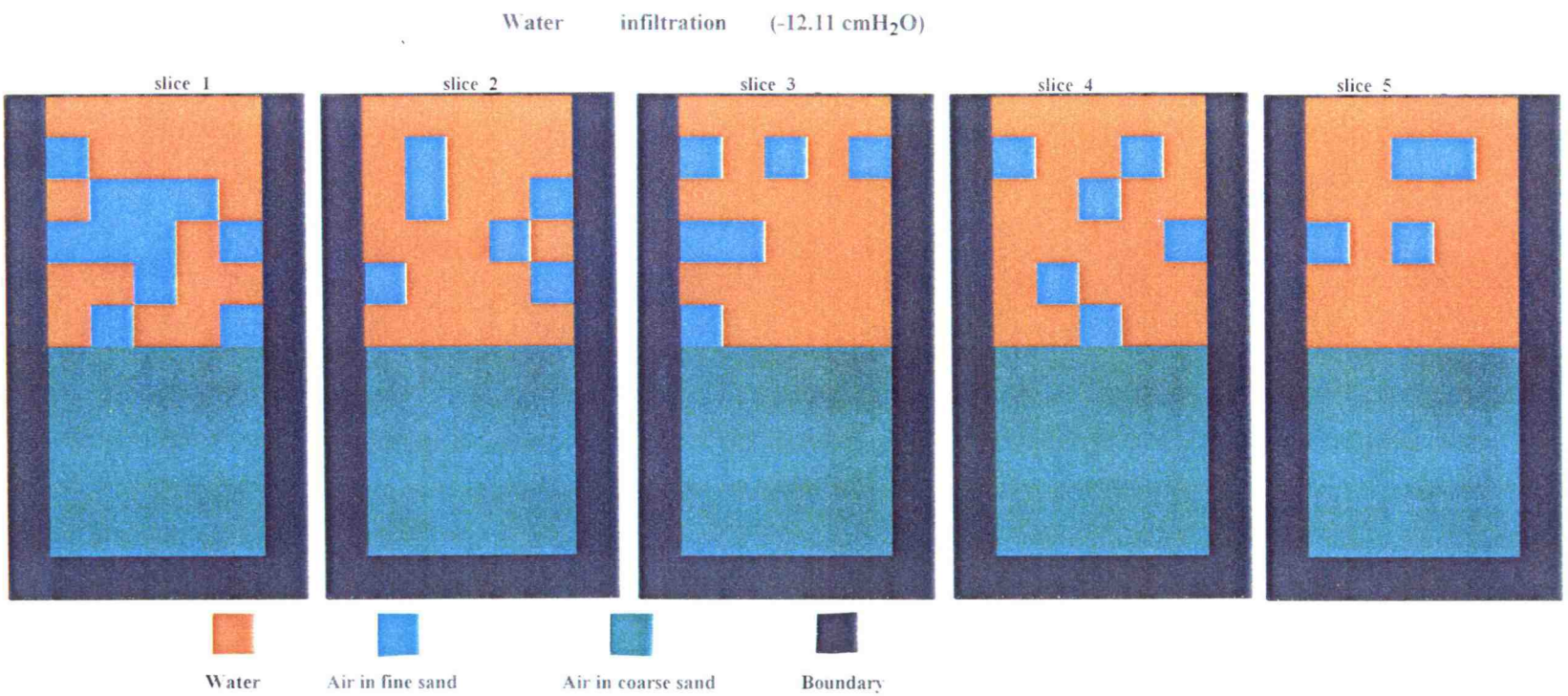

Figure 55. Fluid displacement of water infiltration for double layer sand media with domain size of 10 x 5 x 5 pores

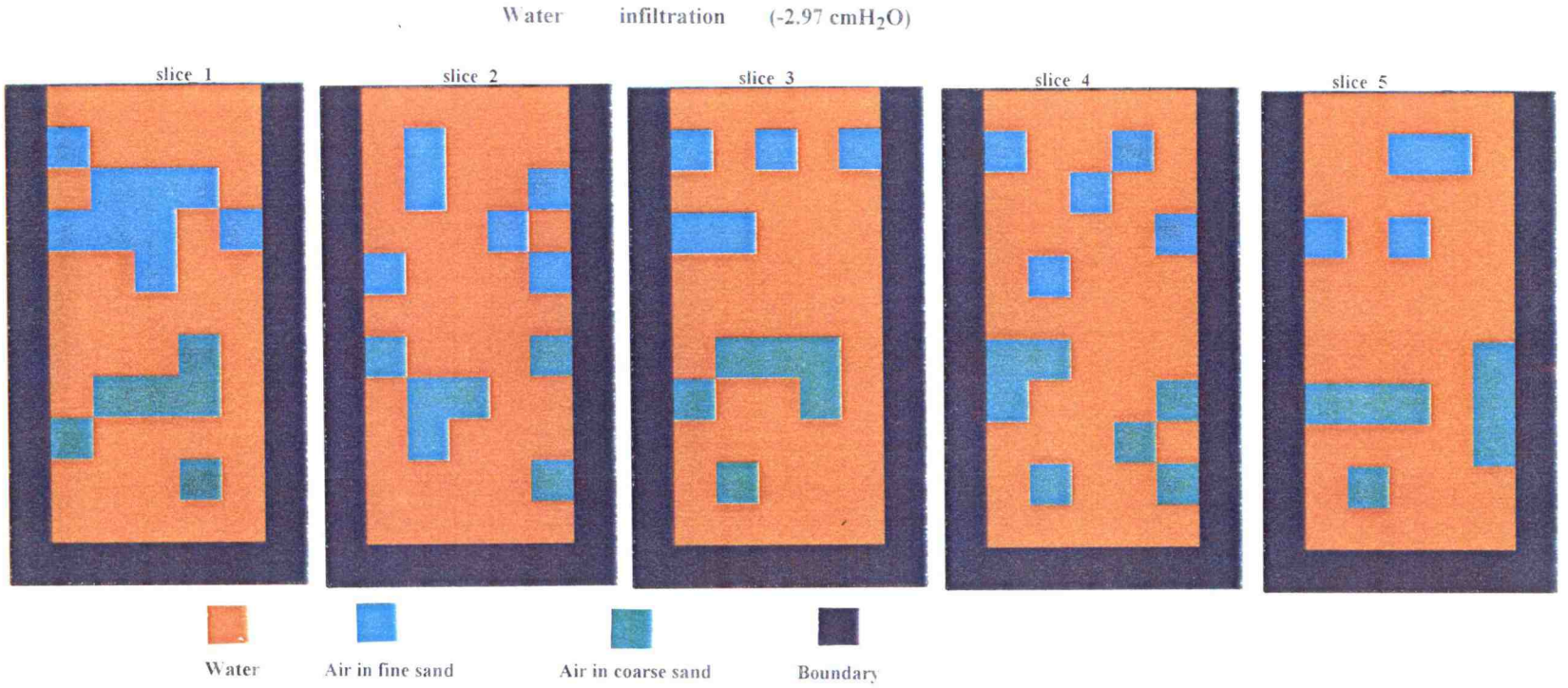

Figure 56 Fluid displacement of water infiltration for double layer sand media with domain size of 10 x 5 x 5 pores.

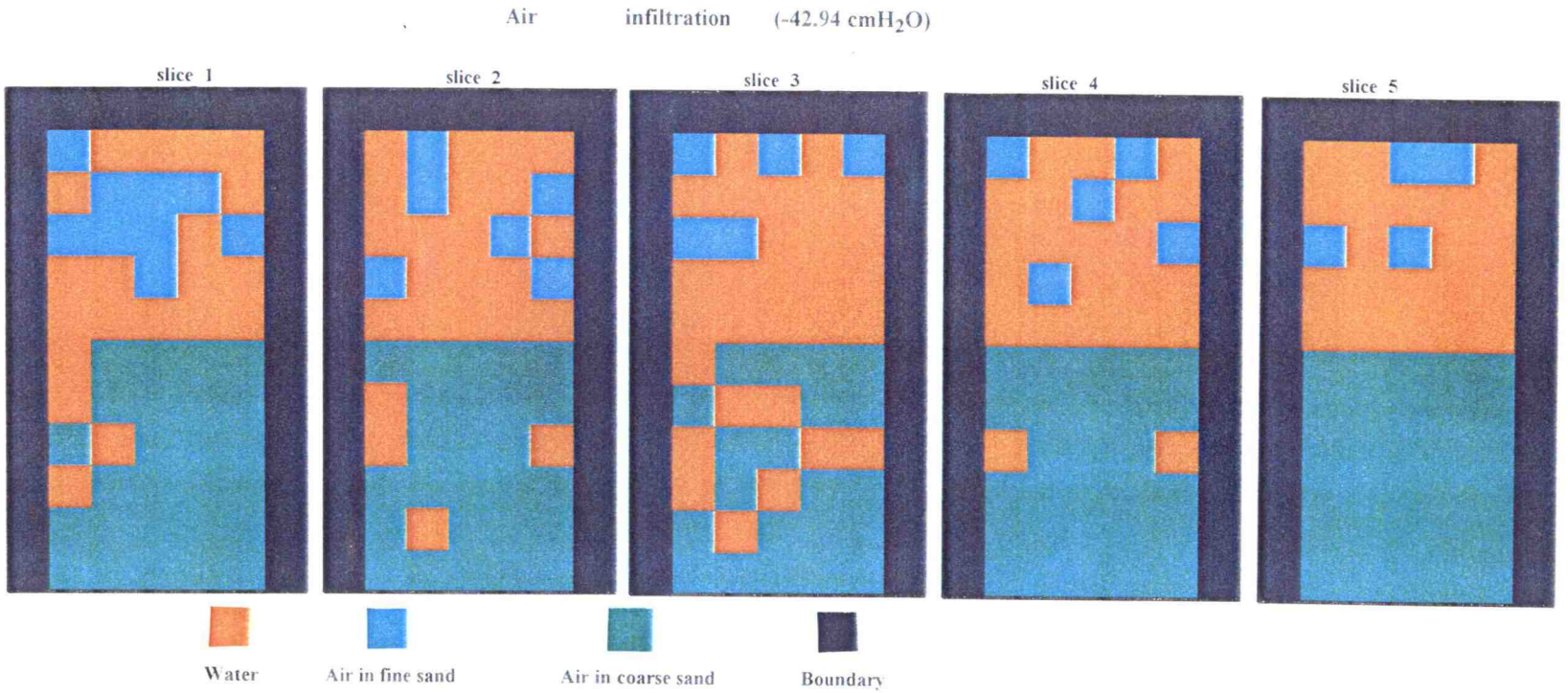

Figure 57 Fluid displacement of air infiltration for double layer sand media with domain size of 10 x 5 x 5 pores

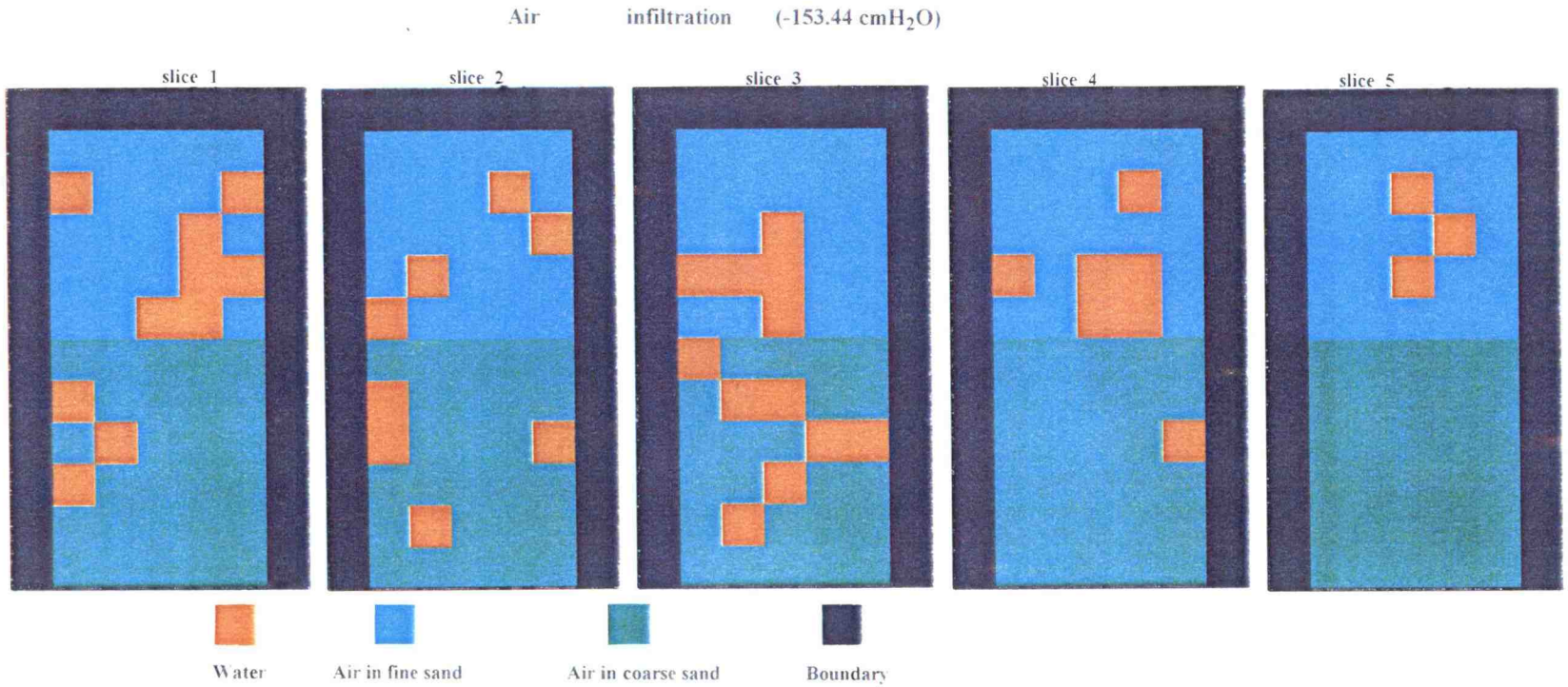

Figure 58 Fluid displacement of air infiltration for double layer sand media with domain size of 10 x 5 x 5 pores

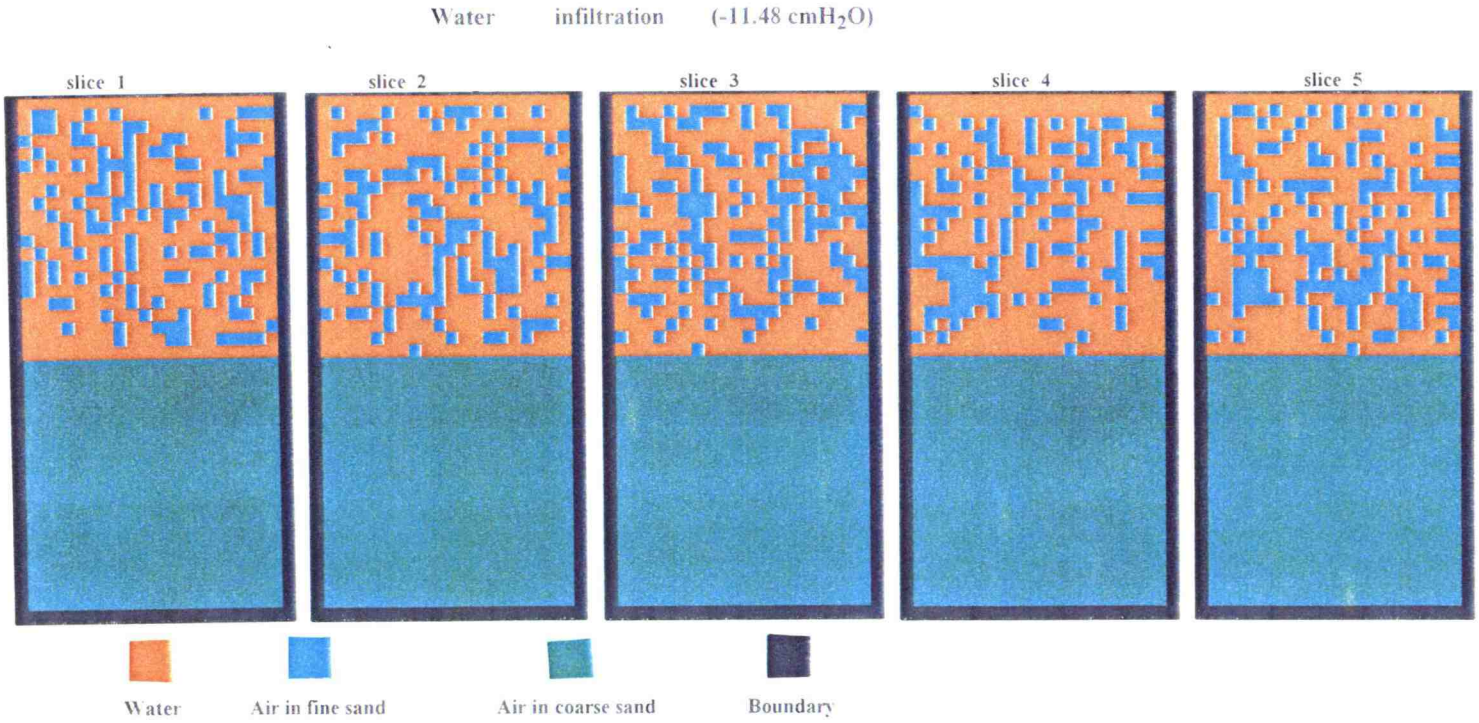

Figure 59 Fluid displacement of water infiltration for double layer sand media with domain size of 40 x 20 x 5 pores

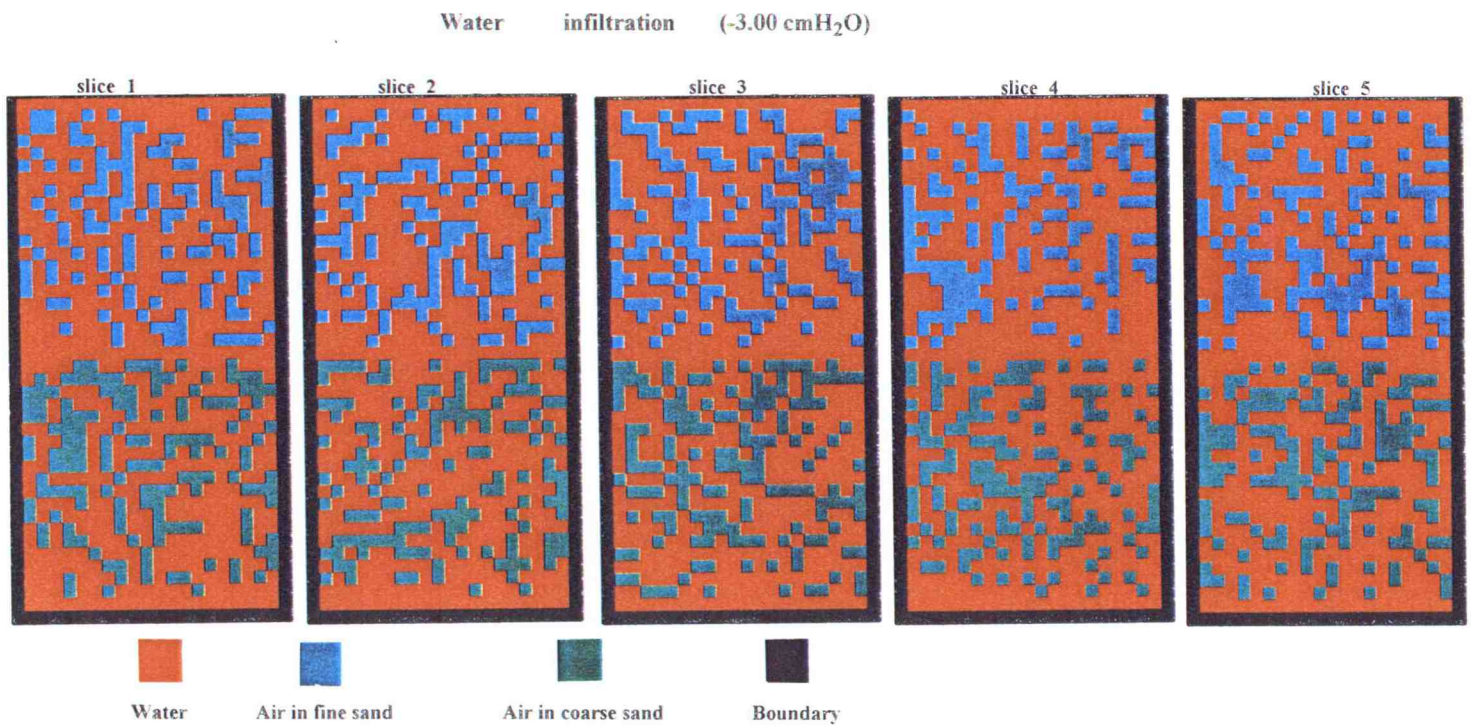

Figure 60. Fluid displacement of water infiltration for double layer sand media with domain size of 40 x 20 x 5 pores

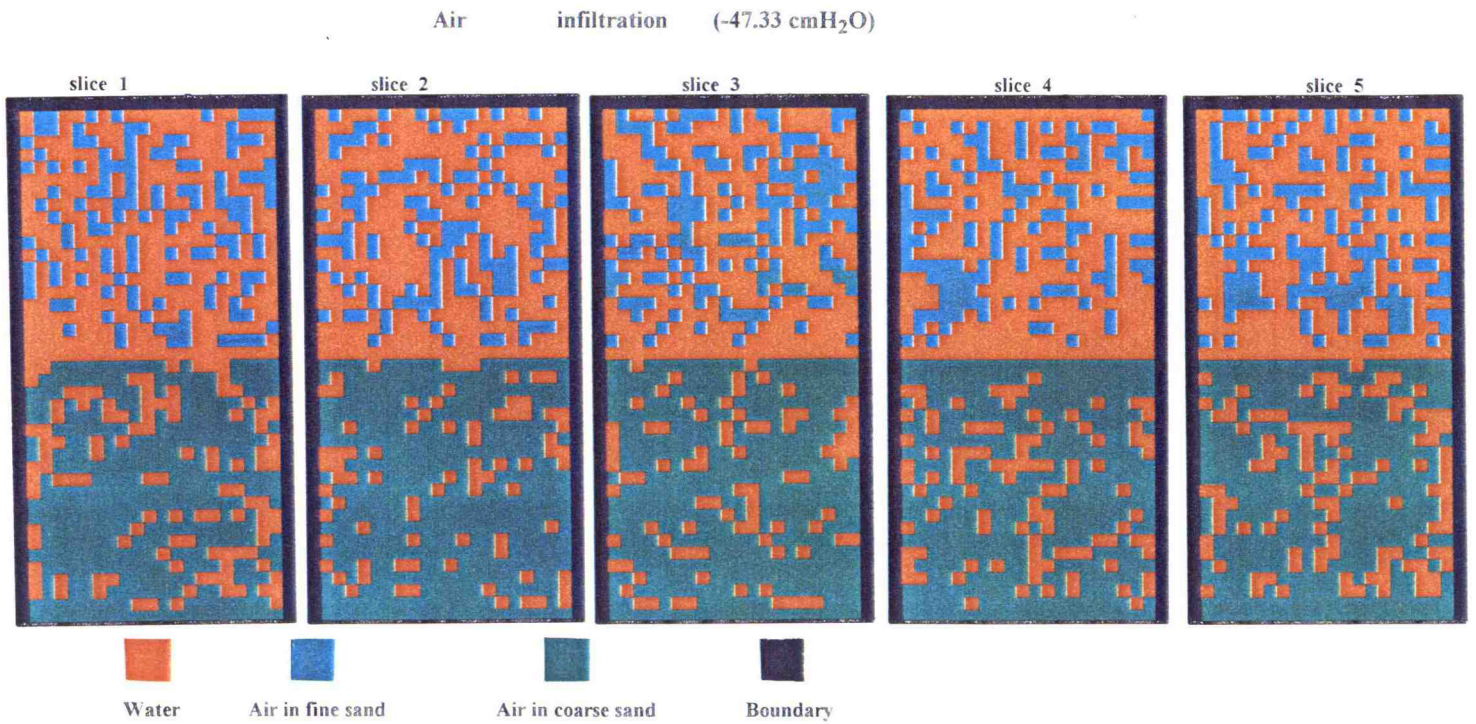

Figure 61 Fluid displacement of air infiltration for double layer sand media with domain size of 40 x 20 x 5 pores

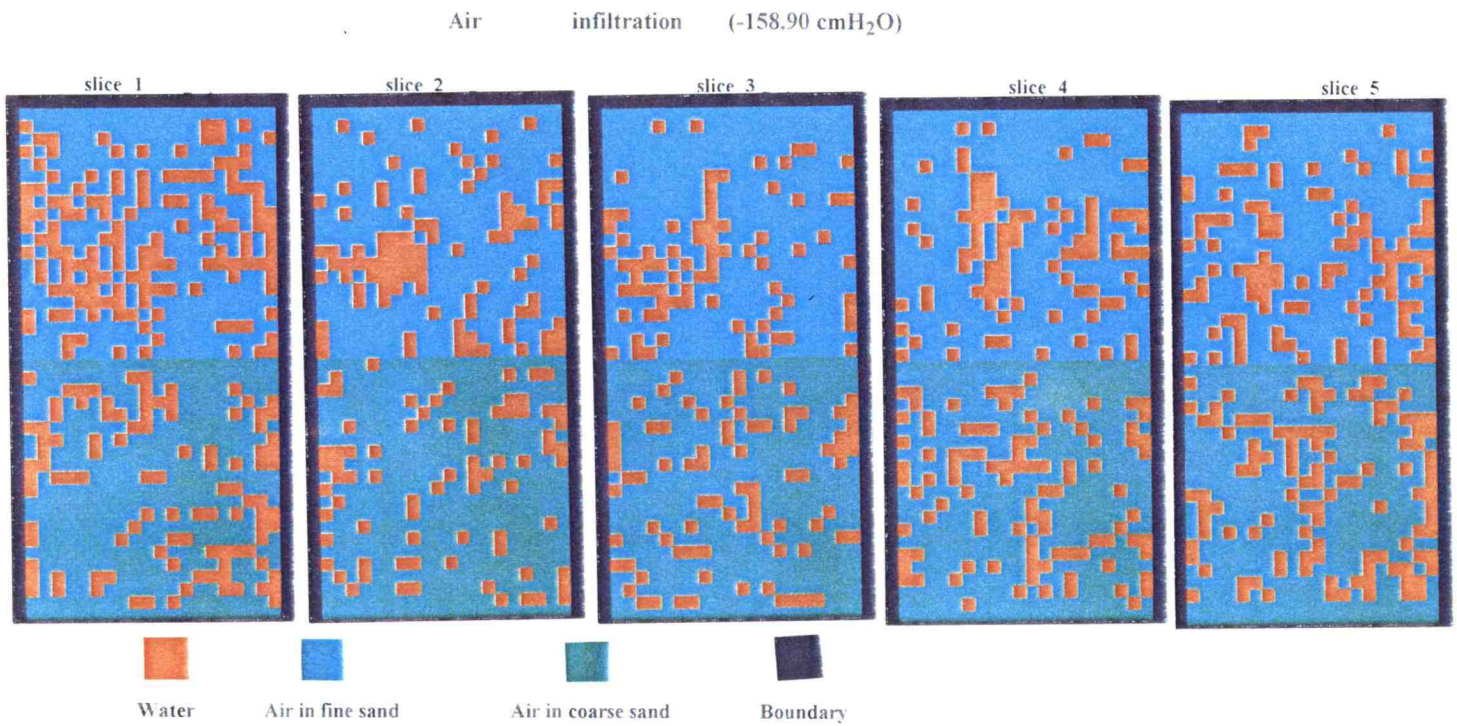

Figure 62 Fluid displacement of air infiltration for double layer sand media with domain size of 40 x 20 x 5 pores

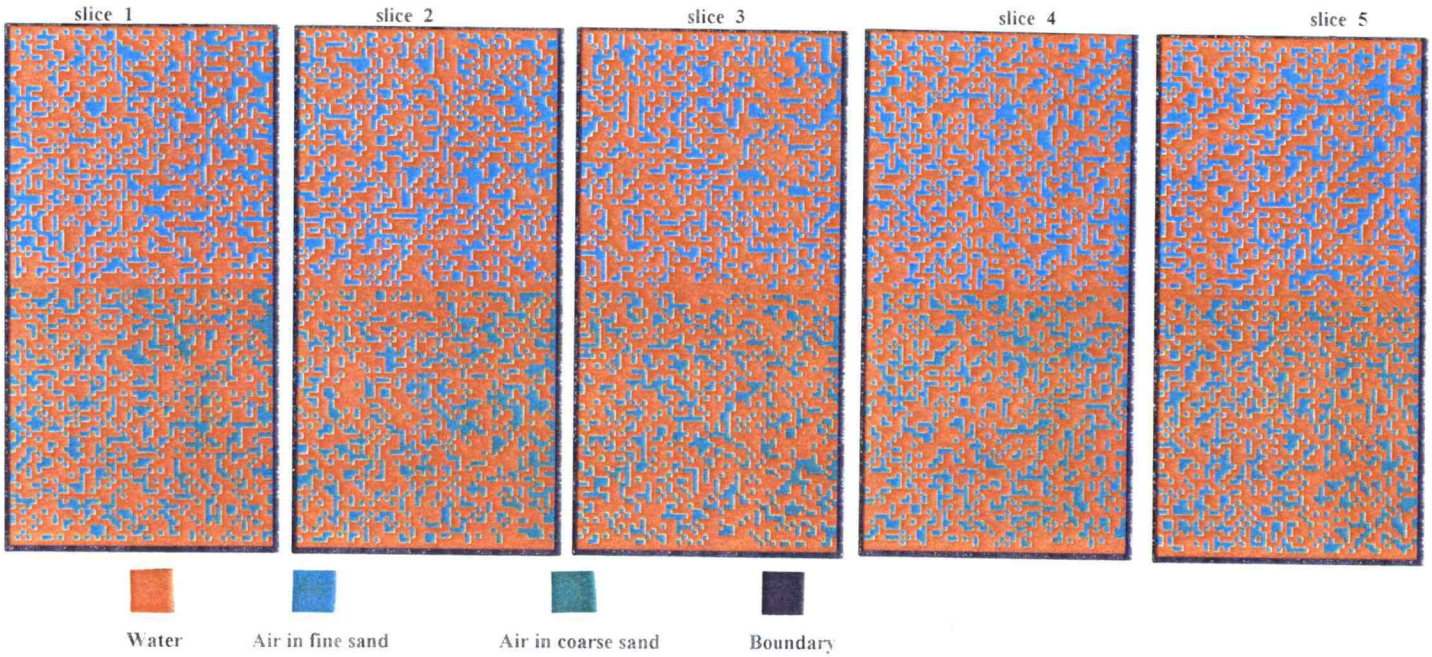

Figure 63. Fluid displacement of water infiltration for double layer sand media with domain size of 100 x 50 x 5 pores.

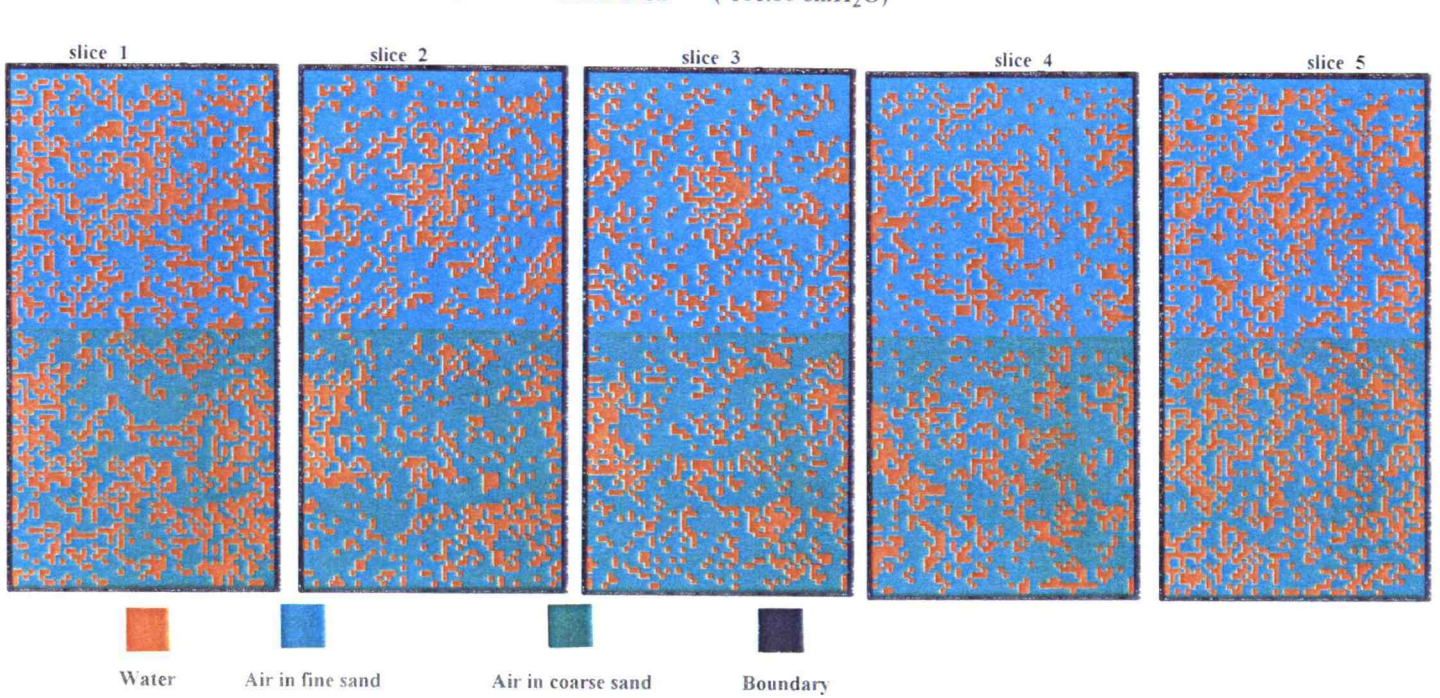

Figure 64. Fluid displacement of air infiltration for double layer sand media with domain size of 100 x 50 x 5 pores.

5.2.3. Double Layer Sand Media with Water-air-oil-air Infiltration Processes

The model domain setting employed here are the same as described in section 5.1.3. Water first infiltrated the initially dry domain from top water reservoir, and drained by air infiltration from bottom air reservoir. Then oil infiltrated the wet domain from top oil reservoir and drained by air infiltration from bottom. The simulation results of water and oil saturation distribution after oil infiltration and air infiltration are shown in Figures 65, 66, 67, and 68 for domain sizes of 10 x 5 x 5, 20 x 10 x 5, 40 x 20 x 5, and 100 x 50 x 5 pores respectively. The fluids appear randomly distributed without large scale blobs or ganglia. It is noted that water saturation distribution after oil infiltration and air infiltration for the same domain size are identical. This can be understood by noting that water and oil reservoir shared the same side of model domain. During oil infiltration, water reservoir was closed. All the water left in the domain were trapped, therefore can not be displaced by oil.

The fluid distributions of intermediate oil and air infiltration steps for domain sizes of 10 x 5 x 5, 40 x 20 x 5, and 100 x 50 x 5 pores are shown by slices in Figures 69 to 78. Water appears uniformly distributed throughout the domain. Oil infiltration is constricted to isolated fingers, similar to the results from two-dimensional models.

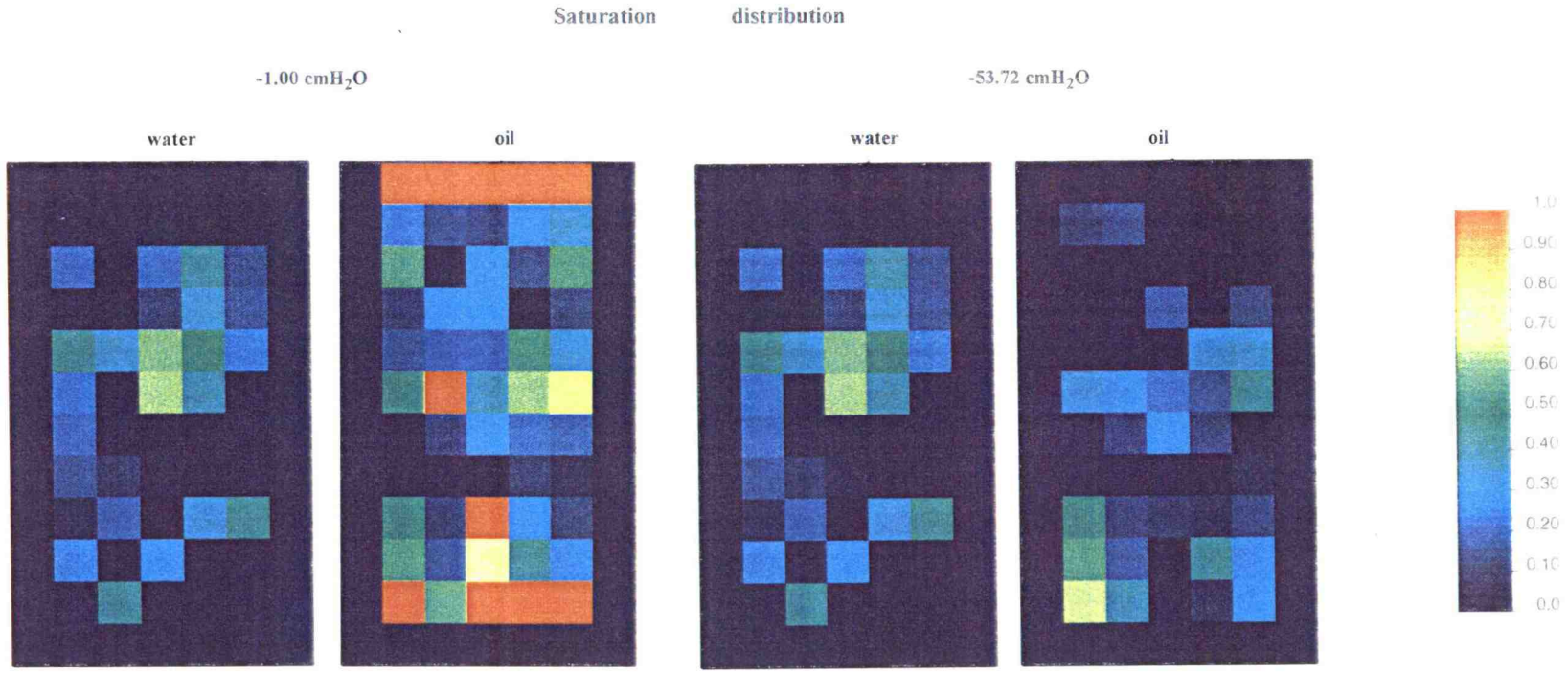

Figure 65. Water and oil saturation distribution after oil and air infiltration for double layer sand media with domain size of 10 x 5 x 5 pores

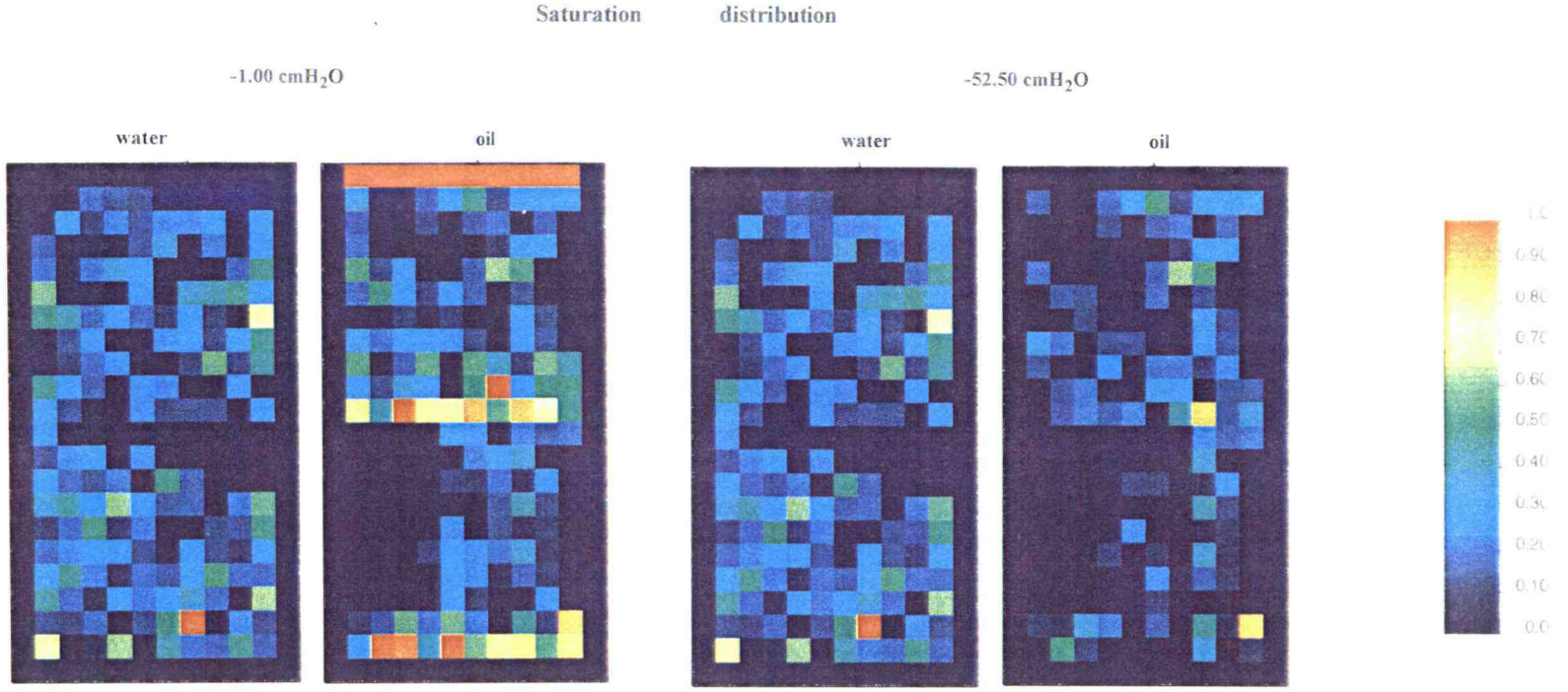

Figure 66. Water and oil saturation distribution after oil and air infiltration for double layer sand media with domain size of 20 x 10 x 5 pores

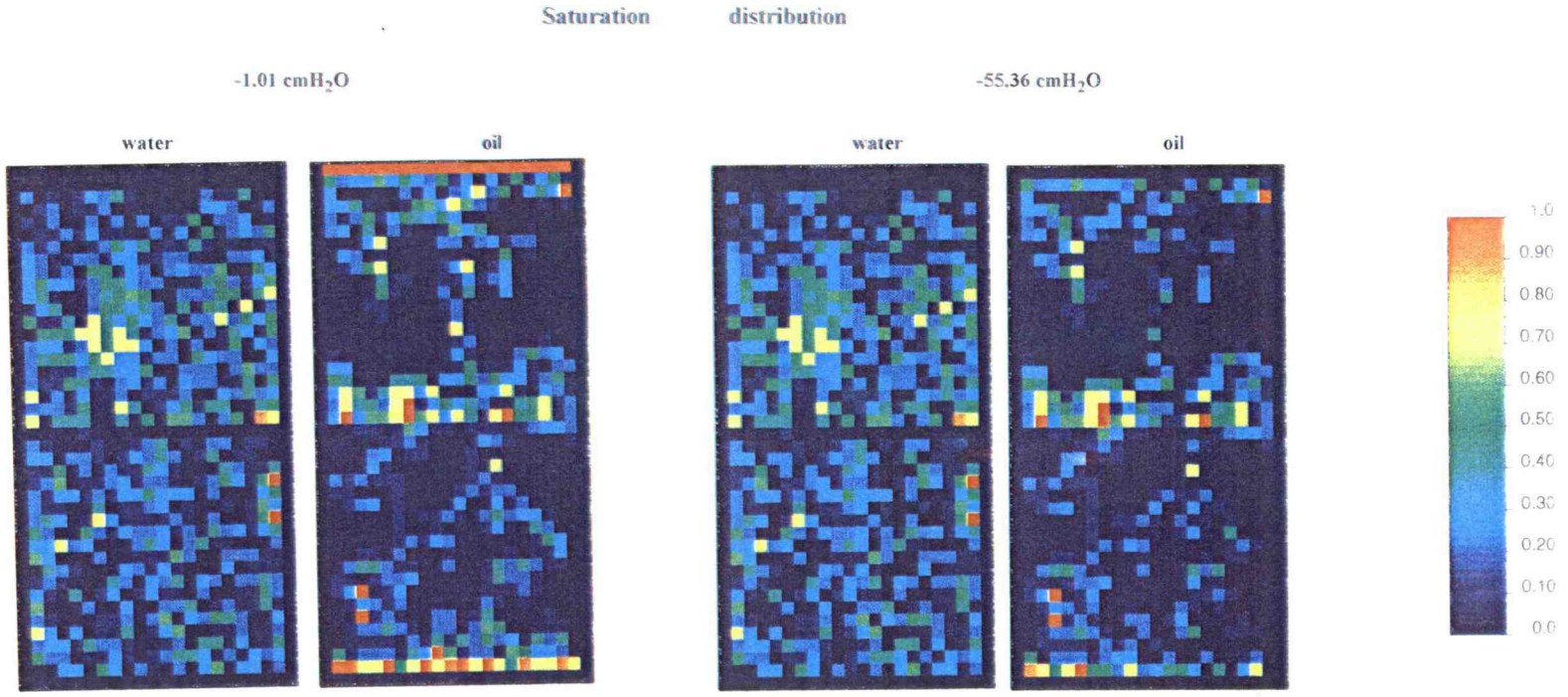

Figure 67 Water and oil saturation distribution after oil and air infiltration for double layer sand media with domain size of 40 x 20 x 5 pores

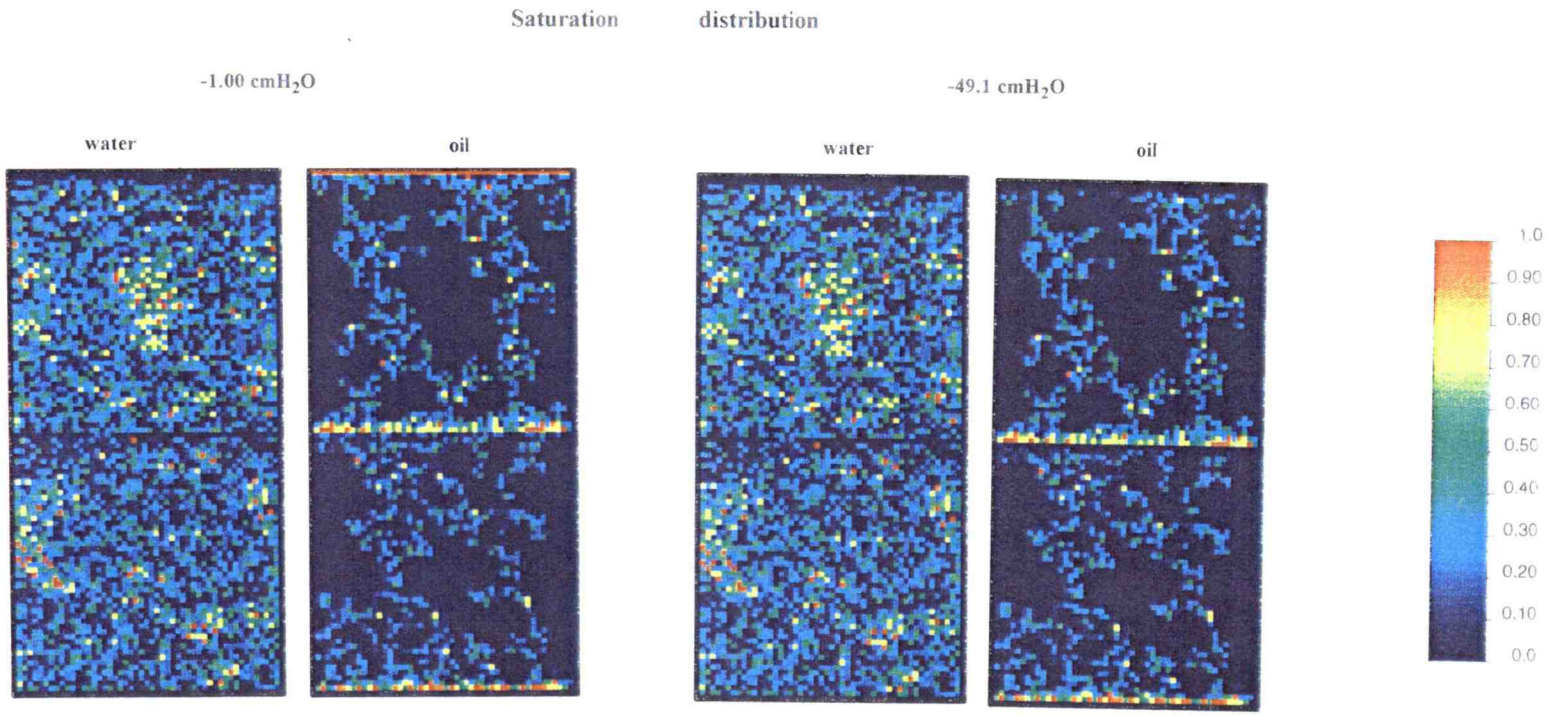

Figure 68. Water and oil saturation distribution after oil and air infiltration for double layer sand media with domain size of 100 x 50 x 5 pores.

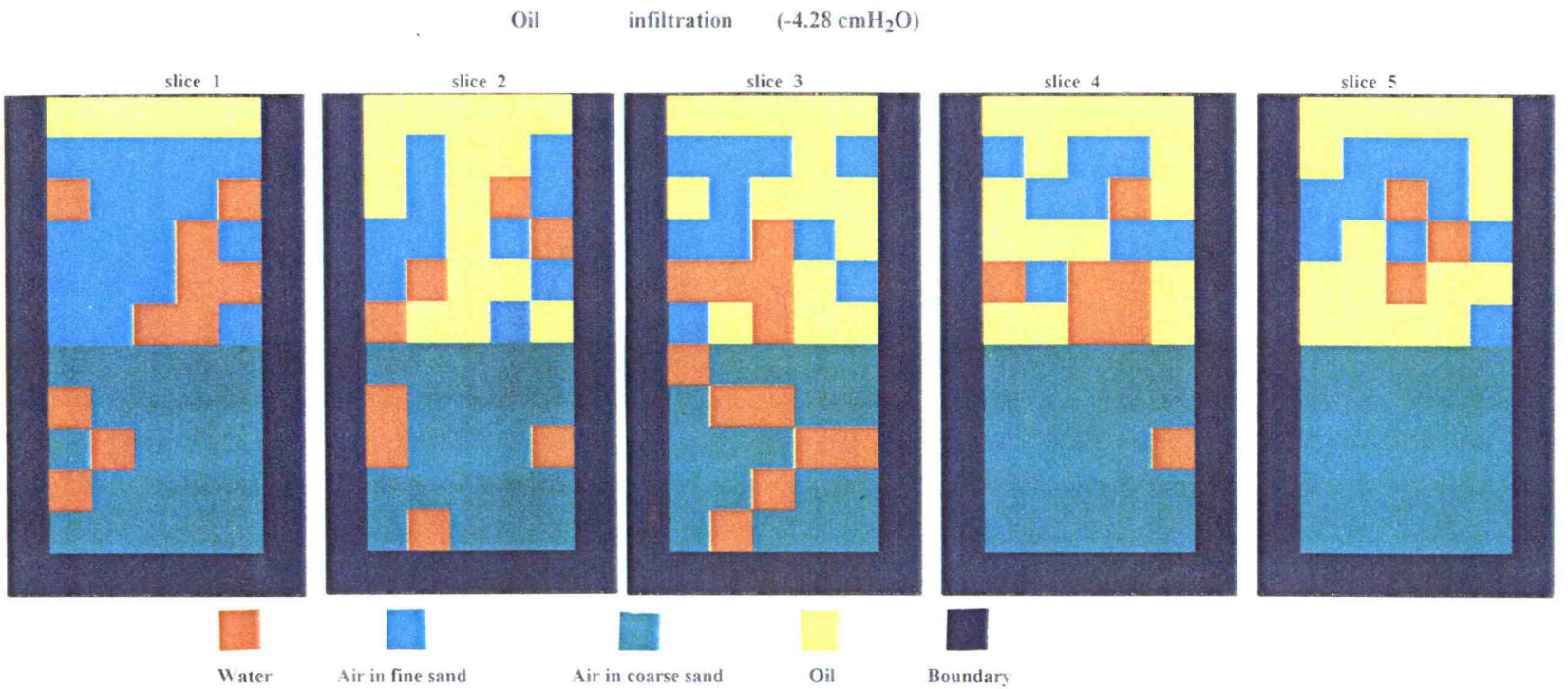

Figure 69. Fluid displacement of oil infiltration for double layer sand media with domain size of 10 x 5 x 5 pores

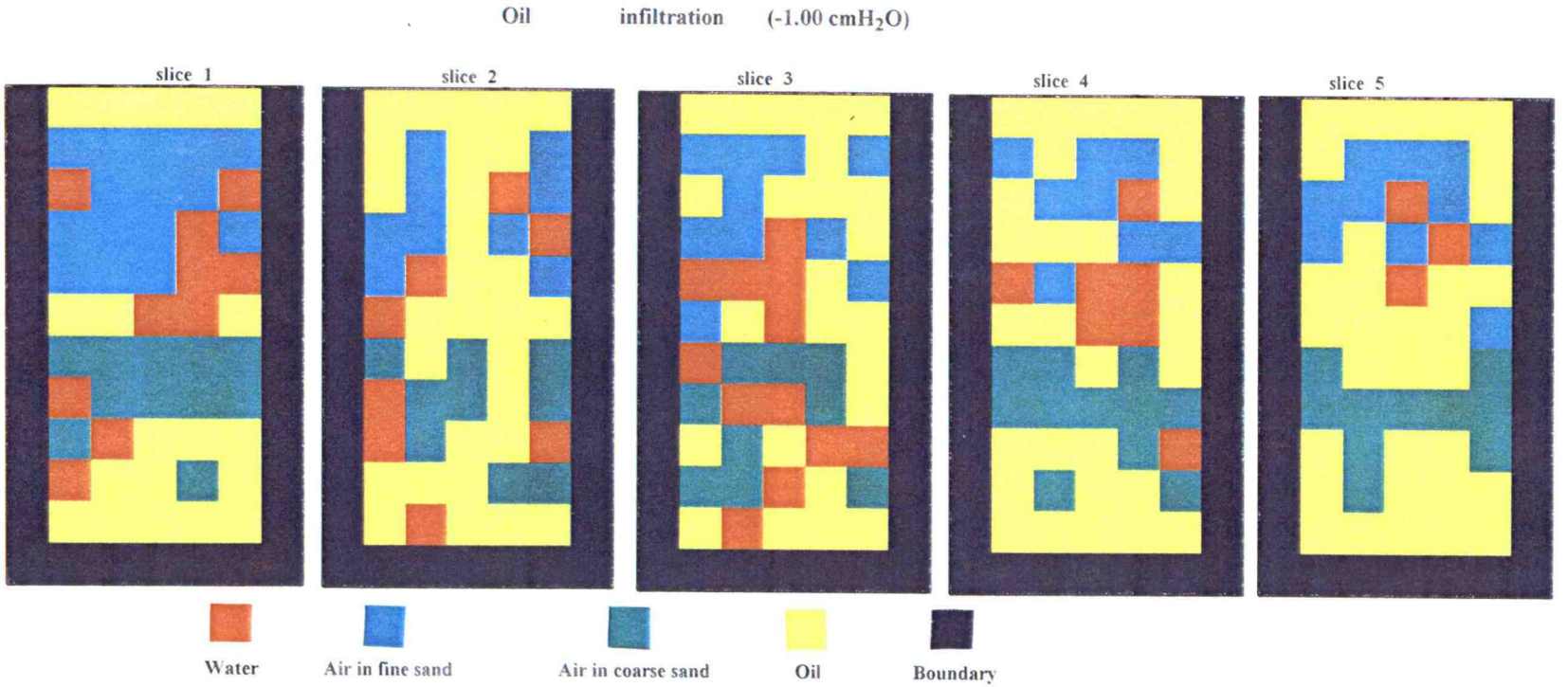

Figure 70. Fluid displacement of oil infiltration for double layer sand media with domain size of 10 x 5 x 5 pores.

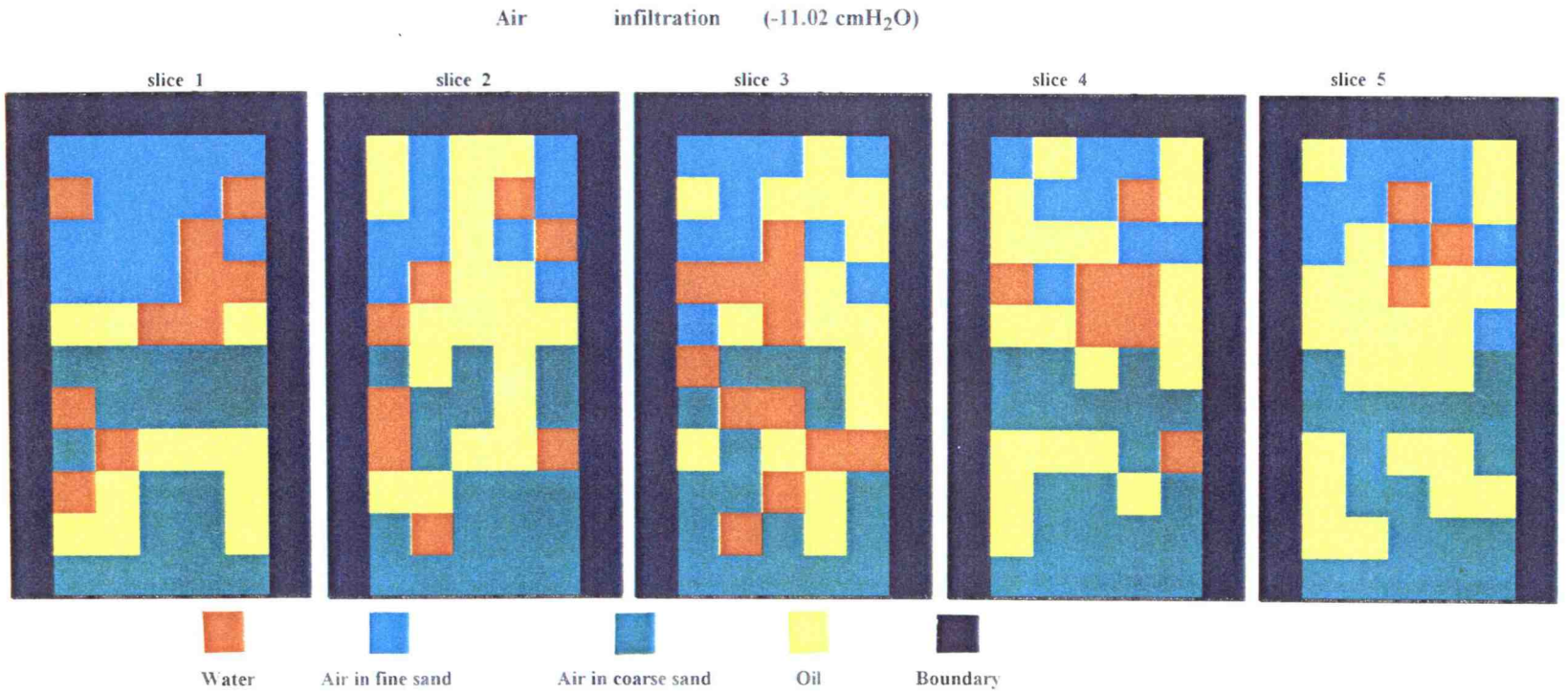

Figure 71. Fluid displacement of air infiltration for double layer sand media with domain size of 10 x 5 x 5 pores

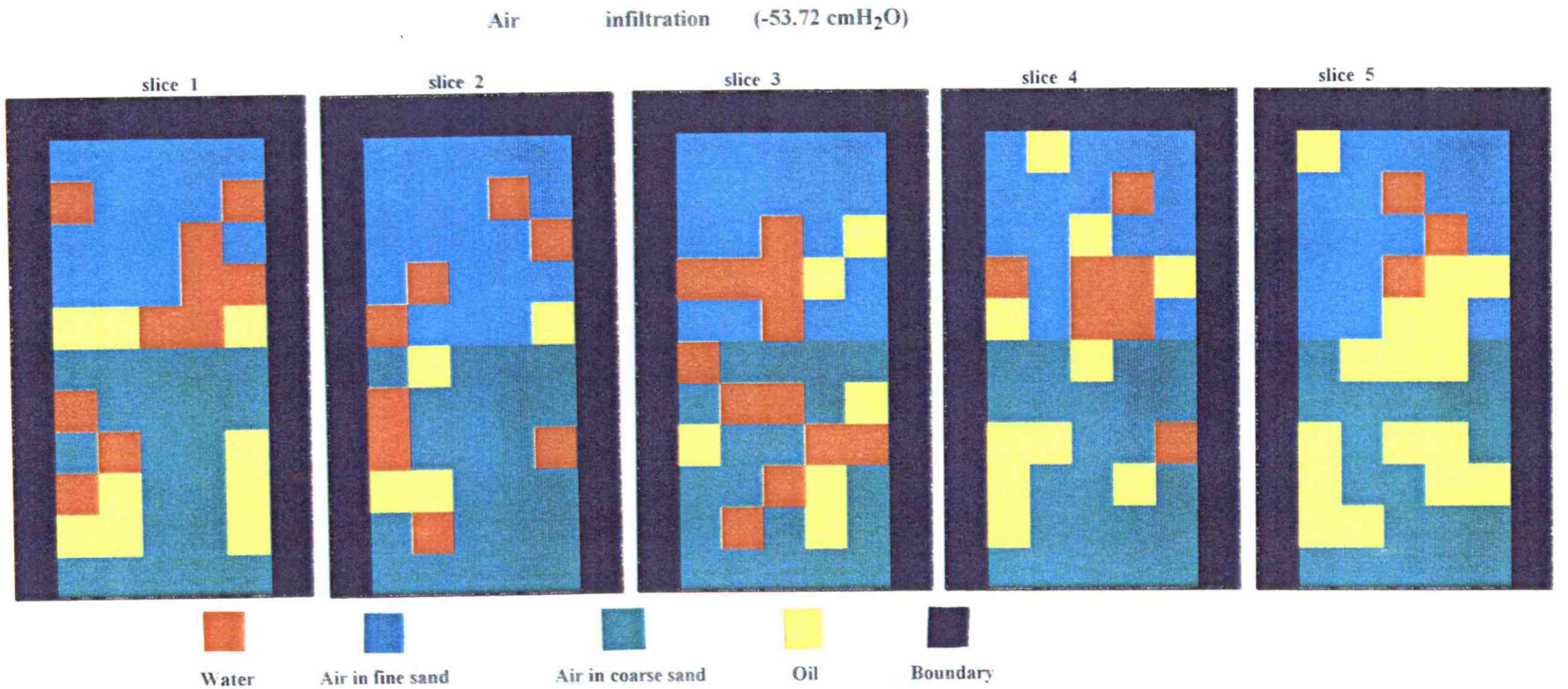

Figure 72. Fluid displacement of air infiltration for double layer sand media with domain size of 10 x 5 x 5 pores.

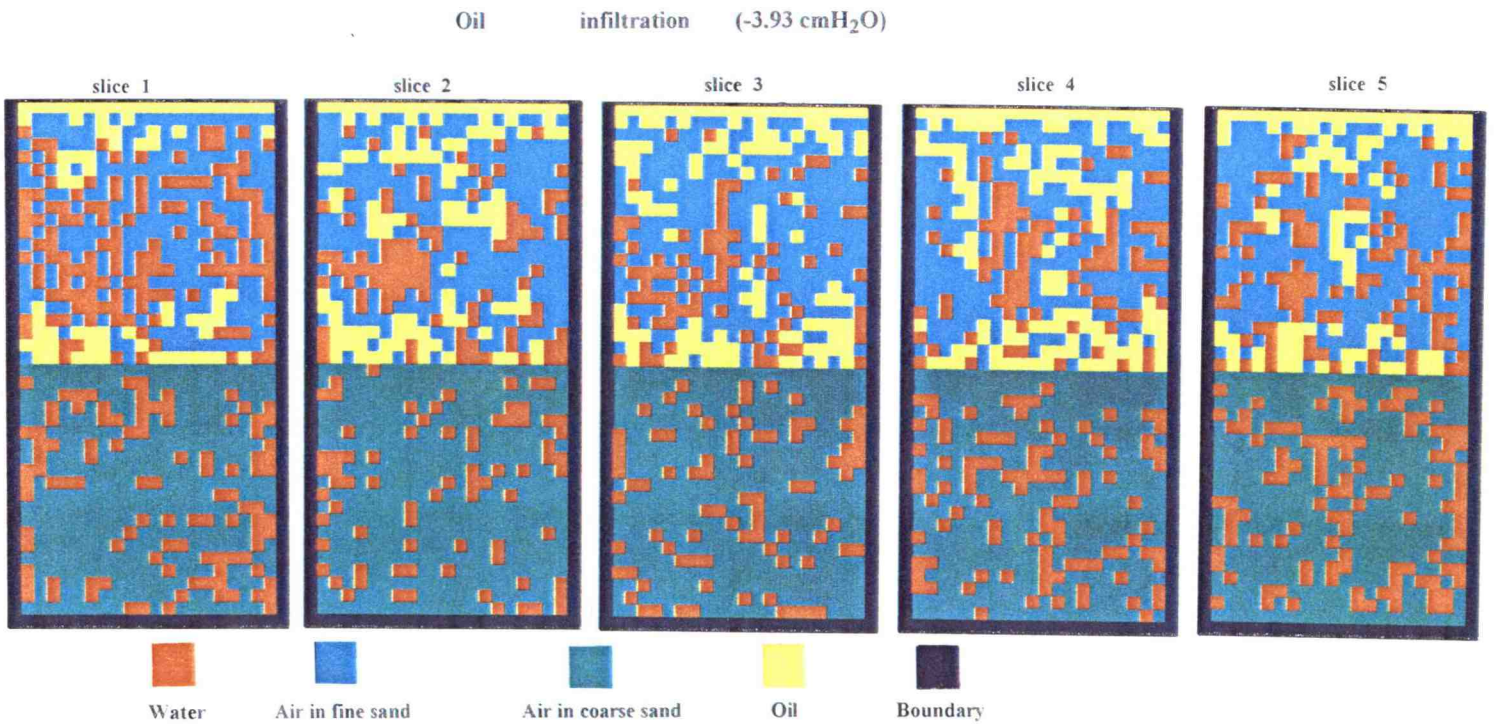

Figure 73. Fluid displacement of oil infiltration for double layer sand media with domain size of 40 x 20 x 5 pores

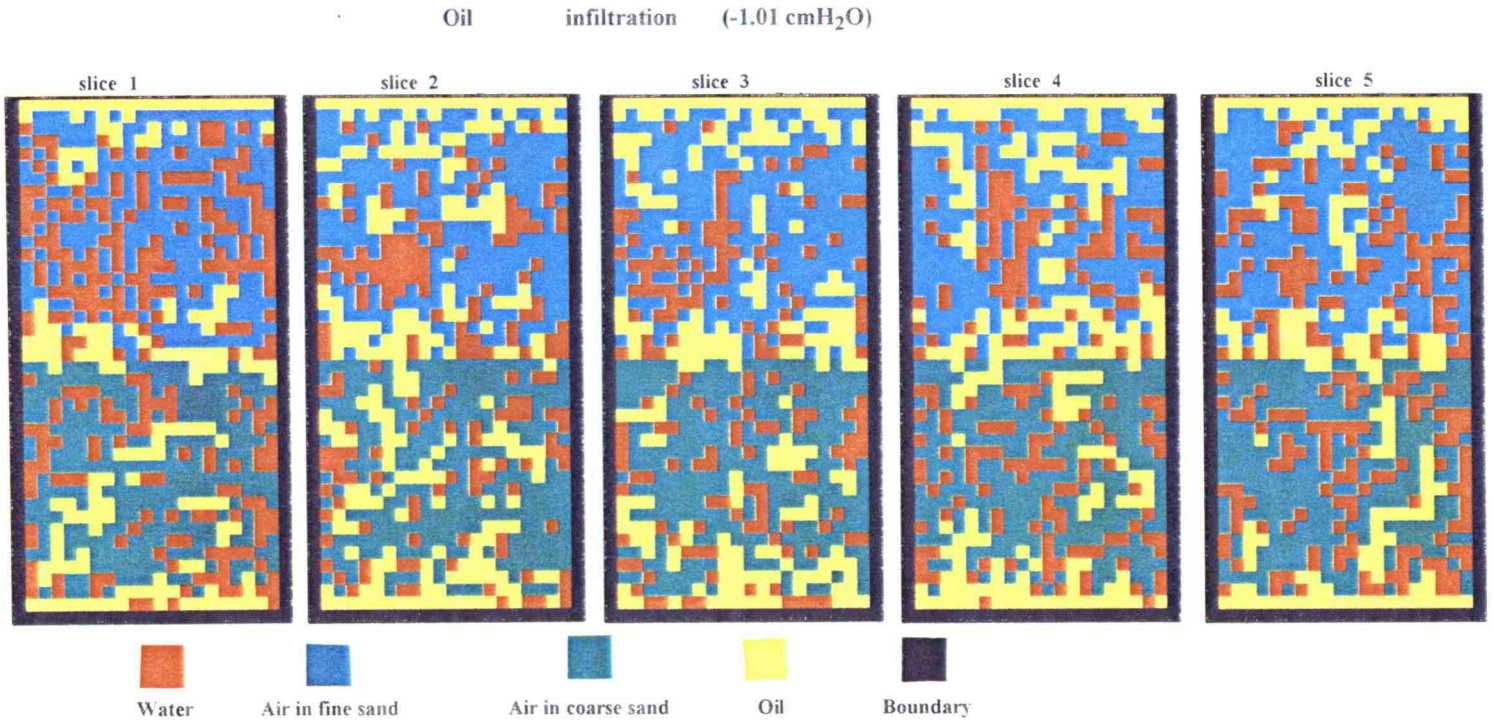

Figure 74 Fluid displacement of oil infiltration for double layer sand media with domain size of 40 x 20 x 5 pores.

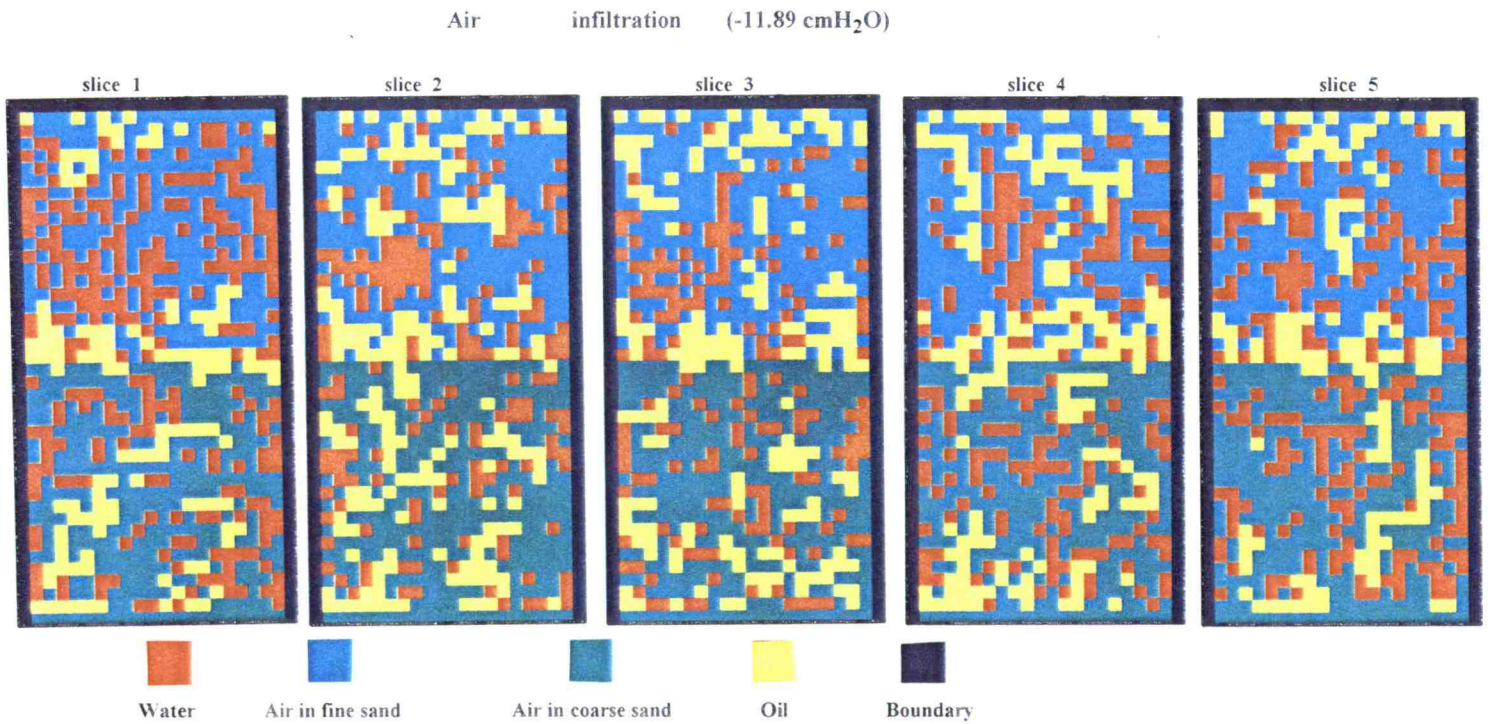

Figure 75. Fluid displacement of air infiltration for double layer sand media with domain size of 40 x 20 x 5 pores

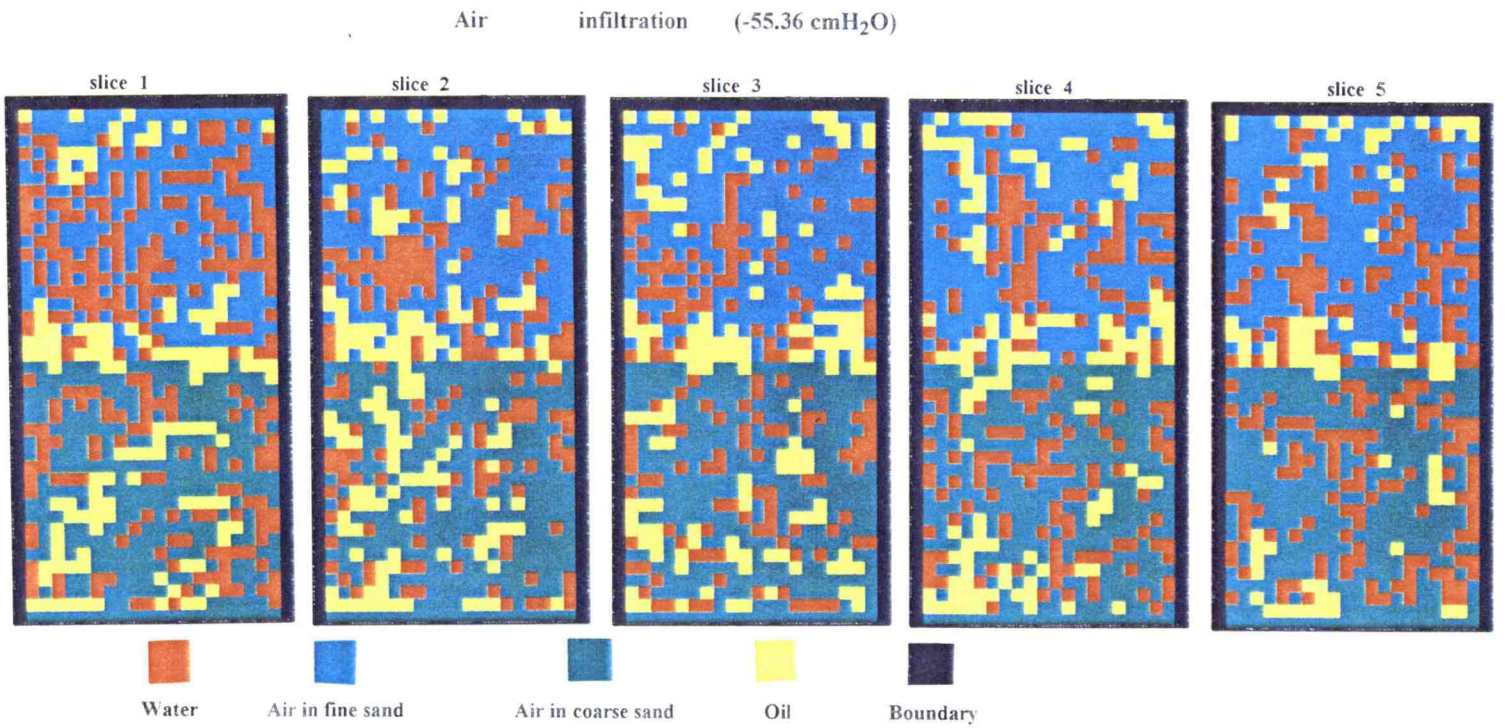

Figure 76. Fluid displacement of air infiltration for double layer sand media with domain size of 40 x 20 x 5 pores.

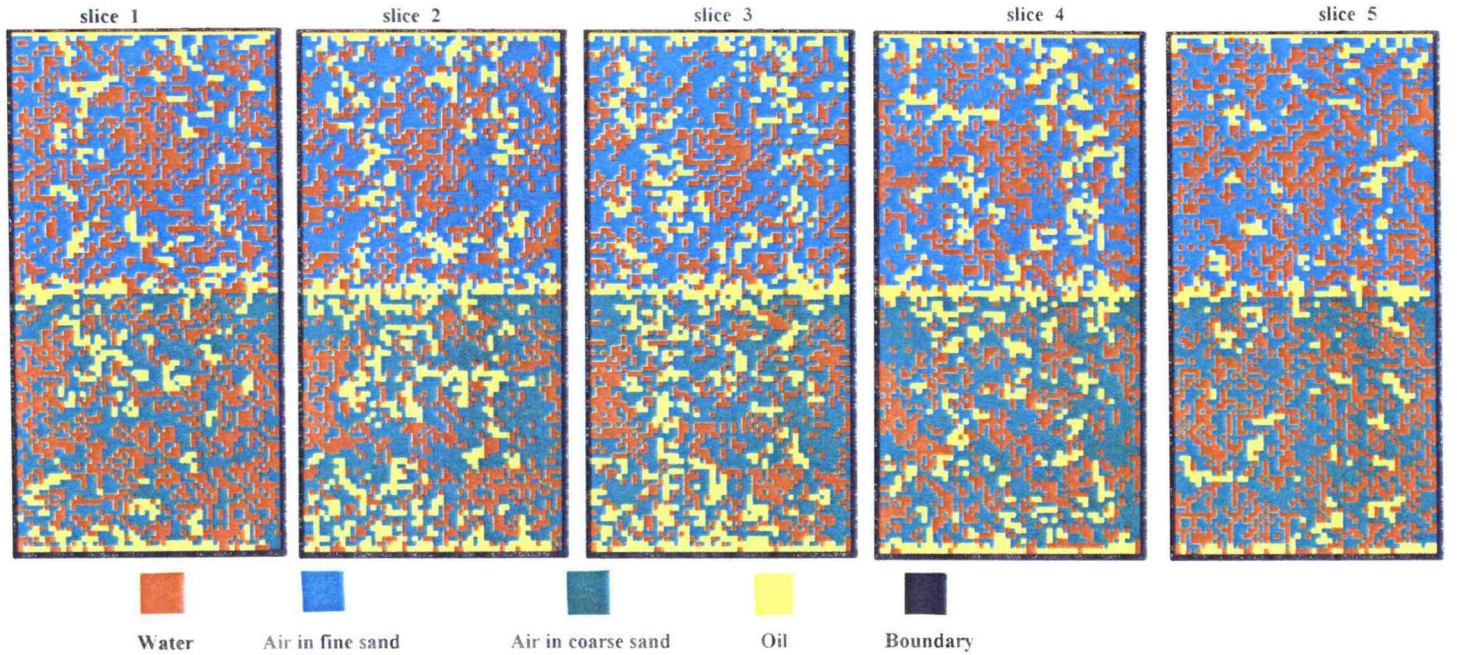

Figure 77. Fluid displacement of oil infiltration for double layer sand media with domain size of 100 x 50 x 5 pores

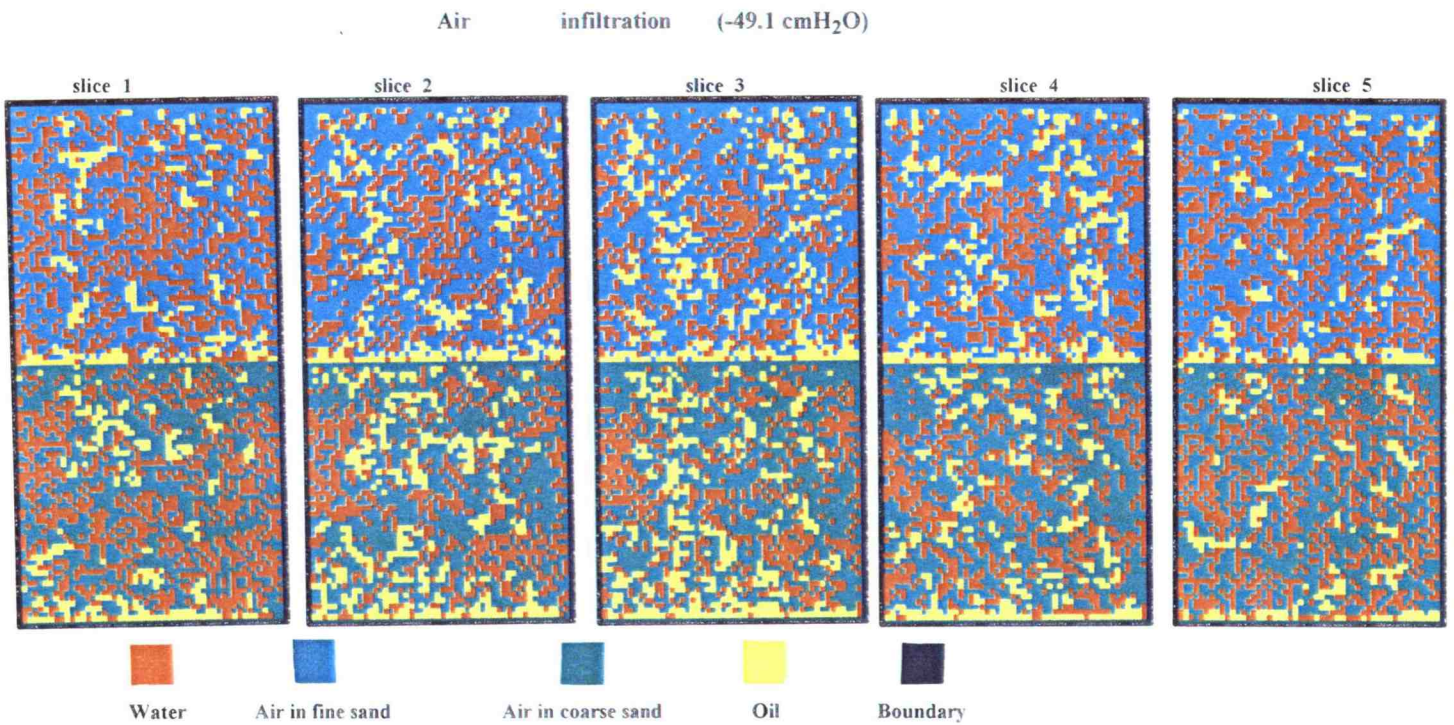

Figure 78. Fluid displacement of air infiltration for double layer sand media with domain size of 100 x 50 x 5 pores

Chapter 6. Discussion and Conclusions

6.1 Discussion

6.1.1 Seed Effect

The pore and tube sizes are the controlling factors in the network modeling. All the fluid displacements are strongly depend on local pore and tube sizes. The pore and tube sizes used in the model are developed by a uniform distribution random number generator. This distribution is generated based on an input random seed which may be any integer. Different random seeds provide different realizations of pore and tube sizes from the same underlying uniform distribution. Because the infiltration processes are strongly dependent on local pore and tube sizes, the random seed may give a significant effect on results from model.

Three seeds (12345, 34521, 54321) were employed in a three-dimensional single layer sand media model runs with the domain size of 10 x 5 x 5 pores. The infiltration processes were water-air-water-air-water-air. The capillary pressure-saturation hysteristic curves are shown in Figures 79, 80, and 81.

With the same domain size and different seeds, the first saturation range from 0.50 to 0.57, the second saturation range from 0.39 to 0.41, and the third saturation range from 0.38 to 0.40. Despite these minor differences, the overall shape of curves are similar between experiments using different seeds. The maximum saturation always occurred in the first infiltration. After each water infiltration, this maximum saturation

decreased by more than 10%. This leads us to the conclusion that choice of seeds affect point values but does not change the overall form of the relationship between the capillary pressure and saturation.

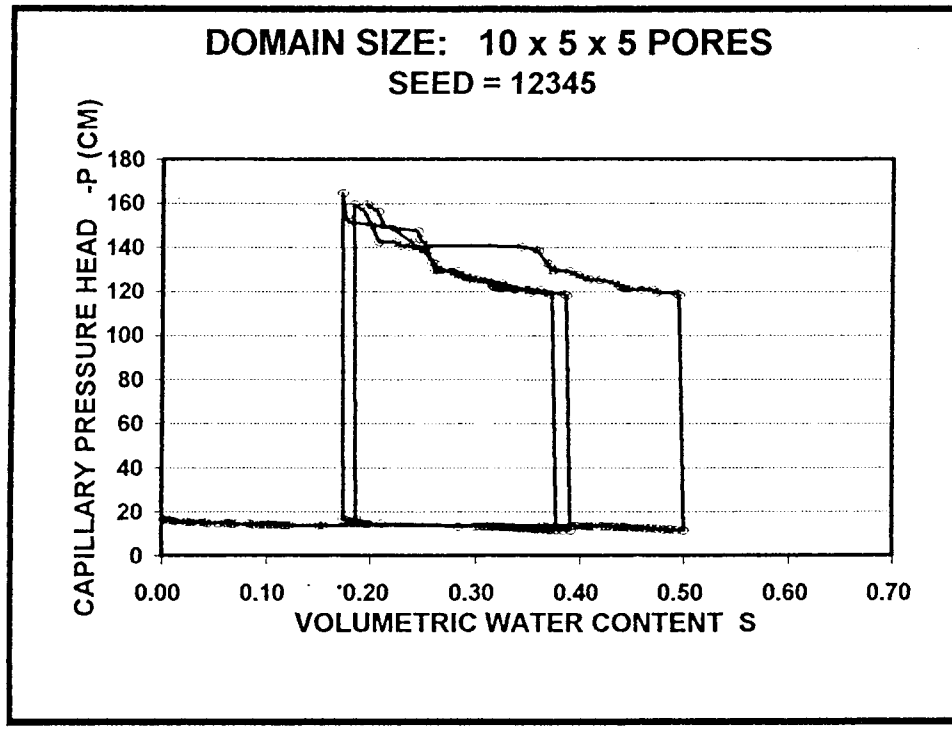

Figure 79. W-A-W-A-W-A capillary pressure-saturation scanning curves for single layer sand media with random seed of 12345.

6.1.2 Domain Size Effect

Domain size is one of the most important factors in pore-scale network modeling. The larger the domain size, the more realistic the results become. At the same time, computational difficulty goes up vastly with domain size (exponential with number of nodes). How big does a domain size have to be to provide a scale-invariant view representation of flow processes? Is there such a size?

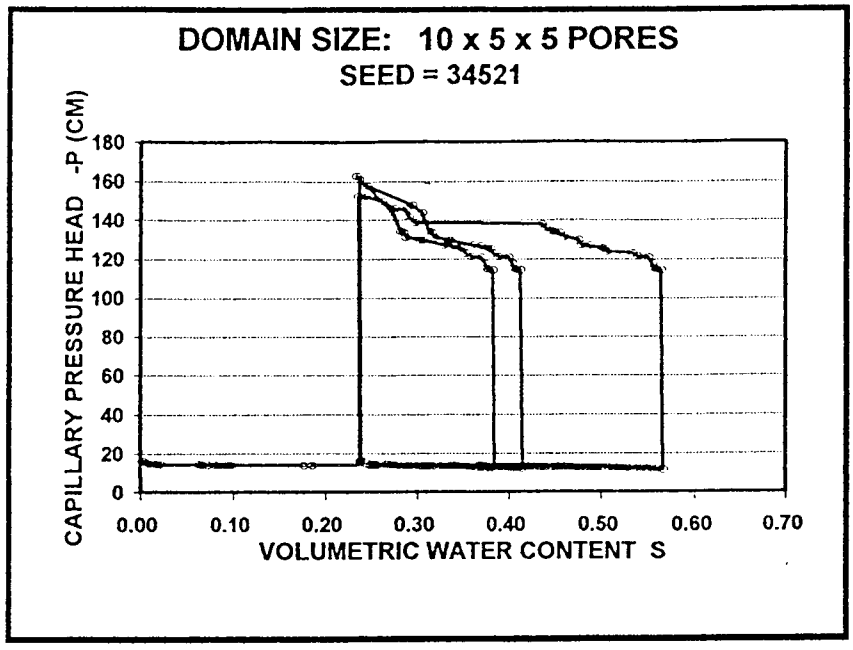

Figure 80. W-A-W-A-W-A capillary pressure-saturation scanning curves for single layer sand media with random seed of 34521.

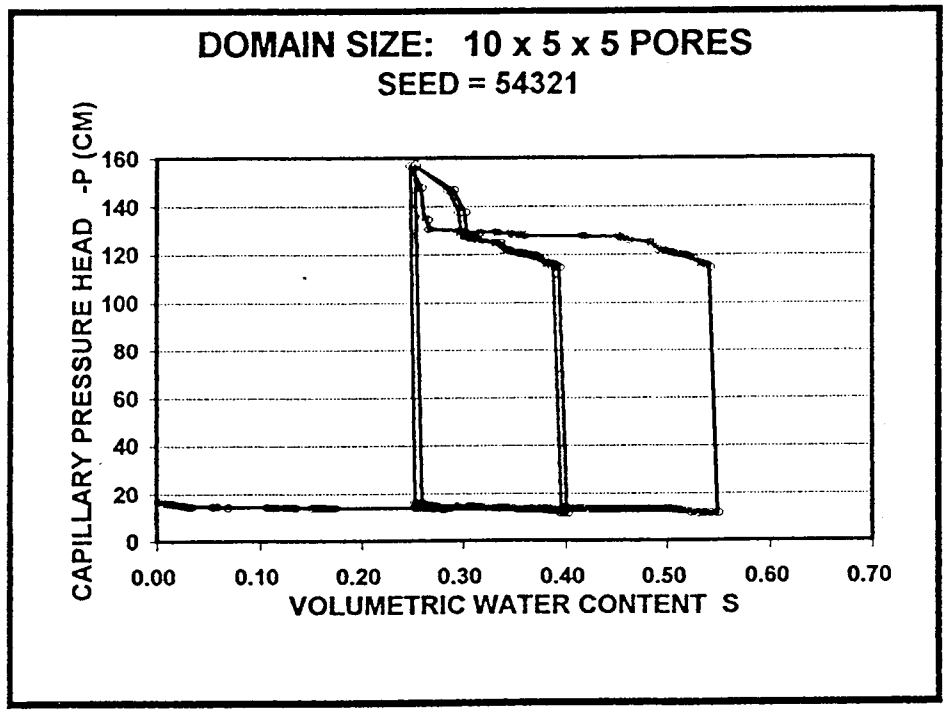

Figure 81. W-A-W-A-W-A capillary pressure-saturation scanning curves for single layer sand media with random seed of 54321.

Take the example of initial saturation data from double-layer, two and three-dimensional domain with water-air-water-air-water-air infiltration processes. The relationships of first saturation and domain size which is described as the number of pores in log scale are shown in Figures 82 and 83.

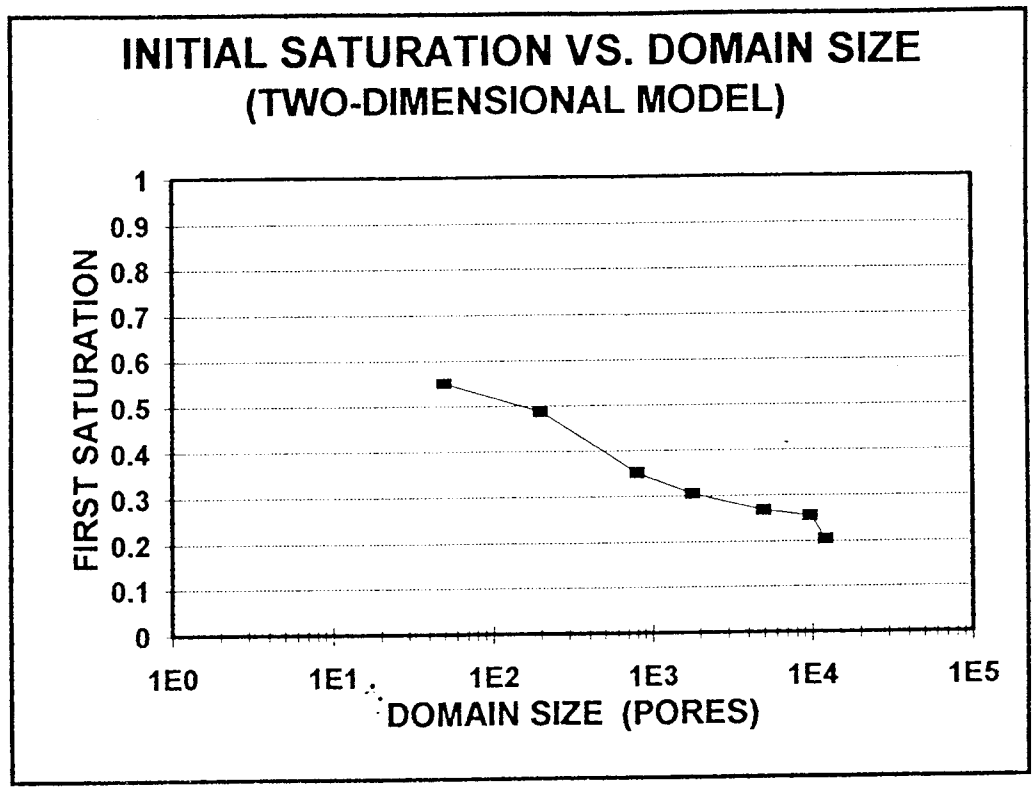

Figure 82. Domain size effect on simulation results from two-dimensional model.

The results from two and three-dimensional models were significantly different. In Figure 82, the initial saturation monotonically decreases with increasing domain size. Up to the domain size of 10,000 pores, the initial saturation keeps on decreasing without showing any sign of reaching an asymptotic value. In contrast, for the three-dimensional simulation (Figure 83), initial saturation initially decreases with increasing domain size. But by the time the domain has 9000 pores, the initial saturation reaches a firm asymptote

which is maintained up to 25,000 pores. Clearly the size of the simulation domain is important. It appears that two-dimensional models do not provide a realistic representation of many features of actual porous media. This will be discussed in detail in next section. Given both the appearance of similar filling pattern between Figures 67 and 68 and the fact that the initial saturation reaches steady-state at the domain size of 60 x 30 x 5 pores, it appears that the domain size of 100 x 50 x 5 pores is big enough to give predictions which are not a function of the domain size.

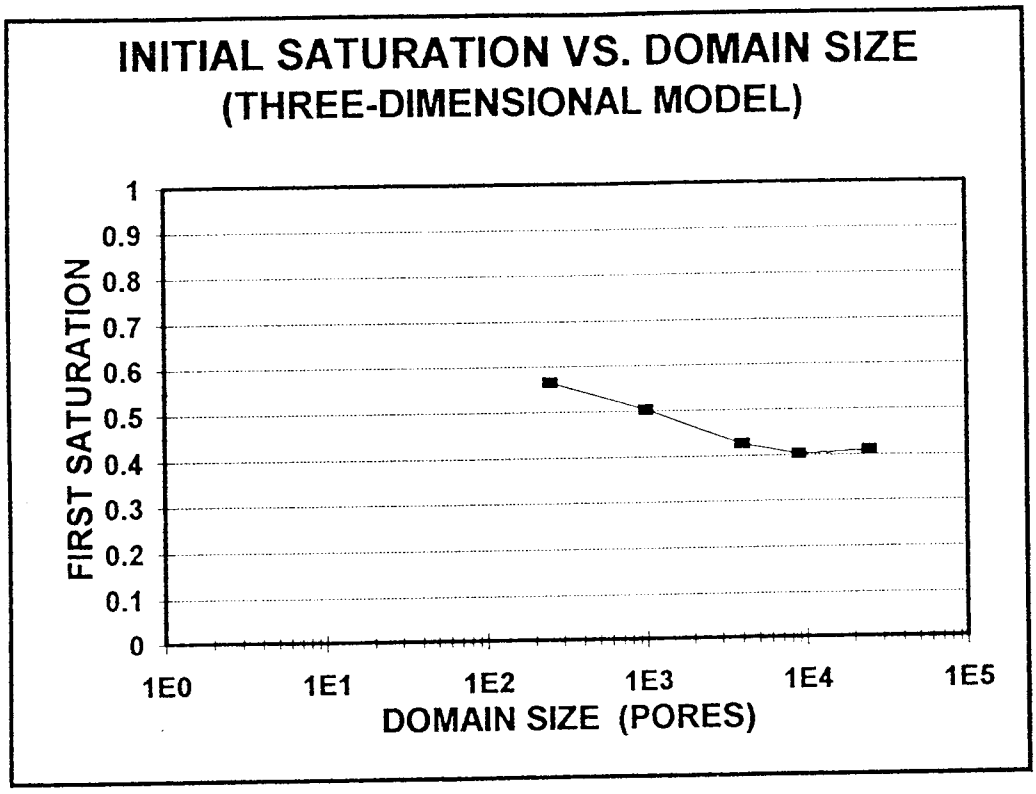

Figure 83. Domain size effect on simulation results from three-dimensional model.

6.1.3 Boundary Effect on Two-dimensional Models

In the simulation using two-dimensional models, it appeared that areas of trapped air developed with the linear extent of the same scale as the domain. However, this phenomena was not found in three-dimensional model results. This supported the hypothesis that the results from two-dimensional models was strictly a function of the domain size which was stated by Chandler et al. in 1982.

This can be seen in the fluid distribution data from double-layer, two-dimensional domain with size of 10 x 5, 20 x 10, 40 x 20, 60 x 30, and 100 x 50 pores. The final fluid distributions after water infiltrating the initial dry domain are shown in Figures 84 and 85. Characteristic trapping sizes are indicated.

From Figures 84 and 85, we measured the largest trapping length for each graph which are 3, 5, 11, 17, and 36 pores respectively. The trapping length which is described as pore distance is increased as the domain size increasing. These are 0.3, 0.25, 0.275, 0.283, and 0.36 the size of the largest domain dimension, demonstrating the direct relationship between entrapment size and domain size. They are all smaller than the width of the their domain. This is also true for single layer sand media (Figures 17 and 19). This phenomena is not found in experiments with natural media. This is one major limitation of two-dimensional models and can be avoided by enlarging to three-dimensional models as shown below.

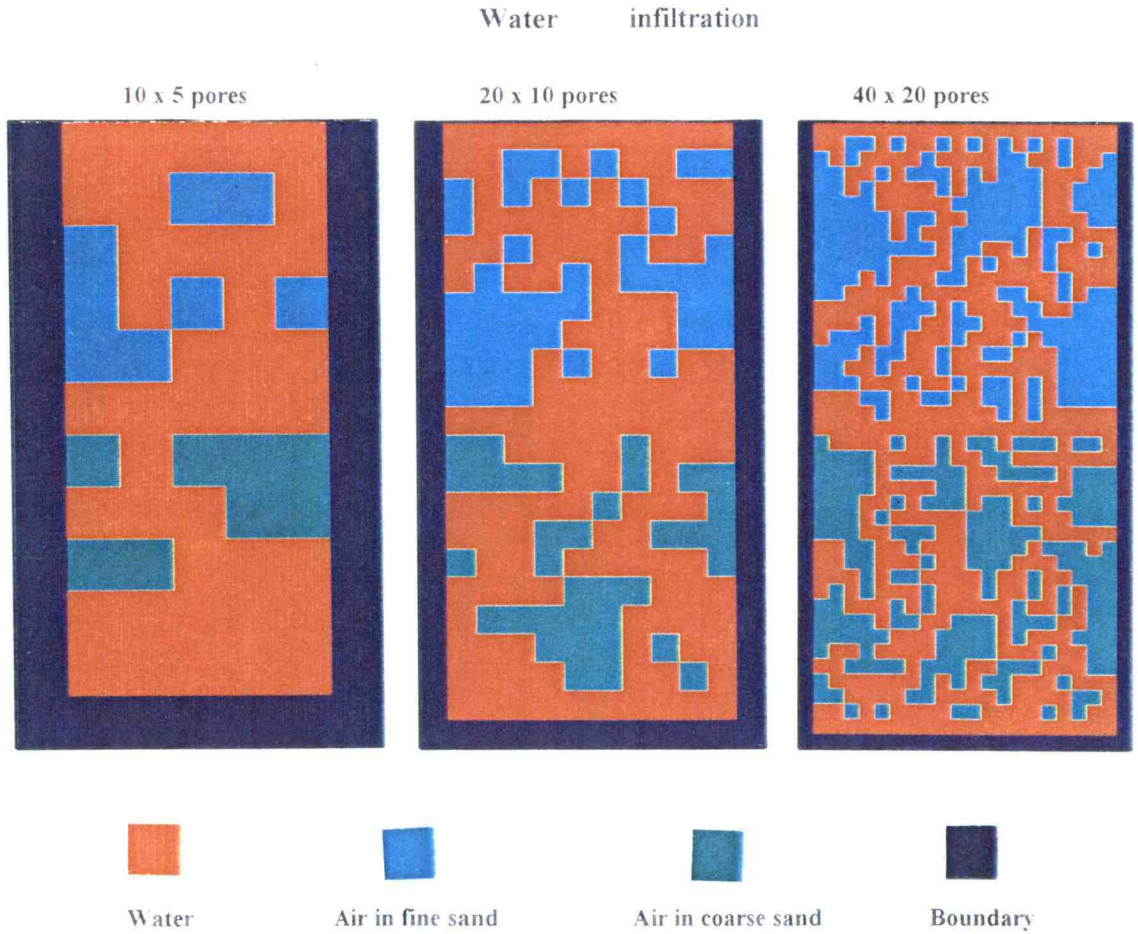

Figure 84. Fluid displacement of water infiltration for double layer sand media with domain size of 10 x 5, 20 x 10, and 40 x 20 pores

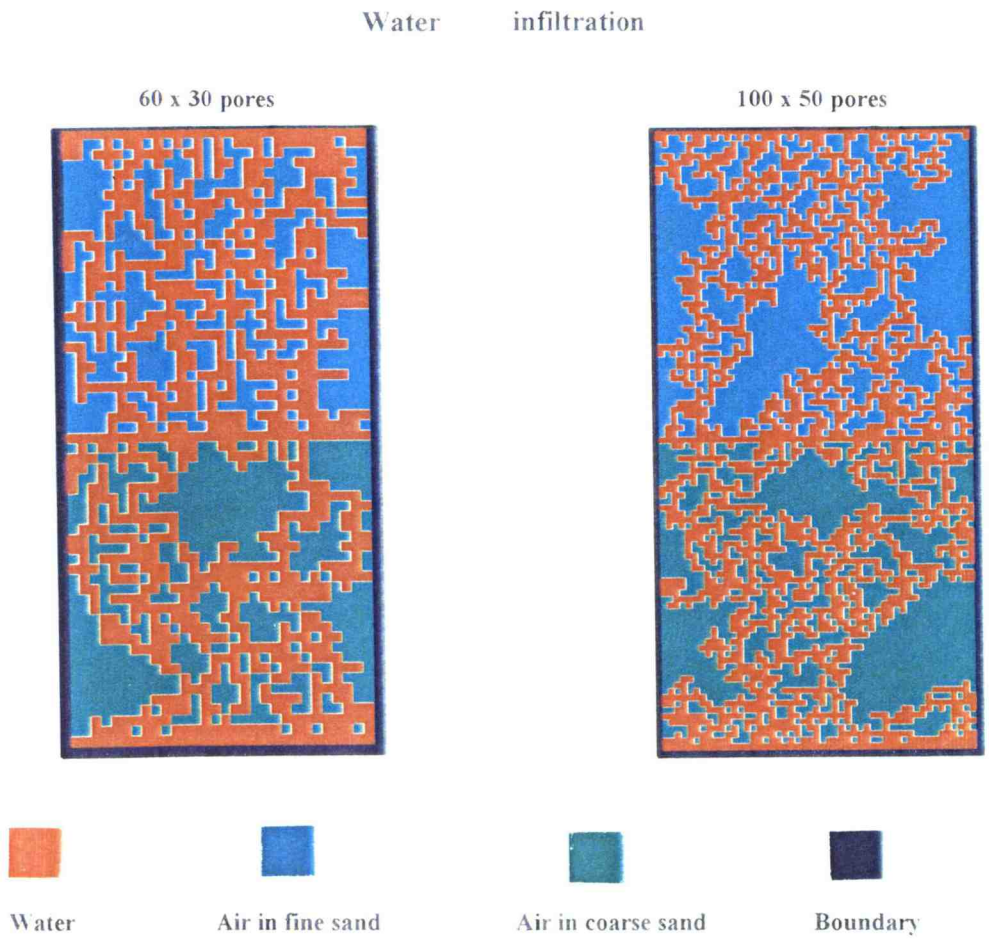

Figure 85 Fluid displacement of water infiltration for double layer sand media with domain size of 60 x 30 and 100 x 50 pores.

6.1.4 Geostatistical Analysis of Fluid Displacement Results from Two-dimensional and Three-dimensional Models

During the simulation with two and three-dimensional models, we found that there were significant differences between fluid distribution matrices after infiltration. The fluid distributions from two-dimensional model have areas of trapping which are the same scale as the domain size. However, the fluid distributions from three-dimensional model have much smaller areas of trapping, and averagely distributed in the whole domain. An example of fluid distributions from two and three-dimensional domain is shown in Figure 86.

Why there were significant differences between two and three-dimensional results? Is there any correlation between those trapping pores? Geostatistical Environmental Assessment Software (GEO-EAS) was used in this study to compare the fluid displacement results from two-dimensional and three-dimensional models. A variogram is defined as the variance of the increment of random variable [Z(u) - Z(u+h)]. It can interpret the spatial correlation structure of the sample data set. A random variable (e.g., Z) is a variable that can take a variety of outcome values (e.g., z) according to some probability distribution. Here u and u+h are the location coordinates vector of the random variable. Using GEO-EAS, variograms may be calculated and plotted for different data sets with up to 1000 points.

The results from double-layer with the domain size of 40 x 20 and 40 x 20 x 5 pores were used in this study. The sample data sets were taken after initial water

infiltration. For three-dimensional case, the middle slice of data set was used. The relationships of variogram of water and pore distance for two sample data sets are shown in Figures 87 and 88.

Figures 87 and 88 show the variogram of water in the small pore distance (from 0 to 10). The variogram from 2-D samples shows regional correlation between variogram and pore distance up to 4 pore lengths (about 0.10 the largest dimension of the domain). However, the variogram from 3-D samples does not show the correlation between variogram and pore distance. This means that 2-D samples will be more likely to have the same fluid filling pores within 4 pore lengths. The physical explanation of this difference is that the connectivity of pores and tubes for different dimension systems are different. In the two-dimensional system, the connectivity of pores and tubes are 4 and 6 respectively. In the three-dimensional system, the connectivity for pores and tubes are 6 and 10. Thus in the three-dimensional space, fluids have more freedom and can infiltrate forward and backward to avoid the difficult infiltrated pores, so less trapped pores left in 3-D model domain.

6.1.5 Environmental Meaning of Bedded Sand Media Study

As stated in Section 3.1, wetting fluid will displace non-wetting fluid from the smallest radius aperture, and non-wetting fluid will displace wetting from the largest radius aperture, along the fluid interface. Applying to bedded sand media, oil is more likely staying in fine media than in coarse media at an oil-air interface. Figures 25 and 27 show that oil filled the fine sand media first then started to infiltrate to coarse sand media.

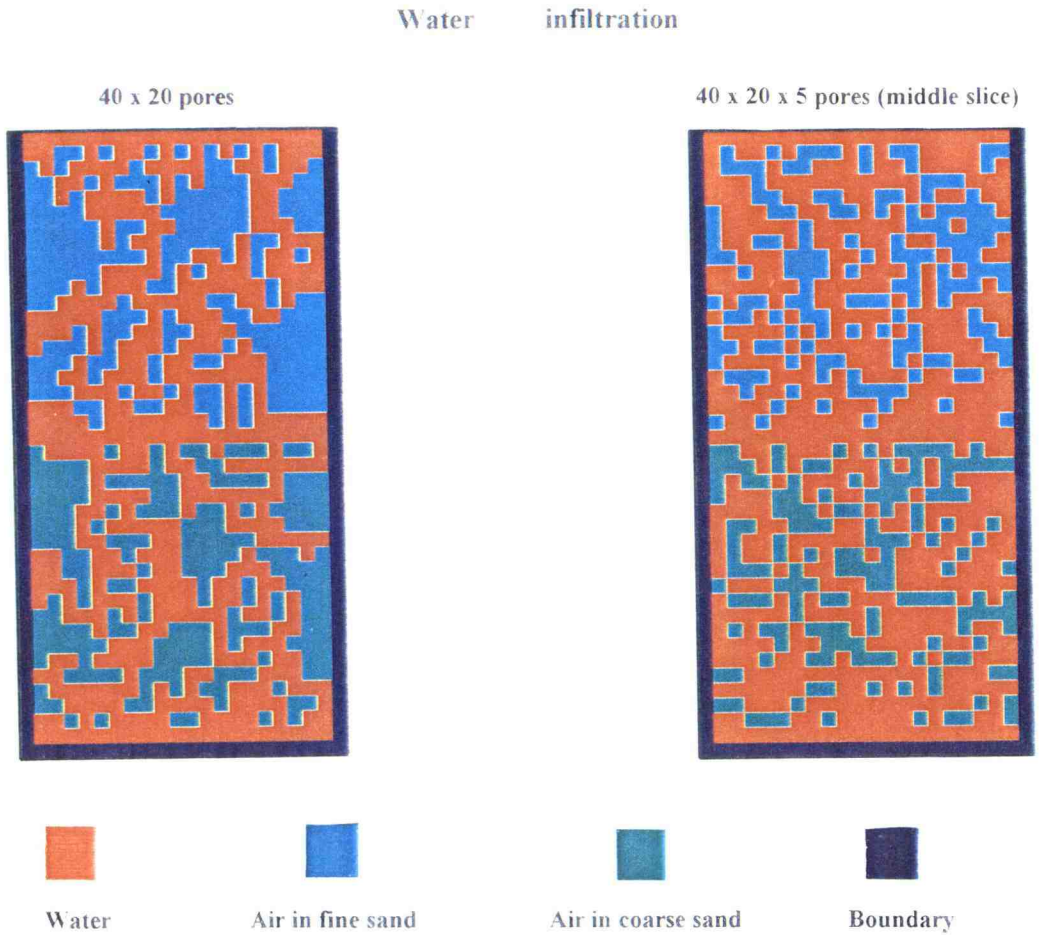

Figure 86 Fluid displacement of water infiltration for double layer sand media with domain size of 40 x 20 and 40 x 20 x 5 pores

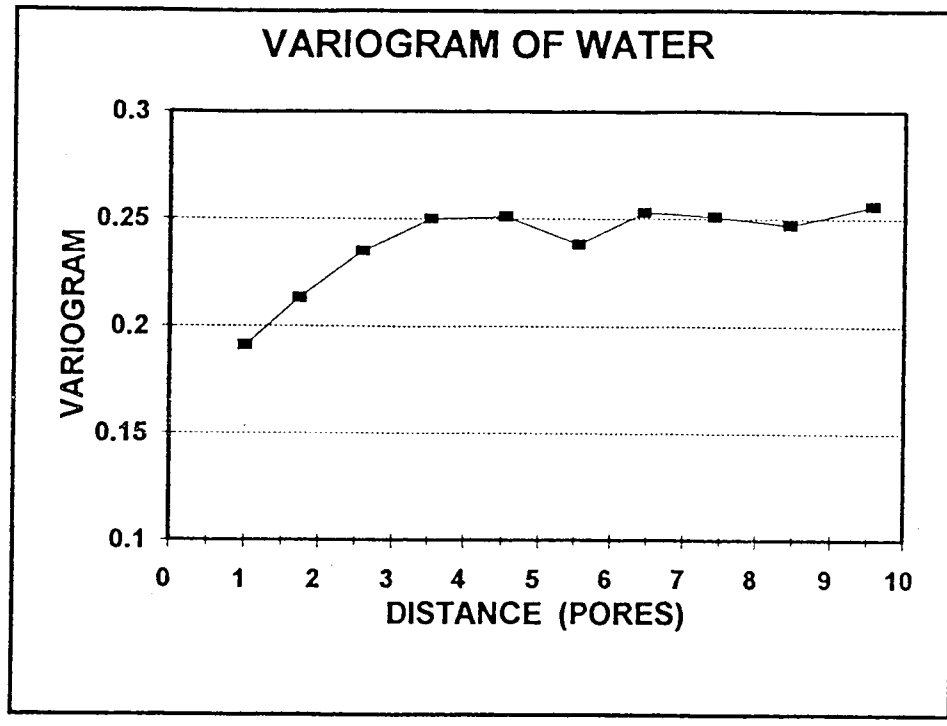

Figure 87. Variogram of Water for the Domain Size of 40 x 20 Pores.

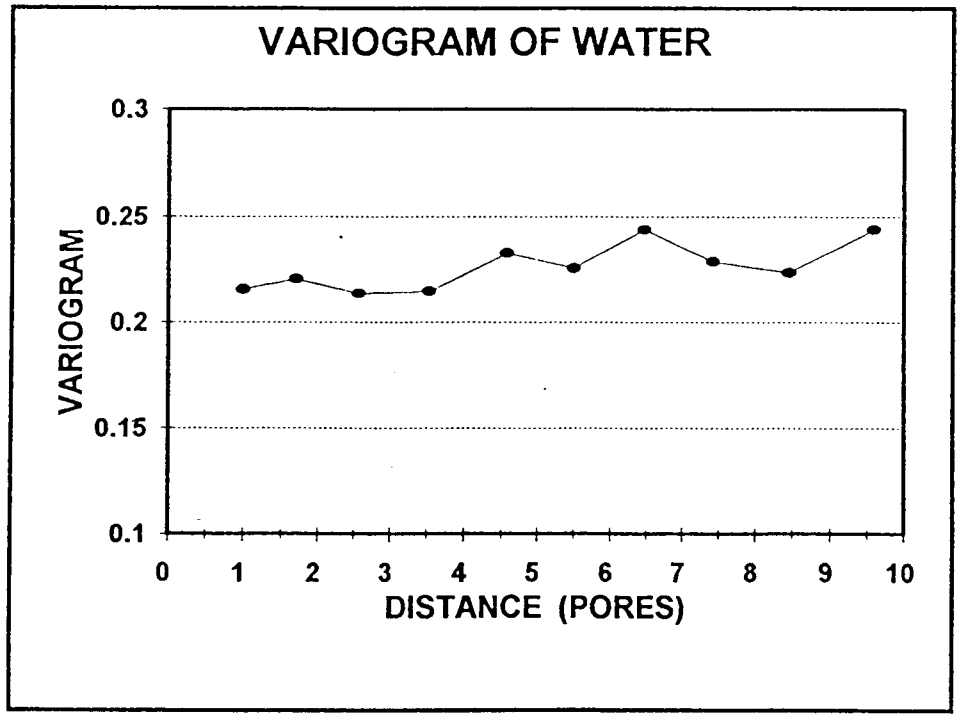

Figure 88. Variogram of Water for the Domain Size of 40 x 20 x 5 Pores.

This property has important environmental implication. When oil transports through the vadose zone, it will stay in fine sand media better than coarse sand media. It is very useful to prevent the contamination of the insoluble organic liquids due to spreading out in the vadose zone by building a slurry wall filled up with more coarse media than the local media. The size of the filling media may be calculated by Laplace Equation to balance the infiltration pressure. However, the possibility of this method needs to be further demonstrated by field experimentation.

6.2 Summary and Conclusions

Two and three-dimensional network models of porous media were constructed to study the movement of NAPL through the bedded sand media containing both air and water. Both hysteristic scanning curves and intermediate fluid distribution were studied. Those intermediate fluid distributions do give insights of mechanisms of fluid emplacement in bedded sand media. The simulation results from hysteristic scanning curves also suggested that the network model may be used to predict the characteristic curves of the three-phase system.

We assumed a uniform distribution of pore and tube sizes. The random seed effect was discussed. The seed does affect the particular values of the characteristic curves but does not change the overall shape of the curves. The network size effect was also discussed. The network sizes used in our study ranged from 10 x 5 (50) to 156 x 78 (12,168) pores for two-dimensional and from 10 x 5 x 5 (250) to 100 x 50 x 5 (25,000) pores for three-dimensional domains. The domain size of 100 x 50 x 5 pores was large enough to provide descriptions independent of the domain scale, whereas there did not appear to be such a size for two-dimensional models.

Different oils (Soltrol-220 and mineral oil) were used in our study. During the same infiltration process, different oil does not change the pattern of the intermediate fluid distribution, only change the capillary pressure at the interface. Several sets of infiltration processes were also tested in our study. The sequence of displacements for a

particular network pore geometry will be identical for any pair of fluids under the same displacement process (e.g., wetting fluid displace non-wetting fluid).

The simulation results from two-dimensional and three-dimensional models were compared in this study. Geostatistical Environmental Assessment Software (GEO-EAS) was used in this analysis. At the same pore distance below 4 pore lengths for the domain size of 40 x 20 and 40 x 20 x 5 pores, the sample results from two-dimensional model have the smaller variogram than those from three-dimensional model. This explained the difference of fluid distribution pattern between two and three-dimensional models (e.g., the fluid distribution patterns from two-dimensional models have the larger entrapping areas than those from three-dimensional models).

The one important limitation of network model is the computational requirement. The use of very high speed computers is essential. The domain size of 100 x 50 x 5 pores was the limit of standard desktop computing tools (486DX-66). It required about one and half months to run one set of the 100 x 50 x 5 domain processes. Except for this limitation, network models provide an invaluable techniques to study fluid transport mechanisms in the vadose zone.

References

Abriola, L. M. and Pinder, G. F., A multiphase approach to the modeling of porous media contamination by organic compounds, I. Equation development, Water Resour. Res., 21(1), 11-18, 1985a.

Abriola, L. M. and Pinder, G. F., A multiphase approach to the modeling of porous media contamination by organic compounds, II. Numerical simulation, Water Resour. Res., 21(1), 19-26, 1985b.

Adler, P. M., *Porous media: Geometry and transports*, Butterworth-Heinemann, Reed Publishing Inc., Stoneham, MA 02180, 9-80 and 375-434, 1992.

Bear, J., *Dynamics of fluids in porous media*, Dover Publications Inc., American Elsevier Publishing Company, Inc., Mineola, N.Y. 11501, 1-21, 38-52, 90-93 and 439-519, 1972.

Blake, F. C., The resistance of packing to fluid flow, Trans. Amer. Inst. Chem. Eng., 14, 415-422, 1922.

Blunt, M. and King, P., Relative permeabilities from two- and three-dimensional pore-scale network modelling, Transport in Porous Media (Netherlands), 6, 407-433, 1991.

Blunt, M., King, M. J. and Scher, H., Simulation and theory of two-phase flow in porous media, Phys. Rev. A, 46(12), 7680-7699, 1992.

Chandler, R., Koplik, J., Lerman, K. and Williamson, J. F., Capillary displacement and percolation in porous media, J. Fluid Mech., 119, 249-267, 1982.

Constantinides, G. N. and Payatakes, A. C., A three dimensional network model for consolidated porous media: Basic studies, Chem. Eng. Comm., 81, 55-81, 1989.

Demond, A. H. and Roberts, P. V., Effect of interfacial forces on two-phase capillary pressure-saturation relationships, Water Resour. Res., 27(3), 423-437, 1991.

Deutsch, C. V. and Journel, A. G., *GSLIB Geostatistical Software Library and User's Guide*, Oxford University Press, Inc., New York, N.Y. 10016, 1992.

Dias, M. M. and Payatakes, A. C., Network models for two-phase flow in porous media, I. Immiscible microdisplacement of non-wetting fluids, J. Fluid Mech., 164, 305-336, 1986a.

Dias, M. M. and Payatakes, A. C., Network models for two-phase flow in porous media, II. Motion of oil ganglia, J. Fluid Mech., 164, 337-358, 1986b.

Dullien, F. A. L., *Porous media: Fluid transport and pore structure*, Academic Press, Inc., San Diego, CA 92107, 5-74, 1979.

Dullien, F. A. L., Characterization of porous media: Pore level, Von Karman Institute for Fluid Dynamics Lecture Series on Modeling and Applications of Transport Phenomena in Porous Media, Belgium, 5-9 February, 1990.

Eckberg, D. K. and Sunada, D. K., Nonsteady three-phase immiscible fluid distribution in porous media, Water Resour. Res., 20(12), 1891-1897, 1984.

Englund, E. and Sparks, A., *GEO-EAS Geostatistical Environmental Assessment Software User's Guide*, Environmental Monotoring Systems Laboratory, Office of Research and Development, U.S. EPA, Las Vegas, NV 89193-3478, September, 1988.

Etter, D. M., *Structured FORTRAN 77 for engineers and scientists*, 3rd edition, The Benjamin/Cummings Publishing Company, Inc., Redwood City, CA 94065, 1990.

Ewing, R. P. and Gupta, S. C., Modeling percolation properties of random media using a domain network, Water Resour. Res., 29(9), 3169-3178, 1993a.

Ewing, R. P. and Gupta, S. C., Percolation and permeability in partially structured networks, Water Resour. Res., 29(9), 3179-3188, 1993b.

Fatt, I., The network model of porous media, I. Capillary pressure characteristics, Petr. Trans. AIME, 207, 144-159, 1956a.

Fatt, I., The network model of porous media, II. Dynamic properties of a single size tube network, Petr. Trans. AIME, 207, 160-163, 1956b.

Fatt, I., The network model of porous media, III. Dynamic properties of network with tube radius distribution, Petr. Trans. AIME, 207, 164-177, 1956c.

Ferrand, L. A., Celia, M. A. and Soll, W. E., Percolation-based models for pore-to-lab scale calculations in multifluid porous media, Cushman, J. H., *Dynamics of Fluids in Hierarchical Porous Media*, Academic Press, Inc., San Diego, CA 92101, 463-480, 1990.

Ferrand, L. A., Sulayman, J. A., Rajaram, H., and Reeves, P. C., Calibration of a pore-scale network model for unsaturated soils, Proceedings of Fourteenth Annual Geophysical Union Hydrology Days, Colorado State University, Fort Collins, Colorado, 99-109, 5-8, April, 1994.

Goodman, S. E. and Hedetniemi, S. T., *Introduction to the design and analysis of algorithms*, McGraw-Hill, Inc., 134-151, 1977.

Green, W. H. and Ampt, G. A., Studies on soil physics, I. The flow of air and water through soils, J. Agr. Sci., 4, 1-24, 1911.

Hazen, A., Some physical properties of sands and gravels, with special reference to their use in filtration, 24th Annual Report of the State Board of Health of Massachusetts, Publ. Document 34, 539-556, 1892.

Heiba, A. A., Davis, H. T. and Scriven, L. E., Statistical network theory of three-phase relative permeabilities, SPE paper no. 12690, SPE-EOR Symposium, Tulsa, OK, 15-18 April, 1984.

Jury, W. A., Gardner, W. R. and Gardner, W. H., *Soil Physics*, John Wiley and Sons, Inc., 1-122, 1991.

Kaluarachchi, J. J. and Parker, J. C., An efficient finite element method for modeling multiphase flow, Water Resour. Res., 25(1), 43-54, 1989.

Kantzas, A. and Chatzis, I., Network simulation of relative permeability curves using a bond correlated-site percolation model of pore structure, Chem. Eng. Commun., 69, 191-214, 1988.

Koplik, J., Creeping flow in two-dimensional network, J. Fluid Mech., 119, 219-247, 1982.

Koplik, J. and Lasseter, T. J., Two-phase flow in random network models of porous media, SPEJ, 2, 89-100, 1985.

Kueper, B. H. and McWhorter, D. B., The use of macroscopic percolation theory to construct large-scale capillary pressure curves, Water Resour. Res., 28(9), 2425-2436, 1992.

Lapidus, G. R., Lane, A. M. and Conner, W. C., Interpretation of mercury porosimetry data using a pore-throat network model, Chem. Eng. Commun., 38, 33-56, 1985.

Lenormand, R., Fingering in two-dimensional porous media: Experiments, network simulators and statistical models, Von Karman Institute for Fluid Dynamics Lecture Series on Modeling and Applications of Transport Phenomena in Porous Media, Belgium, 5-9 February, 1990.

Lenormand, R., Liquids in porous media, First Conference on Liquid Matter, Lyon, France, 7-11 July, 1990.

Lenormand, R. and Zarcone, C., Capillary fingering: Percolation and fractal dimension, Transport in Porous Media (Netherlands), 4, 599-612, 1989.

McBride, J. F., Simmons, C. S. and Cary, J. W., Interfacial spreading effects on one-dimensional organic liquid imbibition in water-wetted porous media, Journal of Contaminant Hydrology, 11, 1-25, 1992.

Moffat, D. V., *Common algorithms in Pascal with programs for reading*, Prentice-Hall, Inc., Englewood Cliffs, NJ 07632, 1984.

Oren, P. E. and Pinczewski, W. V., The effect of wettability and spreading coefficients on the recovery of waterflood residual oil by immiscible gasflooding, SPE paper no. 24881, 67th Annual Technical Conference and Exhibition of the Society of Petroleum Engineers, Washington, DC., 4-7 October, 1992.

Simmons, C. S., McBride, J. F., Cary, J. W., and Lenhard, R. J., Organic liquid infiltration into unsaturated porous media, IAH Conference on Subsurface Contamination by Immiscible Fluids, Calgary, Alberta, 18-20, April, 1990.

Slichter, C. S., Theoretical investigation of the motion of ground waters, U. S. Geological Survey, 19th Annual Report, Part II, 301-380, 1899.

Soll, W. E., Development of a pore-scale model for simulating two- and three-phase capillary pressure-saturation relationships, ScD, dissertation, Massachusetts Institute of Technology, Cambridge, MA, 1991.

Soll, W. E. and Celia, M. A., A modified percolation approach to simulating three-fluid capillary pressure-saturation relationships, Adv. Water Res., 16, 107-126, 1993.

Soll, W. E., Celia, M. A. and Wilson, J. L., Micromodel studies of three-fluid porous media systems: Pore-scale processes relating to capillary pressure-saturation relationships, Water Resour. Res., 29(9), 2963-2974, 1993.

Sorbie, K. S., Network modeling of fluid flow in porous media, Von Karman Institute for Fluid Dynamics Lecture Series on Modeling and Applications of Transport Phenomena in Porous Media, Belgium, 5-9 February, 1990.

Steele, D. D. and Nieber, J. L., Pore scale modeling of porous media: A review, 1989 International ASAE Winter Meeting, New Orleans, LA, 12-15 December, 1989.

Touboul, E., Lenormand, R. and Zarcone, C., Immiscible displacements in porous media: Testing network simulators by micromodel experiments, SPE paper no. 16954, 62nd Annual Technical Conference and Exhibition of the Society of Petroleum Engineers, Dallas, TX, 27-30 September, 1987.

Zhang, W. W., Selker, J. S., and Istok, J. D., Use of pore-scale network to model three phase flow in a bedded unsaturated zone, Abstract No. H32A-04, American Geophysical Union 1993 Fall Meeting, Civic Auditorium, San Francisco, CA, 6-10, Dec., 1993.

Zhang, W. W., Selker, J. S., and Istok, J. D., Use of 3-D pore-scale network to model three phase flow in a bedded unsaturated zone, 1994 ASA-CSSA-SSSA Annual Meeting, Seattle, WA, 13-18, November, 1994.